



pvDesign Energy Yield Methodology

A methodology for calculating the annual energy yield of a solar photovoltaic plant

April 3, 2024

Félix Ignacio Pérez Cicala
Miguel Ángel Torrero Rionegro
Juan Romero González
Álvaro Pajares Barroso



Abstract

This document describes a methodology to compute the annual energy yield of a utility-scale solar photovoltaic power plant. The aim of this document is to provide the reader with a comprehensive review and analysis of the methodology, describing in detail the calculations involved in each part of the process.

The methodology described in this models covers simulation of fixed structures and trackers, and mono-face and bifacial photovoltaic modules.

The general outline of the problems studied in order to compute the annual energy yield is:

- The transposition of the radiation components to the tilted plane.
- Using a library to compute the sun position.
- The sun-tracking algorithm used in single-axis trackers (backtracking).
- Computation of the effects of shadows on the irradiance received by a tilted plane.
- Computation of the irradiance perceived by the back-face, used for bifacial simulations.
- Electrical generation of a photovoltaic module being irradiated, and it's associated losses.
- Estimating the effect of partial shadows on strings of modules.
- Performance of an electrical inverter and window of operation.
- Electrical losses in a utility-scale photovoltaic plant.

Contents

Abstract	1
1 Problem definition and structure	8
1.1 Problem definition	8
1.2 Inputs used	9
1.3 Bifacial simulations	10
1.4 Sub-hourly simulations	11
1.5 Program structure	11
2 Solar position and tracking angle	13
2.1 Solar position	13
2.1.1 Definition of solar angles	14
2.2 Incidence angle on a tilted surface	15
2.2.1 Surface orientation and tilt angles used in the program	15
2.3 Tracking angle in one axis sun-tracking systems	16
2.3.1 True tracking algorithm	16
2.3.2 Backtracking algorithm	17
3 Irradiance transposition to the tilted plane of array	20
3.1 Transposition of the beam component	20
3.2 Transposition of the diffuse component	21
3.3 Calculation and transposition of the ground-reflected component	23
3.4 Transposition to the back-face for bifacial simulation	25
4 Front-face effective irradiance	27
4.1 Beam component shading	27
4.1.1 Calculation of shaded area	28
4.2 Diffuse component shading	31
4.2.1 Integration limits	33
4.2.2 Formulation using the integration limits	36
4.3 Ground-reflected component shading	38
4.4 Incidence angle modifier loss	38
4.4.1 ASHRAE incidence angle modifier model	40
4.4.2 Air-glass incidence angle modifier model	41
4.5 Soiling loss	42
4.5.1 Measured incidence angle modifier model	42
4.6 Effective irradiance on the plane of array	43
4.7 Virtual field dimensions	44

5	Back-face effective irradiance	46
5.1	Geometrical reference system definition	47
5.1.1	Ground intersection point calculation	48
5.2	Beam irradiance perceived by the ground	50
5.3	Diffuse irradiance perceived by the ground	52
5.4	Contribution of ground reflected irradiance to the back face	55
5.4.1	Near vision obstacles obstructing the ground reflected irradiance	56
5.5	Contribution of diffuse irradiance to the back face	58
5.6	Contribution of beam irradiance to the back face	59
5.7	Effective back face irradiance	60
6	Photovoltaic module model	61
6.1	The one-diode model	61
6.1.1	Correction of the shunt resistance	64
6.1.2	Reference parameters	65
6.1.3	Correction of the diode ideality factor	68
6.1.4	Numerical resolution using an iterative method	68
6.1.5	Input parameters	69
6.2	Cell temperature	70
6.3	Bifacial photovoltaic modules	71
6.4	Module degradation	72
6.5	Module losses: quality, LID and mismatch	74
6.5.1	Bifacial mismatch	76
6.6	CdTe photovoltaic modules	77
6.6.1	Spectral correction	77
6.6.2	Recombination losses	79
7	Production of an array of photovoltaic modules	80
7.1	Electrical connections in an array	80
7.2	Power production of an array	82
7.2.1	Losses in DC power cables	83
7.2.2	Array production loss due to partial shadings	84
8	Electrical inverter production and performance	86
8.1	Inverter conversion performance model	86
8.1.1	Synthetic performance model	87
8.1.2	Interpolated performance model	88
8.2	Inverter operation window	89
8.3	Multiple MPPT inverter configuration	90
8.4	Inverter apparent power output limit and power factor adjustment	91
8.5	Process diagram of the inverter power calculation	93
8.6	Auxiliary consumption inverter losses	94
8.7	Inverter model input parameters	95
9	Photovoltaic plant AC losses	97
9.1	AC power cable losses	97
9.2	Transformer losses	98
9.2.1	Active power losses	99
9.2.2	Reactive power losses	99
9.3	Auxiliary consumption	100

9.4	Availability losses	101
10	Annual aggregate results and losses	102
10.1	Annual energy production	102
10.2	Photovoltaic plant performance ratio	103
10.3	Specific production	103
10.4	Bifaciality gain	104
10.5	Computing the aggregate loss factors	104
10.5.1	Irradiance losses and shadows	105
10.5.2	Photovoltaic module and DC array losses	105
10.5.3	Inverter losses	106
10.5.4	AC transmission losses	107
10.6	Energy production in sub-hourly timesteps	108
	Bibliography	109

List of Figures

1.1	World map of solar resource [1]	9
1.2	Simplified resolution process of a single interval	12
2.1	Definition of sun position angles [6]	14
2.2	Sun incidence angle on a tilted surface [5]	16
2.3	Axis azimuth	17
2.4	True tracking angle	17
2.5	Backtracking angle	19
3.1	The sky representation used in the simplified Perez model [9]	21
3.2	Contributions to the front and back-face of the plane of array [5]	26
4.1	Beam component shading from one row to another	28
4.2	Beam shadow projections on the perpendicular vertical plane	29
4.3	Unshaded length along the east-west axis	30
4.4	Polar coordinate system	32
4.5	Diffuse shading factor along table height	33
4.6	Diffuse irradiance obstructions	34
4.7	Diffuse irradiance obstructions, including obstructing rows	35
4.8	Obstructions caused by a row upon itself	36
4.9	Obstructions caused by a row upon the next row	37
4.10	Air-glass model IAM profile, with profile corrected for the azimuth effect.	40
4.11	IAM calculated using the ASHRAE model	41
4.12	A diagram of the equivalent virtual field, using trackers	44
5.1	Single axis tracker with torque tube model in Radiance [25]	47
5.2	Reference systems used for the back-face irradiance calculation	48
5.3	Diagram showing the variables used to calculate the distance to axis coordinate	49
5.4	Diagram showing the shades cast by the tables on the ground	50
5.5	Diagram showing the position of the direct shade on the ground	51
5.6	Picture of a 2V tracker using bifacial modules [27]	52
5.7	Arcs of sky vault visible through the gaps between structures.	53
5.8	Configuration factor between a point in the ground and an arc of the sky vault [28]	55
5.9	Evaluation of a ground segment from the back face	56
5.10	Ground reflected irradiance loss due to the near obstacles (torque beam and contiguous structure), evaluated at the middle point of the table for a worse case scenario representation.	57
6.1	Equivalent circuit of a photovoltaic module [5]	62

6.2	Example of the obtained IV curve for a photovoltaic module	63
6.3	Effect of modifying the module resistances on the IV curve	73
6.4	Degradation of maximum power point values [37]	74
6.5	Degradation of the module maximum power after 25 years	75
6.6	Loss caused by mismatch when using bifacial modules [41]	76
7.1	Electrical connections in a photovoltaic power plant [47]	81
7.2	Array disposition in plant and connection to power station [47]	82
7.3	Partially shaded photovoltaic module	84
8.1	Example of efficiency curve obtained with synthetic model	87
8.2	Example of inverter efficiency curves provided by a manufacturer [53]	89
8.3	Graphical representation of the inverter operation window	90
8.4	Losses due to MPP outside operation window	91
8.5	Array of MPPT systems in an inverter	92
8.6	A sample kVA curve	93
8.7	Simplified resolution process of a single interval	96
9.1	AC system losses	98

List of Tables

3.1	Perez model coefficients for irradiance [8]	23
3.2	Perez model sky clearness categories [8]	24
6.1	Parametrization coefficients for spectral correction [42]	77
10.1	Irradiance loss factors	105
10.2	Photovoltaic module and DC array loss factors	106
10.3	Inverter loss factors	107
10.4	AC transmission loss factors	107

Chapter 1

Problem definition and structure

In this chapter, the problem is defined, and the program structure and inputs are described. This chapter should be used as a general guide to the methodology and program, and it gives an overview of how the problem is solved.

1.1 Problem definition

The aim of this methodology is to compute the annual energy injected to grid by utility scale solar photovoltaic plants. This is a two-step process, in which the first step is to evaluate the solar resource at a given location and the second step is to compute the energy yield of a hypothetical photovoltaic plant in that site. This document is only concerned with the second step of this process, and the solar resource will be the main input in the process. A world map of solar resource (available irradiance) is shown in Figure 1.1.

In order to find the production of a plant, the following problems must be solved:

- Calculation of the position of the sun for any given date.
- If the plant has sun-tracking structures, the tracking angle must be calculated.
- Evaluation of the portion of the available irradiance which can be converted to electrical energy. This involves the transposition of the irradiance to the tilted plane and the evaluation of the effect of shadows. Effects of partial shadings on the photovoltaic module arrays.
- Photovoltaic conversion and energy produced by a single photovoltaic module of the plant. The photovoltaic modules must be modeled accurately, which involves the module physical and electrical characteristics, and the module operating temperature must be calculated according to the meteorological conditions.
- Electrical losses from the photovoltaic modules to the electrical inverter (DC losses).
- Electrical inverter conversion performance and power output.
- Electrical losses in the AC side of the plant (cables and transformers).

The solution which will be generated by the program is the hourly (every one hour) or sub-hourly (every 15 minutes, 5 minutes or 1 minute) electrical production of the plant during one

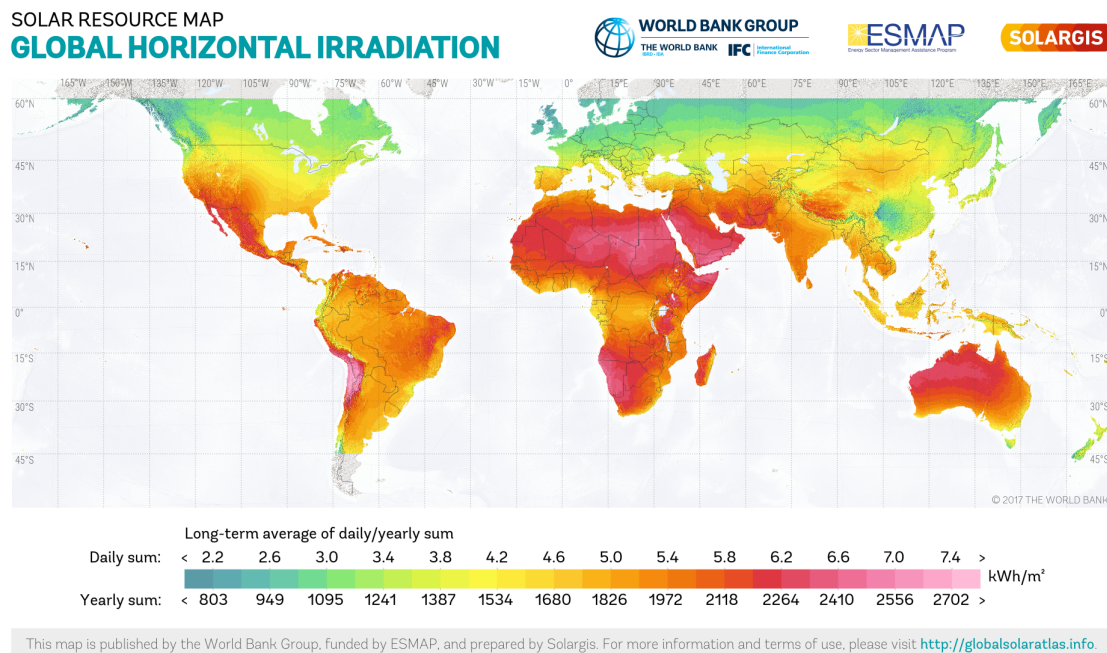


Figure 1.1: World map of solar resource [1]

year. Using this result, the annual aggregate results can be calculated, as well as the losses caused by the different processes and equipment used.

1.2 Inputs used

The following inputs are required to start the calculation process:

1. The site coordinates, timezone and elevation.
2. A Typical Meteorological Year (TMY), with an hourly or sub-hourly (15-minute, 5-minute or 1-minute) resolution and at least the following variables:
 - Global horizontal irradiance (GHI) in $[W/m^2]$.
 - Either diffuse horizontal irradiance (DHI) or beam horizontal irradiance (BHI) in $[W/m^2]$.
 - Air ambient temperature in $[^{\circ}C]$.
 - Ground surface albedo (blue-sky albedo) ρ , unitless.

Additionally, as an optional variable the wind speed in $[m/s]$ may be provided.

3. Whether or not the plant uses sun-tracking structures, and the plane of array tilt if the structures are of the fixed type.
4. Physical characteristics of the structures, such as the pitch distance, the table width, or the ground clearance.
5. The characteristics of the photovoltaic modules, electrical inverters and transformers used.
6. The plant topology, describing the number of components of each type used in the plant, and their physical disposition.

7. The losses which will be applied and their numerical value if they have one.

A Typical Meteorological Year for the site may be obtained by setting up a weather station in the plant site and measuring the required variables during a time period. However, as this data is usually not available in the design phase of building a photovoltaic plant, synthetic TMYs are usually used instead. The process of generating a synthetic TMY consists of using mean monthly irradiance and temperature data (generally obtained using satellite data or interpolating from ground stations) to create an hourly-resolution year of data with a stochastic methodology.

This has a great influence on the final result obtained using the methodology described in this document, as the TMY will usually be the greatest source of error in the model. Given that it is the first and most important input of the program, any errors present in the TMY will be carried downstream and greatly affect the accuracy final result. This is specially true for the irradiance, given that the photovoltaic production is approximately proportional to it.

The errors introduced by other parts of the model are generally of lesser magnitude. The ones which are affected by the program inputs, such as the photovoltaic module model, were found to have very small errors, e.g. Mermoud and Lejeune [2] found the error of the IV model used to calculate the production of a photovoltaic module to be around 1% in periods up to six years.

1.3 Bifacial simulations

To calculate the production of bifacial photovoltaic modules, two different problems must be solved. The first problem is to compute the irradiance perceived by the back-face of the modules. The biggest contribution is the ground reflected irradiance, but other contributions such as the sky vault or the reflections from near structures may be considered.

The second problem is to compute the electrical power output of a bifacial photovoltaic module, using a model which is very similar to the one diode model used for monofacial modules.

Solving these problems presents presents challenges which must be addressed in order to obtain an acceptable yield estimation:

- Surface albedo data, which is the most important input for calculating the ground reflected irradiance, may not be available. Satellite data may be used in the absence of more accurate ground-measured data. In Section 3.3 a more detailed explanation is provided.
- The shading scene for the back-face is much more complicated than the front-face, because of the presence of shades in the ground and near shading obstacles such as the torque beam. Some simplifications must be made to ensure the calculation program is fast enough.
- The PVSyst .pan file only defines the bifaciality factor for bifacial modules, which limits the electrical models which can be used in the simulation when using the .pan as data source.

The simplifications made to calculate the shading effects in the back-face irradiance are described in Chapter 5.

The electrical model used to calculate the electrical output of bifacial modules described in this methodology is very simple. There are better models available, as described in Chapter 6. However, because of the requirement to use the data available in .pan files, the one diode model used

by the PVSyst software [3] was used, which adds up the back-face irradiance to the front irradiance weighted by the bifaciality factor.

1.4 Sub-hourly simulations

Sub-hourly TMYs have a larger number of intervals than hourly TMYs. While hourly TMYs have 8760 intervals per year, 15-minute TMYs have 35040, 5-minute TMYs have 105120 and 1-minute TMYs have 525600.

Sub-hourly simulations are carried out for detailed assessments of PV projects. They can better estimate the inverter power limit losses in sites with higher than usual cloud cover, as well as improving the estimation of the plane of array gains when transposing the irradiation values.

Even if the number of intervals to evaluate is larger, the methodology followed to calculate the energy yield for sub-hourly simulations is the same as for hourly simulations.

1.5 Program structure

In Figure 1.2 a simplified process diagram of the program is shown. The process described in the diagram is the resolution of a single interval. In order to compute the whole year, this process would be repeated for each interval of the whole year.

The individual steps taken in each part of the process will be detailed in the following chapters. There exist iterative steps which may require to repeat the previous step (e.g. when the inverter modifies the operating voltage and the photovoltaic module production must be computed again), however this is unusual in well designed plants and generally there is no need to repeat any step.

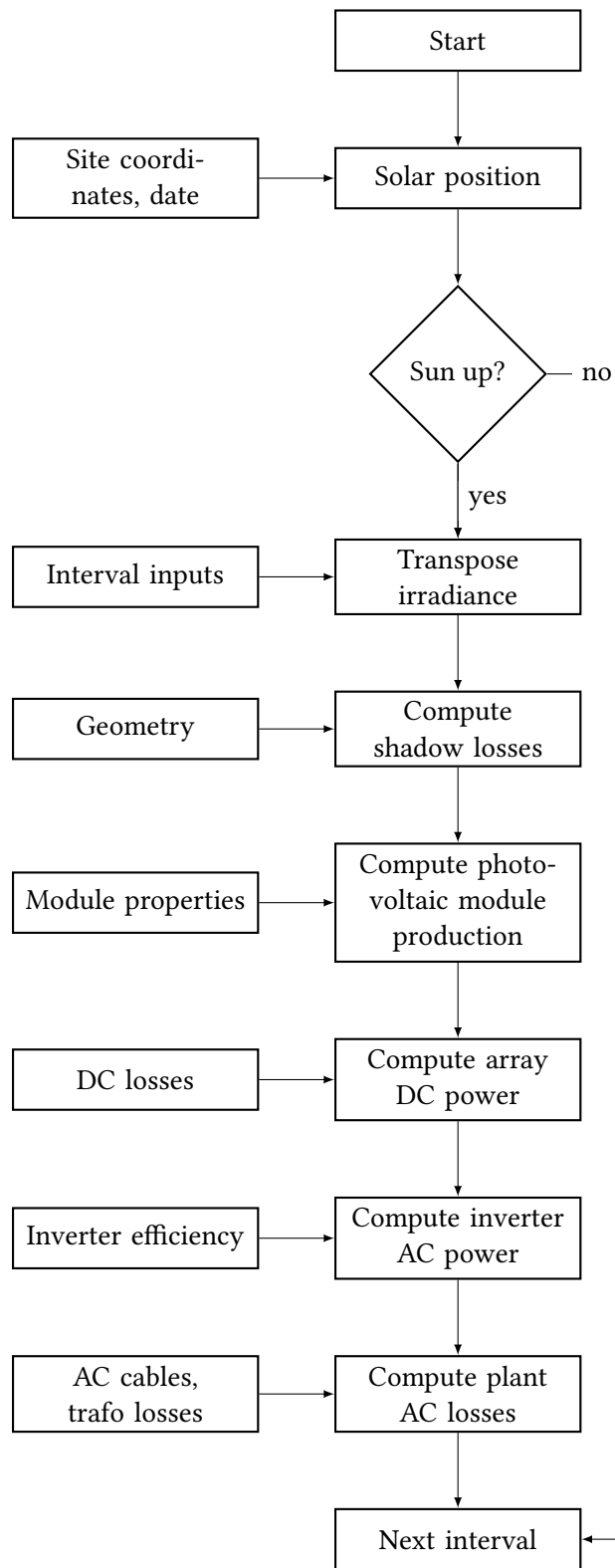


Figure 1.2: Simplified resolution process of a single interval

Chapter 2

Solar position and tracking angle

The computation of the solar position is critical to the accuracy of the model, given its direct influence on the irradiance values seen by the photovoltaic module. The approach taken in this methodology was to use the SOLPOS library [4], which was developed by the NREL (National Renewable Energy Laboratory) of the United States.

The SOLPOS library can be tested online for free ¹.

The sun tracking system implemented is a one-axis tracking system, with the options of using true tracking or back tracking.

2.1 Solar position

The SOLPOS [4] library has an assortment of functions which take as inputs the site coordinates, timezone and date, and return the following parameters (not all parameters listed):

- Solar zenith and azimuth angles (as defined in Subsection 2.1.1).
- Sunrise and sunset for the given date.
- Solar time.
- Relative air mass.
- Extraterrestrial (top of atmosphere) irradiance.

The solar position is computed at the middle of the interval. When the sunrise or sunset occurs during the interval being calculated, the sun position is re-computed at the middle of the actual sun-up time, according to equation (2.1).

$$midpoint_{interval}(i) = \begin{cases} min_{sunrise} + \frac{t_{interval} - min_{sunrise}}{2} & \text{if } i = i_{sunrise} \\ \frac{min_{sunset}}{2} & \text{if } i = i_{sunset} \\ \frac{t_{interval}}{2} & \text{otherwise} \end{cases} \quad (2.1)$$

Where:

¹MIDC SOLPOS Calculator <http://midcdmz.nrel.gov/solpos/solpos.html>

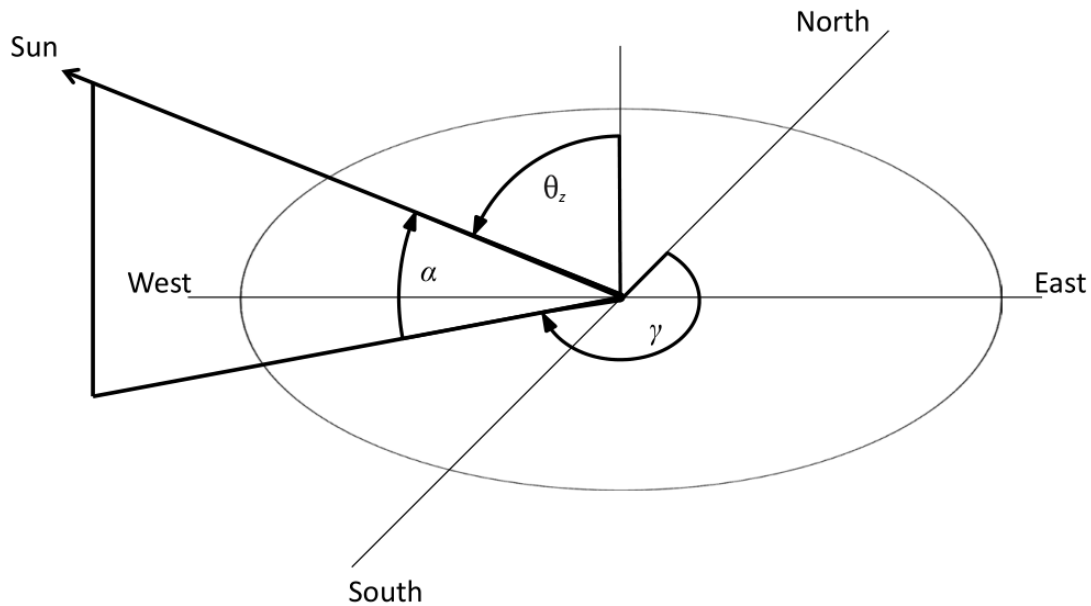


Figure 2.1: Definition of sun position angles [6]

- $midpoint_{interval}(i)$ is the minute at which the sun position will be calculated for any given interval.
- $min_{sunrise}$ is the minute at which the sun rises.
- $t_{interval}$ is the resolution of the interval in minutes.
- $i_{sunrise}$ is the interval at which the sun rises.
- min_{sunset} is the minute at which the sun sets.
- i_{sunset} is the interval at which the sun sets.

2.1.1 Definition of solar angles

A diagram defining the sun angles is shown in Figure 2.1. The angles and their bounds are:

- γ Sun azimuth angle, angular displacement from north of the projection of the sun beam on the horizontal plane [5]. At zero degrees the sun is over the north axis, with the azimuth value increasing in the clockwise direction, so that the east axis would be 90 degrees, the south axis 180 degrees, and the west axis 270 degrees.
- θ_z Sun zenith angle, the angle between the vertical to the horizontal plane and a line drawn from the reference point to the sun [5]. The zenith angle is zero degrees when the sun is directly overhead and 90 degrees when the sun is on the horizon.
- α Sun elevation angle, complement of the sun zenith angle [5]. It is computed using equation (2.2).

$$\alpha = 90 - \theta_z \tag{2.2}$$

2.2 Incidence angle on a tilted surface

The angle of incidence is the angle between the normal to a tilted surface and the sun beam, as shown in Figure 2.2 (the sun incidence angle is θ in this representation). A tilted surface can be defined by its orientation and inclination. The inclination in tracking systems will vary throughout the day, and it will have an effect in both the orientation and inclination parameters.

- γ_{sur} Surface orientation angle (surface azimuth), defined as the azimuth angle of the vector normal to the tilted surface. The angle bounds are defined using the same system used for the sun azimuth angle, such that a surface looking south will have a γ_{sur} equal to 180 degrees, and a north-looking surface will have γ_{sur} equal to 0 degrees. The γ_{sur} of a tracking system with its axis oriented to the north-south axis will have a value of 90 degrees in the morning a 270 degrees in the afternoon (for a northern hemisphere system).
- β Surface inclination angle (surface tilt), defined as the angle between the surface and the ground, and calculated using the equations described in Section 2.3 for sun-tracking one axis systems.

Using these definitions, and the solar angles defined in Subsection 2.1.1, the incidence angle of the sun beam on the surface can be calculated using (2.3) [7].

$$\cos \theta_{\text{inc}} = \cos \beta \cdot \cos \theta_z + \sin \beta \cdot \sin \theta_z \cos(\gamma - \gamma_{\text{sur}}) \quad (2.3)$$

Where:

- θ_{inc} is the angle of incidence on the tilted surface.
- β is the surface inclination angle.
- θ_z is the sun zenith angle.
- γ is the sun azimuth angle.
- γ_{sur} is the surface azimuth angle.

Equation (2.3) can also be used to compute the incidence angle on the back-face of the plane of array, which is necessary for bifacial simulations. If the β surface inclination value is flipped by calculating $180 - \beta$, a new β' angle can be obtained which corresponds to turning the plane of array to look towards the ground. The γ_{sur} must also be flipped 180 degrees to look towards the back.

The resulting cosine of the incidence angle will be negative if the sun beam does not directly impinge on the back-face, but if it does, the incidence angle will be lower than 90 degrees.

2.2.1 Surface orientation and tilt angles used in the program

The program takes as input an additional angle to those defined in Section 2.2. The angles taken as inputs are:

- γ_{axis} Axis orientation angle (axis azimuth), defined as the azimuth angle of the structure axis. The axis definition is clear in the case of a tracking structure, as shown in Figure 2.3 (a), and it is defined as the azimuth angle of a virtual axis set along the largest dimension of a fixed structure, Figure 2.3 (b).
- γ_{sur} is the surface azimuth angle, defined in Section 2.2. This input is unused for tracking systems (in this case, the surface azimuth is calculated using γ_{axis} and β).

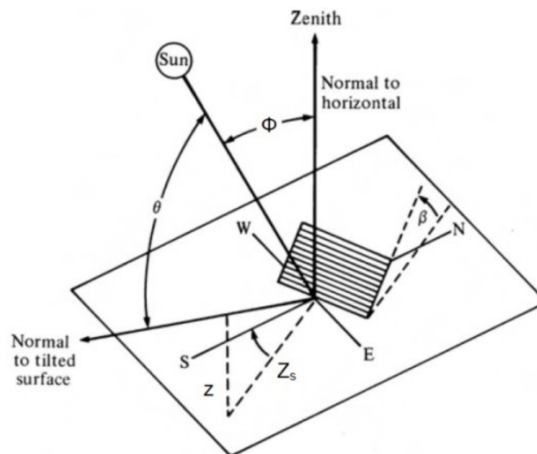


Figure 2.2: Sun incidence angle on a tilted surface [5]

- β is the surface inclination angle (surface tilt), defined in Section 2.2. This input is unused for tracking systems.

2.3 Tracking angle in one axis sun-tracking systems

Calculating the tilt angle in a sun-tracking system consists of finding a tilt such that the incidence angle is minimized (the sun beam is as close to being normal to the plane of array as possible). This ideal tracking angle is given by the true-tracking algorithm, defined in Subsection 2.3.1.

However, the true tracking algorithm is not ideal for conventional solar photovoltaic modules, as it will produce row to row shading whenever the sun is low. In order to avoid losses induced by this shading, which can be very severe due to the effects which will be described in Subsection 7.2.2, a different algorithm is usually used which avoids producing row to row shading. This algorithm is known as the back-tracking algorithm, and it is described in Subsection 2.3.2.

2.3.1 True tracking algorithm

The true tracking algorithm is defined in equation (2.4), using the formula given by [7]. The final tilt angle must respect the maximum and minimum tilt angles defined by the tracker manufacturer, so that they are never exceeded.

In Figure 2.4 (a), an example is shown where the true tracking algorithm exceeds the maximum allowed tilt, and in Figure 2.4 (b) the tilt is set to the maximum allowed tilt, thus the angle of tilt is no longer optimal but it respects the provided bounds.

The final β_{tt} surface inclination true tracking angle is the absolute value of R .

$$R = \tan^{-1} (\tan \theta_z \cdot \sin(\gamma - \gamma_{axis})) \quad (2.4)$$

Where:

- R is the surface tilt. The sign of R indicates in which direction the surface is tilted, being positive whenever $\gamma - \gamma_{axis}$ is smaller than 180 degrees and negative otherwise. Consequently, in a north-south axis aligned system, if the sun is to the east the angle is positive

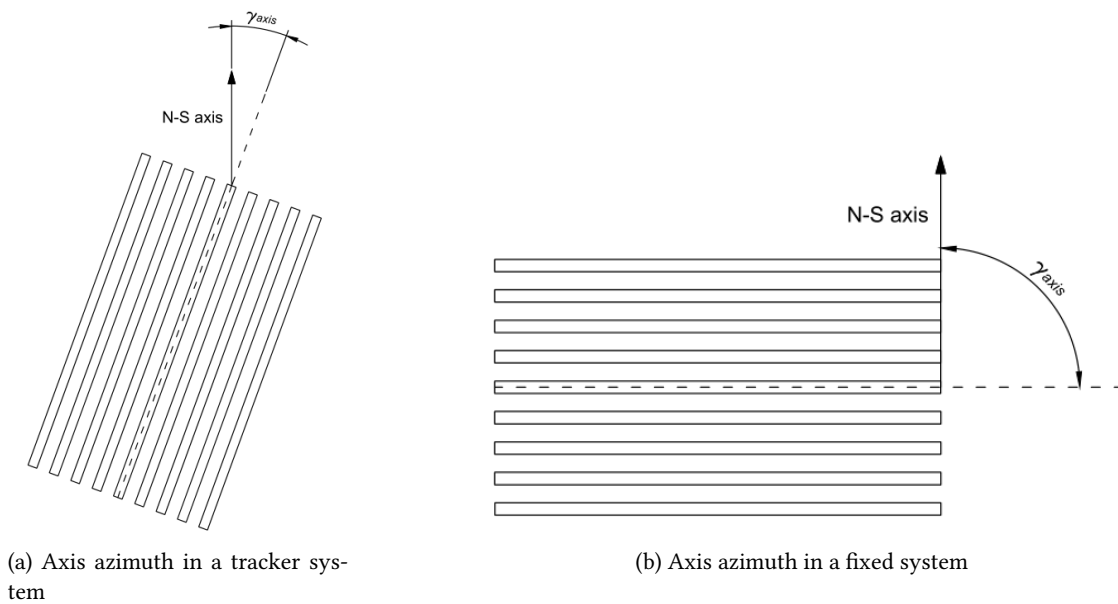


Figure 2.3: Axis azimuth

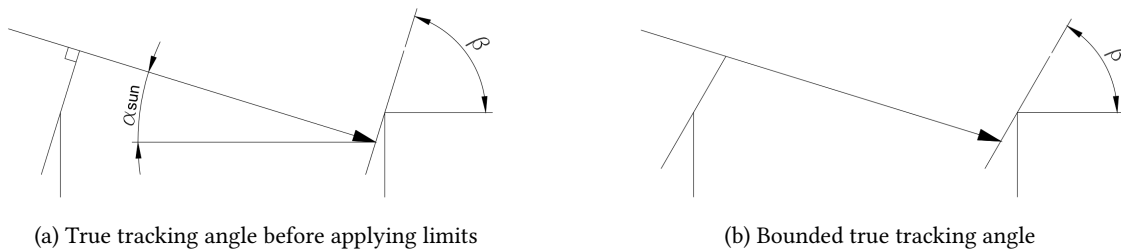


Figure 2.4: True tracking angle

and otherwise it is negative. Thus the surface view azimuth can be calculated using the R value.

- θ_z is the sun zenith angle.
- γ is the sun azimuth angle.
- γ_{axis} Axis orientation angle (axis azimuth).

2.3.2 Backtracking algorithm

In order to compute the backtracking tilt angle, the true tracking tilt angle is used as an input. This angle can, due to its definition, be used to easily compute the angle between the sun beam projected on a vertical plane normal to the plane of array and the horizontal. Given that it is the angle which makes the plane of array perpendicular to the sun rays (when they are projected on a vertical plane normal to the plane of array), the angle between the sun rays and the horizontal plane can be calculated using

$$\alpha_{sun} = 90 - \beta_{tt} \tag{2.5}$$

Where:

- α_{sun} is the angle between the sun rays projected on a vertical plane normal to the plane of array and the horizontal, shown in Figure 2.4 (a).
- β_{tt} is the true tracking tilt angle, obtained using equation (2.4).

In order to compute the back tracking tilt, it must be checked whether or not the true tracking optimal tilt is producing any shades at all. This can be done by computing a cutoff angle, which is the maximum allowed true tracking angle. The cutoff angle is calculated using equation (2.6), by solving the problem shown in Figure 2.5 (a), where the projection of the sun ray is assumed to be perpendicular to the plane of array.

$$\beta_{\text{cutoff}} = \cos^{-1} \left(\frac{w}{PP} \right) = \cos^{-1} (GCR) \quad (2.6)$$

Where:

- β_{cutoff} is the cutoff angle, at which shades appear.
- w is the table width.
- PP is the post to post spacing.
- GCR is the Ground Coverage Ratio, $GCR = w/PP$.

If the true tracking tilt angle obtained using equation (2.4) is smaller than the cutoff obtained with equation (2.6), then the back tracking angle is equal to the true tracking angle (because the true tracking angle does not produce shading, thus it is the optimal angle).

If the true tracking angle does exceed the cutoff angle, then a new tilt angle which does not produce shading must be computed. In order to do this, it is assumed that the selected tilt will give a shadow such that its projection on the ground will be equal to the post to post spacing, as shown in Figure 2.5 (b).

Therefore the backtracking tilt will be the angle which gives the best possible angle of incidence without producing any row to row shading. It is calculated using equation (2.7).

$$\beta_{\text{bck}} = 180 - \alpha_{\text{sun}} - \sin^{-1} \left(\frac{1}{GCR} \cdot \sin(\alpha_{\text{sun}}) \right) \quad (2.7)$$

Where:

- β_{bck} is the backtracking tilt angle.
- α_{sun} is the angle between the sun rays projected on a vertical plane normal to the plane of array and the horizontal, shown in Figure 2.4 (a) and computed using equation (2.5).
- GCR is the Ground Coverage Ratio, $GCR = w/PP$.

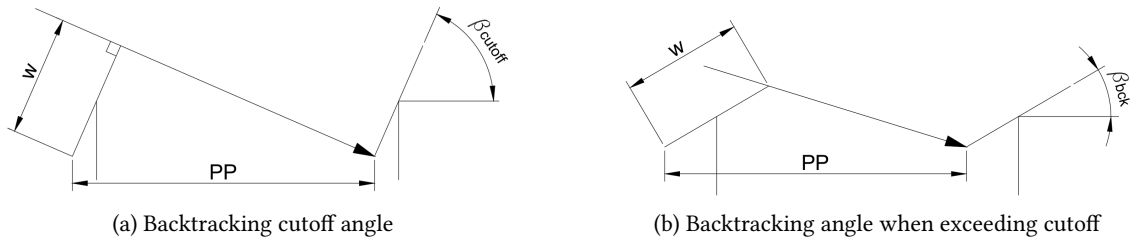


Figure 2.5: Backtracking angle

Chapter 3

Irradiance transposition to the tilted plane of array

The irradiance values taken as inputs are values for irradiance on a horizontal surface. The irradiance seen by a tilted surface will be different, given the cosine effects and different view factors for the diffuse and ground reflected components.

Thus the beam and diffuse components must be transposed to the plane of array, and the ground reflected components must be calculated and transposed (usually done in a single step).

3.1 Transposition of the beam component

The transposition of the beam horizontal irradiance to a tilted plane is a simple calculation, dependent on the angle of incidence on the surface and the sun zenith [5].

The beam irradiance on the plane of array is computed using equation (3.1), which first transposes the *BHI* to *DNI* (Direct normal irradiance), and then applies the cosine effect which is a consequence of the angle of incidence. The *DNI* can be computed separately using equation (3.2).

$$B_{\text{POA}} = BHI \cdot \frac{\cos \theta_{\text{inc}}}{\cos \theta_z} \quad (3.1)$$

Where:

- B_{POA} is the beam irradiance transposed to the plane of array.
- BHI is the beam horizontal irradiance component.
- θ_{inc} is the incidence angle of the sun rays on the plane of array, calculated according to Section 2.2.
- θ_z is the sun zenith angle.

$$DNI = \frac{BHI}{\cos \theta_z} \quad (3.2)$$

Where:

- DNI is the direct normal irradiance.

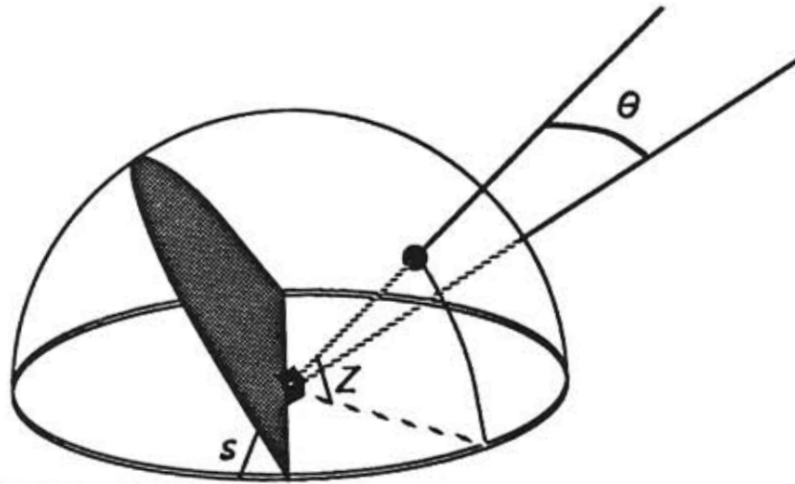


Figure 3.1: The sky representation used in the simplified Perez model [9]

- BHI is the beam horizontal irradiance component.
- θ_z is the sun zenith angle.

3.2 Transposition of the diffuse component

The model used to perform the transposition of the diffuse component to the plane of array is the simplified Perez model presented in [8], which complies with both hourly and sub-hourly intervals. It is an anisotropic diffuse model, which represents the sky as an isotropic background with circumsolar and horizon effects superimposed on it. The circumsolar effect is a point source of irradiance at the sun's position, and the horizon effect is a linear source at the horizon.

This representation of the sky is shown in Figure 3.1, where the sun is represented as point in the surface of the semi sphere (isotropic background), and the horizon band is represented as a line on the ground.

The diffuse irradiance on the tilted plane is equation (3.3). The first term of this equation, $1 - F_1$, is the fraction of isotropic irradiance, which is emitted by the isotropic background. The second term F_1 a coefficient for the circumsolar anisotropy, and the third term expresses the horizon/zenith anisotropy [8].

$$D_{POA} = DHI \cdot \left((1 - F_1) \cdot \frac{1 + \cos \beta}{2} + F_1 \cdot \frac{a}{b} + F_2 \cdot \sin \beta \right) \quad (3.3)$$

Where:

- D_{POA} is the diffuse irradiance transposed to the POA.
- DHI is the diffuse horizontal irradiance component.
- F_1 is the coefficient expressing the circumsolar anisotropy, calculated using equation (3.6).
- β Surface inclination angle (surface tilt).
- a is a term computed using equation (3.4), a function of the angle of incidence on the plane of array.
- b is a term computed using equation (3.5), a function of the sun zenith angle.

- F_2 is the coefficient expressing the horizon/zenith anisotropy, calculated using equation (3.7).

The a and b coefficients are calculated with equations (3.4) and (3.5) respectively.

$$a = \max(0, \cos \theta_{\text{inc}}) \quad (3.4)$$

Where:

- a is a term used in equation (3.3).
- θ_{inc} is the incidence angle of the sun rays on the plane of array.

$$b = \max(0.087, \cos \theta_z) \quad (3.5)$$

Where:

- b is a term used in equation (3.3).
- θ_z is the sun zenith angle.

The model coefficients F_1 and F_2 were obtained empirically by the authors of [8] using data from 9 sites. The variations of these coefficients were found to be consistent from site to site [9], and the choice of any particular set of coefficient values is not critical according to Perez et al. [8].

The F_1 and F_2 coefficients are computed using equations (3.6) and (3.7) respectively.

$$F_1 = F_{11} + F_{12} \cdot \Delta + F_{13} \cdot \theta_z \quad (3.6)$$

Where:

- F_1 is the coefficient expressing the circumsolar anisotropy.
- F_{11} is a coefficient interpolated from Table 3.1, using equation to calculate the bin to be used.
- F_{12} is a coefficient interpolated from Table 3.1, using equation to calculate the bin to be used.
- Δ_{sky} is the sky's brightness, computed with equation (3.8).
- F_{13} is a coefficient interpolated from Table 3.1, using equation to calculate the bin to be used.
- θ_z is the sun zenith angle, in radians.

$$F_2 = F_{21} + F_{22} \cdot \Delta + F_{23} \cdot \theta_z \quad (3.7)$$

Where:

- F_2 is the coefficient expressing the horizon/zenith anisotropy.
- F_{21} is a coefficient interpolated from Table 3.1, using equation to calculate the bin to be used.
- F_{22} is a coefficient interpolated from Table 3.1, using equation to calculate the bin to be used.
- Δ_{sky} is the sky's brightness, computed with equation (3.8)
- F_{23} is a coefficient interpolated from Table 3.1, using equation to calculate the bin to be used.

ϵ_{sky} category (Bin)	F_{11}	F_{12}	F_{13}	F_{21}	F_{22}	F_{23}
1	-0.008	0.588	-0.062	-0.06	0.072	-0.022
2	0.13	0.683	-0.151	-0.019	0.066	-0.029
3	0.33	0.487	-0.221	0.055	-0.064	-0.026
4	0.568	0.187	-0.295	0.109	-0.152	-0.014
5	0.873	-0.392	-0.362	0.226	-0.462	0.001
6	1.132	-1.237	-0.412	0.288	-0.823	0.056
7	1.06	-1.6	-0.359	0.264	-1.127	0.131
8	0.678	-0.327	-0.25	0.156	-1.377	0.251

Table 3.1: Perez model coefficients for irradiance [8]

- θ_z is the sun zenith angle, in radians.

The sky brightness is calculated using equation (3.8)

$$\Delta_{\text{sky}} = DHI \cdot \frac{AM}{I_0} \tag{3.8}$$

Where:

- Δ_{sky} is the sky's brightness.
- DHI is the diffuse horizontal irradiance component.
- AM is the relative optical air mass, obtained using the SOLPOS library described in Chapter 2.
- I_0 is the extraterrestrial irradiance at the top of the atmosphere, obtained using the SOLPOS library described in Chapter 2.

The sub coefficients of F_1 and F_2 are obtained from Table 3.1. The bin value to be used is obtained from Table 3.2, and it is a function of ϵ_{sky} , the sky's clearness, calculated using equation (3.9).

This bin value represents how clear the sky is for any given value of ϵ_{sky} . A value of 1 would be equivalent to overcast skies, and a value of 8 would represent clear skies.

$$\epsilon_{\text{sky}} = \frac{\frac{DHI + DNI}{DNI} + \kappa \cdot \theta_z^3}{1 + \kappa \cdot \theta_z^3} \tag{3.9}$$

Where:

- ϵ_{sky} is the sky's clearness.
- DHI is the diffuse horizontal irradiance component.
- DNI is the direct normal irradiance, computed using (3.2).
- κ is a constant which has a value of 1.041 for a θ_z in radians.
- θ_z is the sun zenith angle, in radians.

3.3 Calculation and transposition of the ground-reflected component

To calculate the ground-reflected irradiance, three hypothesis are made [10]:

ϵ_{sky} category	ϵ_{sky} lower bound	ϵ_{sky} upper bound
1	1	1.065
2	1.065	1.23
3	1.23	1.5
4	1.5	1.95
5	1.95	2.8
6	2.8	4.5
7	4.5	6.2
8	6.2	–

Table 3.2: Perez model sky clearness categories [8]

- The ground reflects irradiance isotropically (that is, it behaves as a lambertian surface).
- The ground is homogeneously illuminated by the corresponding irradiance component (shades are not applied at this stage).
- All reflected irradiance comes from the ground, no additional surfaces are considered for this calculation.

These hypothesis are reflected in the formulation of equation (3.10), which is used to compute the ground-reflected irradiance which reaches the tilted plane of array.

The first and second hypothesis translate into the first part of equation (3.10), $\rho \cdot GHI$. The albedo value ρ is the blue-sky broadband albedo. The calculation could be improved by differentiating between the black-sky albedo (directional-hemispherical reflectance) and the white-sky albedo (bi-hemispherical reflectance) if data is available on the value of each. If the values of those two components are available, then the contribution of the beam horizontal irradiance (black-sky albedo) and the diffuse horizontal irradiance (white-sky albedo) can be calculated separately. The contribution of each component would then be added up to calculate the total isotropic reflected irradiance.

The second part of equation (3.10) is the view factor of a tilted plane to the ground.

$$GR_{\text{POA}} = \rho \cdot GHI \cdot \frac{1}{2} (1 - \cos \beta) \tag{3.10}$$

Where:

- GR_{POA} is the ground reflected irradiance transposed to the plane of array.
- ρ is the albedo coefficient (blue-sky albedo if using the GHI). A value of 0.2 is recommended if no site data is available. Recommended values for different surface types can be found in [10].
- GHI is the global horizontal irradiance.
- β is the surface inclination angle (surface tilt).

The value of the albedo coefficient should be chosen carefully, specially if simulating bifacial modules. Satellite data is available with world coverage (two examples are [11] and [12]). However, satellite data presents two challenges when used for PV performance modelling:

- Spatial resolution may not be high enough to accurately model certain locations, specially for smaller photovoltaic plants.

- The construction of the PV plant alters the characteristics of the ground below the photovoltaic modules, due to ground clearing and other civil works. Although over time the ground may return to a state similar to its natural condition before construction, the albedo value will be different from measurements before construction, specially in the first years of operation.

These challenges result in the recommendation to use on-site measured data when possible.

Another concern is temporal resolution. An increase in accuracy can be obtained using monthly-resolution albedo data. If so, seasonal effects due to rain and moisture can be taken into account. Moisture presence changes the albedo values significantly [13].

Finally, although the surface albedo is strongly dependent on the spectral distribution of the light being reflected [14], this effect is not taken into account because of the lack of information regarding the spectral distribution of light in the hourly or sub-hourly interval data, and the difficulties associated with obtaining albedo values segregated by wavelength range (MODIS satellite data is available raw in such a form [11]).

3.4 Transposition to the back-face for bifacial simulation

The methodology for calculating the back-face effective irradiance in bifacial simulations does not strictly require calculating the irradiance perceived by the back-face of the plane of array, as will be explained in Chapter 5. This does not mean the transposition does not occur, the transposition takes place implicitly when applying the configuration factors from the ground to the back-face.

However, it is useful to calculate the irradiance on the backface to keep track of the losses due to the shades cast on the ground by the structures. By comparing the results of the ideal irradiance transposition with the results of the calculations described in Chapter 5, it is possible to extrapolate the value of the loss due to shades on the ground.

The beam component contribution can be calculated using equation (3.1). Using the incidence angle on the back-face, calculated as described in Section 2.2, the resulting beam contribution on the back-face is obtained. If the incidence angle on the back-face is greater than 90 degrees, then the sun is in front of the plane of array, and the beam contribution to the back-face is zero.

Similarly, the diffuse component contribution can be calculated using the Perez model as described in Section 3.2. When computing the a coefficient using equation (3.4), the back-face incidence angle must be used. The β tilt angle used in (3.3) must be flipped, obtaining a β' value calculated as $180 - \beta$.

Finally, the same β' tilt angle can be used in equation (3.10) to calculate the contribution of the ground reflected irradiance.

A diagram with all the contributions to the plane of the array is shown in Figure 3.2. If the direct sunlight beam was behind the plane of array, then it would be added up to the back-face irradiance instead of the front face.

An additional result is required for the calculation described in Chapter 5, the segregation of diffuse components on the ground. It is necessary to apply the Perez model to the horizontal plane to calculate the contribution of each Perez model component (vault, circumsolar and horizon).

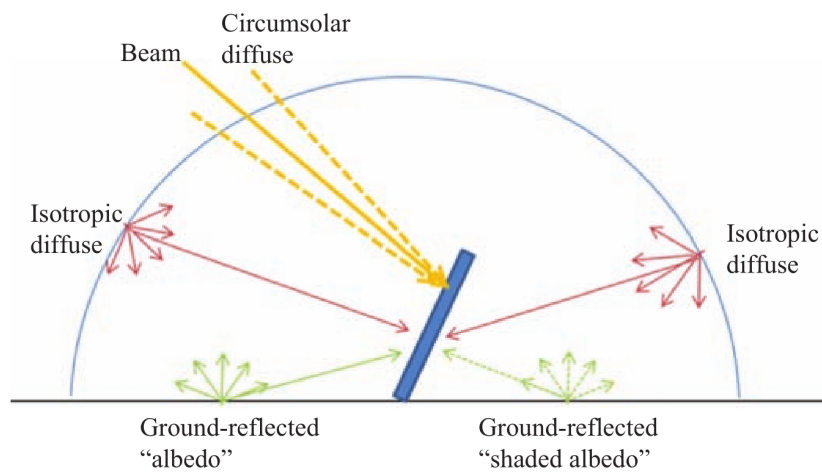


Figure 3.2: Contributions to the front and back-face of the plane of array [5]

To segregate the diffuse horizontal irradiance in its components using the Perez model, the β tilt angle is set to zero. This nullifies the horizon component $F_2 \cdot \sin \beta$, and leaves the circumsolar and vault components.

Chapter 4

Front-face effective irradiance

The losses due to shading, IAM (Incidence Angle Modifier) and soiling are the last losses to be computed and applied before the solar energy is converted to electrical energy by the photovoltaic module. The shading losses are among the most complicated calculations to be performed by the program, and could potentially take the most computation time out of all the steps unless a simplified and optimized approach is taken.

In this methodology, the approach is to model the photovoltaic plant as a number of tilted planes set above a completely flat ground. Additionally, the planes (or rows, as they may be called) are considered to be of infinite length for the calculation of the diffuse and ground reflected components.

The edge effects are taken into account in a simplified manner for the beam component, using an idealized DC field described in Section 4.7. These simplifications allow for both reducing the complexity of the equations involved and the computation time.

4.1 Beam component shading

The beam component will usually be shaded during the first and last hours of the day, given the usual design rules used when calculating the post to post spacing.

The sun rays can be blocked by two differentiated geometrical objects:

- The next (adjacent) row in the field. This will produce a partial shade on the shaded row.
- The horizon, which will block the beam component for the entire field.

The shading produced by a row upon another is potentially the most penalizing effect on the production a photovoltaic power plant, as will be explained in Subsection 7.2.2. However, it is usually mitigated by the use of simple design rules and completely eliminated in tracking systems using the backtracking algorithm.

The horizon shading is usually less penalizing, as the horizon is low in most locations and it would anyway block the sun beam components in the earlier and later hours the day, when the angle of incidence is low. The horizon shading factor can only take the values 0 and 1, as it can

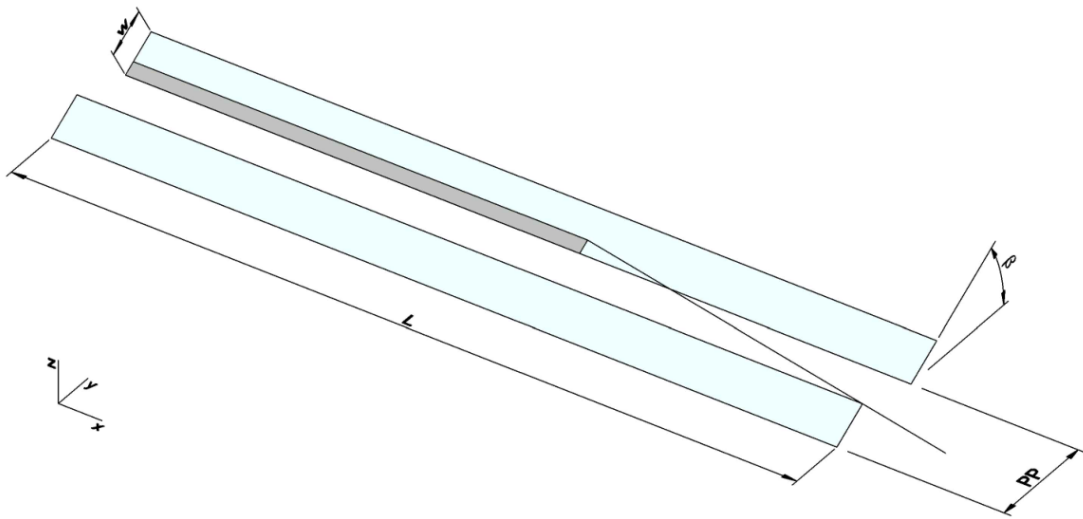


Figure 4.1: Beam component shading from one row to another

either block the entire beam component or not. It is defined in equation (4.1).

$$F_{B, \text{hor}}(\alpha, \gamma) = \begin{cases} 0 & \text{if } \alpha < \alpha_{\text{hor}}(\gamma) \\ 1 & \text{otherwise} \end{cases} \quad (4.1)$$

Where:

- $F_{B, \text{hor}}(\alpha, \gamma)$ is the horizon shading factor on the beam component. It is dependent on the sun elevation (α) and azimuth (γ) angles.
- $\alpha_{\text{hor}}(\gamma)$ is the elevation of the horizon for a given azimuth (γ) angle.

4.1.1 Calculation of shaded area

The calculation of the shading area is geometrical, and can be greatly optimized so that it is computed quickly. The shades are dependent on the position of the sun, so they must be computed on a per-interval basis to achieve the maximum possible accuracy. The simplifications assumed in this methodology are:

- The field on which the rows are is completely flat.
- The distance between one row and the next one is the same for all rows.
- The shade from one row to the next is perfectly rectangular.

This simplifications allow to compute the shades for only one row, as they will apply equally to the whole field. The rectangular shades mean only that only the intersecting point of a ray passing the corner of the next row and the plane of array needs to be calculated, as shown in Figure 4.1.

The first step of the process is to compute the cast shadow length on the ground (length along the Figure 4.1 y axis). The angle calculated in Subsection 2.3.1 can be used, because as explained in Subsection 2.3.2, the angle is the complimentary to the sun elevation projected on the vertical plane perpendicular to the plane of array (yz plane in Figure 4.1).

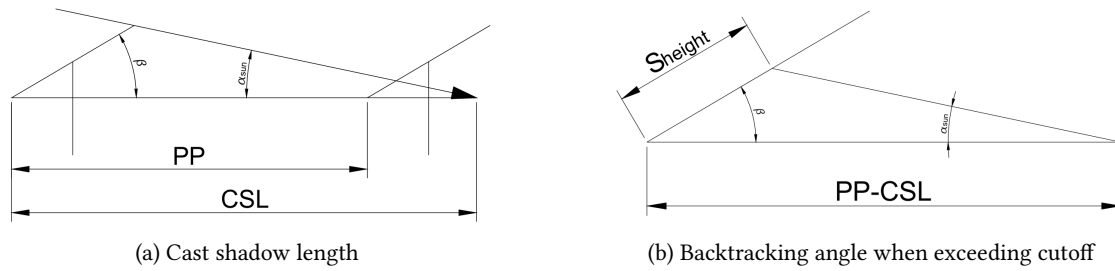


Figure 4.2: Beam shadow projections on the perpendicular vertical plane

The cast shadow length can be calculated using equation (4.2), by solving the triangle shown in Figure 4.2 (a).

$$CSL = w \cdot \frac{\sin(180 - \beta - \alpha_{sun})}{\sin \alpha_{sun}} \quad (4.2)$$

Where:

- CSL is the cast shadow length on ground (y axis on Figure 4.1).
- w is the table width.
- β is the plane tilt.
- α_{sun} is the sun elevation projected on the yz plane of Figure 4.1, as shown in Figure 2.4.

If the cast shadow length computed using equation (4.2) is greater than the post to post distance, then there is row to row shading. In this case, the length of the shadow when projected must be computed, as well as the x axis (Figure 4.1) shaded length.

The projected shadow height can be calculated using equation (4.3), solving the triangle shown in Figure 4.2 (b).

$$S_{height} = \sin \alpha_{sun} \cdot \frac{PP - CSL}{\sin(180 - \beta - \alpha_{sun})} \quad (4.3)$$

Where:

- S_{height} is the shadow height when projected on the plane of array.
- α_{sun} is the sun elevation projected on the yz plane of Figure 4.1, as shown in Figure 2.4.
- PP is the post to post distance.
- CSL is the cast shadow length on ground (y axis on Figure 4.1).
- β is the plane tilt.

The un-shaded length along the Figure 4.1 x axis can be calculated using (4.4), by solving the problem shown in Figure 4.3. The azimuth angles are defined according to Subsection 2.1.1.

$$d_{unshaded} = \tan \gamma_R \cdot (PP + (S_{height} - w) \cdot \cos \beta) \quad (4.4)$$

Where:

- $d_{unshaded}$ is the unshaded distance along the Figure 4.1 x axis, shown in Figure 4.3.
- PP is the post to post distance.
- S_{height} is the shadow height when projected on the plane of array, calculated using equation (4.3) (in Figure 4.3 $s_y = S_{height} \cdot \cos \beta$).

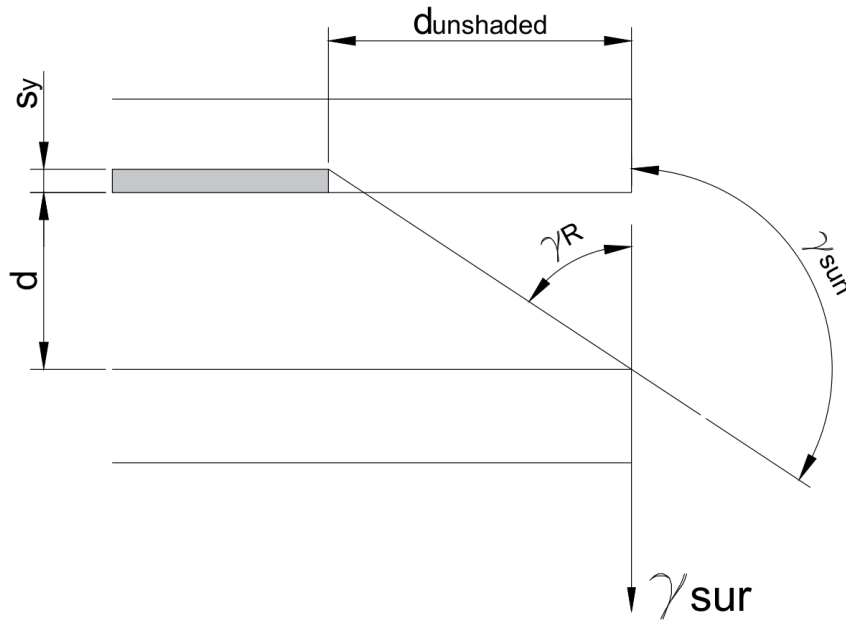


Figure 4.3: Unshaded length along the east-west axis

- w is the table width, shown in Figure 4.1.
- β is the plane tilt.
- γ_R is the angular difference $\gamma_{sur} - \gamma_{sun}$, where γ_{sur} is the surface azimuth view angle defined according to Subsection 2.2.1 and γ_{sun} is the sun azimuth angle defined according to Subsection 2.1.1.

When both shadow dimensions have been calculated, it is possible to compute the ratio of shaded area to total table area and the number of modules shaded per table.

The shadow area can be calculated using (4.5).

$$A_{shaded} = s_{height} \cdot s_{len} = s_{height} \cdot (L - d_{unshaded}) \quad (4.5)$$

Where:

- A_{shaded} is the shaded area inside the table.
- s_{height} is the shadow height when projected on the plane of array, calculated using equation (4.3).
- s_{len} is the shadow length along the Figure 4.1 x axis, which can be calculated using the table length and the unshaded length.
- L is the table length, shown in Figure 4.1, calculated as explained in Section 4.7.
- $d_{unshaded}$ is the unshaded distance along the Figure 4.1 x axis, shown in Figure 4.3.

The shaded area factor can be calculated using (4.6).

$$F_{sh\ area} = \frac{A_{shaded}}{A_{table}} = \frac{A_{shaded}}{L \cdot w} \quad (4.6)$$

Where:

- $F_{\text{sh area}}$ is the shaded area factor.
- A_{shaded} is the shaded area inside the table.
- A_{table} is total table area.
- L is the table length, shown in Figure 4.1, calculated as explained in Section 4.7.
- w is the table width, shown in Figure 4.1.

With the shadow dimensions, it is also possible to calculate the number of strings which have any module shaded. This can be calculated knowing the distribution of strings in any given table. The number of shaded strings will be needed for the shading effects described in Subsection 7.2.2.

4.2 Diffuse component shading

The diffuse component of the global horizontal irradiance can account to up 25 % of the available irradiance in midday, and much more in the early and later hours of the day. Furthermore, while the beam component is only shaded during the sunrise and sunset (in well-designed plants), the diffuse component is shaded throughout the whole day. Thus the calculation of the diffuse shading factor will have a constant influence on the photovoltaic plant production.

The calculation of the diffuse shading factor is a complex and time consuming process. The main two assumptions driving the calculation are:

- The diffuse irradiance is isotropic. While the transposition model described in Section 3.2 is anisotropic, for the purpose of computing a shading factor the isotropic assumption is sufficient.
- The rows have infinite length (that is, the L dimension in Figure 4.1 is infinite). This allows for simplified equations and better performance, while having a negligible impact in accuracy for the usual lengths and post to post distance values used in the photovoltaic industry.

The diffuse shading factor will be the flux (rate of energy flow through unit area) across the area any panel can view of the sky, divided by the maximum area the panel could view if it was completely unobstructed (either by the horizon or by adjacent rows). Given that the flux is calculated in polar coordinates, a polar system is defined in Figure 4.4, which will be used in this section and in Section 4.3.

In Figure 4.4, the azimuth coordinate γ is defined as in Subsection 2.1.1, and the zenith coordinate θ is defined equally to the θ_{sun} (sun zenith).

The general equation to calculate the flux of energy through any plane v [5] is shown in equation (4.7). In this equation, the $\cos \theta$ reflects the cosine effect on the angle of incidence. Since equation (4.7) is formulated for a horizontal plane, the angle of incidence on the plane is equal to the zenith. If the plane was tilted, the angle would have to be substituted by the actual angle of incidence, calculated using equation (2.3). The $\sin \theta$ reflects the varying area of a slice of the sphere, where the lower the zenith angle is, the lower the slice area is, for equal azimuth angles.

$$G_v = \int_0^{2\pi} \int_0^\pi I_v \cdot \cos \theta \cdot \sin \theta \, d\theta \, d\gamma \quad (4.7)$$

Where:

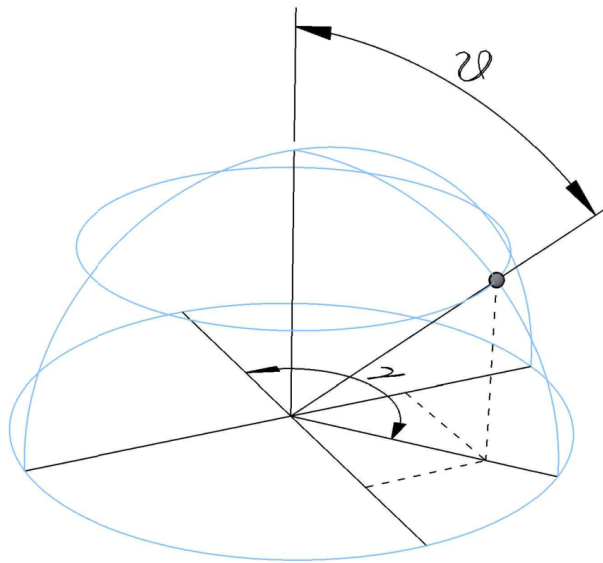


Figure 4.4: Polar coordinate system

- G_v is the energy flux through the horizontal plane.
- I_v is the flux intensity of the isotropic radiation.
- θ is the zenith angle.
- γ is the azimuth angle.

In order to use equation (4.7), the integration limits must be computed for the geometrical problem. The integration limits will contain the information pertaining the system dimensions, as well as the incidence angle.

A problem arises due to the need to separate the influence of the horizon and the near shadings effect on the diffuse irradiance. Because they are superimposed areas on the sphere (that is, a near object can't block irradiance which has already been blocked by a higher obstacle in the horizon), they cannot be easily separated. To overcome this issue, a partial shading factor is computed using equation (4.8), which only takes into account the effect of the horizon. This factor is used only to compute a far-shadings available irradiance, which is itself used only to compute losses.

The factor actually used to compute the effective diffuse irradiance will be calculated in equation (4.9), which uses as its integration area the superposition of the self row, horizon and near objects. The area visible with no obstructions is the area left after applying the obstruction due to the tilted plane where the point of origin is situated. In Figure 4.6, these obstructions are shown, and a detailed explanation is given in Subsection 4.2.1.

$$F_{sh\ diff, hor} = \frac{G_{hor}}{G_{vis}} \tag{4.8}$$

Where:

- $F_{sh\ diff, hor}$ is the horizon diffuse shading factor.
- G_{hor} is the flux left after applying the horizon obstruction (and the area obstructed by the row itself), calculated using equation (4.14).

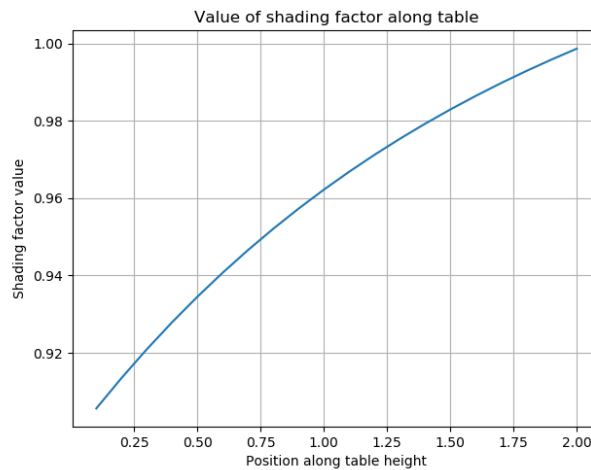


Figure 4.5: Diffuse shading factor along table height

- G_{vis} is the flux visible with no obstruction (only the area obstructed by the row itself), calculated using equation (4.12).

$$F_{sh\ diff} = \frac{G_{near}}{G_{vis}} \tag{4.9}$$

Where:

- $F_{sh\ diff}$ is the diffuse shading factor.
- G_{near} is the flux left after applying the self-row, next row and horizon obstructions, calculated using equation (4.13).
- G_{vis} is the flux visible with no obstruction (only the area obstructed by the row itself), calculated using equation (4.12).

It must be noted that the shading factor will not be the same at the bottom of a row (lowest point) than at the top. The effect of the next row will be null on the top, and will reach its maximum value when at the bottom. This may or may not be important depending on the site horizon. To compute an accurate shading factor, a mean factor is computed by integrating the shading factor along the table from bottom to top, at the middle of its length.

In Figure 4.5, it is shown that the diffuse shading factor is not linear along the table height.

When the structure is a tracker, the diffuse shading factor is computed for an array of plane tilt values comprised between the maximum and minimum tilts specified by the manufacturer. During the calculation of each interval's effective diffuse irradiance, the diffuse shading factor is interpolated from this list of previously computed factors using the actual plane tilt of the interval.

4.2.1 Integration limits

In Figure 4.6, the obstructions to be applied when computing the vision factors are shown. The obstructions are the row where the origin point is situated, the next adjacent row, and the horizon. In Figure 4.6 the self row is shown as a black line behind the origin point, the next row as

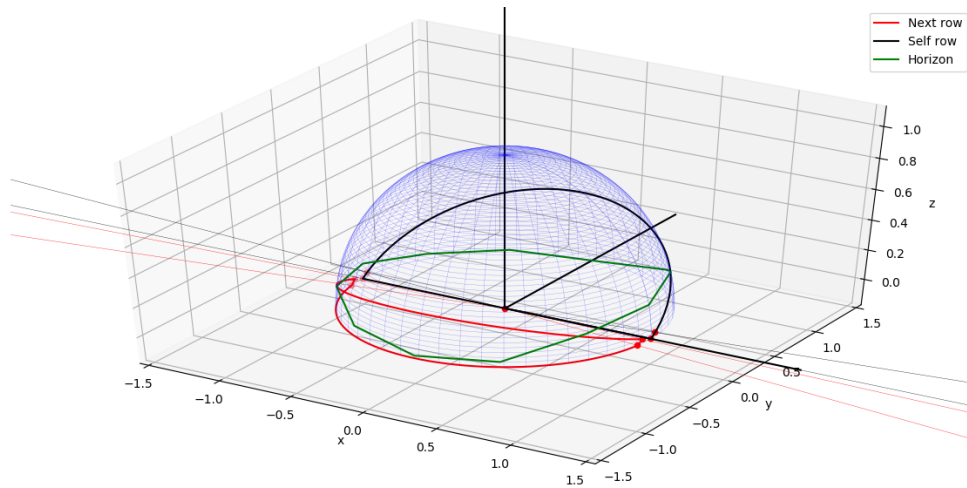


Figure 4.6: Diffuse irradiance obstructions

a red line in front of it, and the horizon as a green line which spans the whole circumference of the sphere.

In Figure 4.7, the rows are shown in a zoomed-out view.

The self obstruction view angle is computed using equation (4.10). A drawing of the problem is shown in Figure 4.8. The self obstruction is due to the plane tilt, which is already taken into account by the Perez diffuse irradiance transposition model detailed in Section 3.2. Thus the self obstruction integration limit will define the available area if no other obstructions were present (that is, the ideal case). The equation (4.10) is formulated using the infinite rows assumption.

$$\theta_{\text{self}}(\gamma_{\text{view}}) = 90 - \tan^{-1} \left(\frac{w_{\text{al}} \cdot \sin \beta}{\frac{w_{\text{al}} \cdot \cos \beta}{\cos \gamma_{\text{R}}}} \right) = 90 - \tan^{-1} \left(\frac{\tan \beta}{\cos \gamma_{\text{R}}} \right) \quad (4.10)$$

Where:

- θ_{self} is the zenith angle obstructed by the self-row.
- γ_{view} is the azimuth view angle for which the self-row zenith obstruction angle is being evaluated.
- w_{al} is the distance along the table width.
- β is the plane tilt.
- γ_{R} is the difference between the angle of a vector normal to the back of the plane of array, and the azimuth being evaluated: $\gamma_{\text{R}} = \gamma_{\text{sur, back}} - \gamma_{\text{view}}$.

The value of θ_{self} should be 90 degrees if γ_{R} is greater than 90 degrees (the azimuth view angle is in front of the plane of array), so that the only obstruction in this case is the ground.

The obstruction view angle due to the next row can be calculated using equation (4.11). The problem is shown in Figure 4.9, with finite rows for easier understanding. The equation (4.11) is

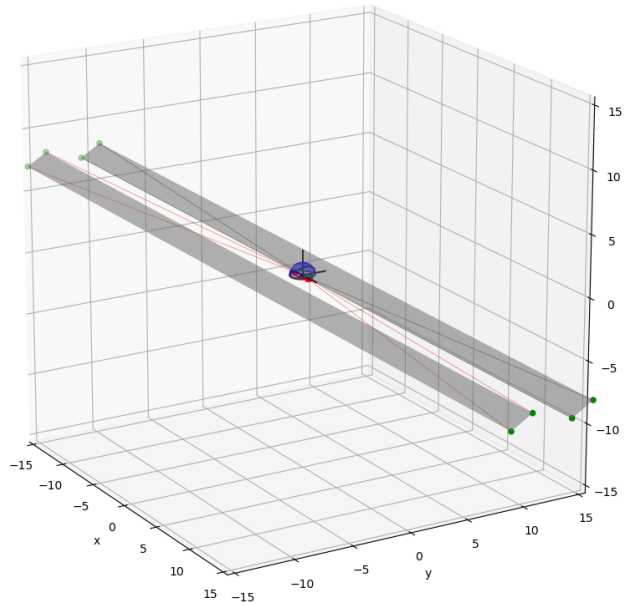


Figure 4.7: Diffuse irradiance obstructions, including obstructing rows

formulated using the infinite rows assumption.

$$\theta_{\text{next}}(\gamma_{\text{view}}) = 90 - \tan^{-1} \left(\frac{(w - w_{\text{al}}) \cdot \sin \beta}{\frac{PP - (w - w_{\text{al}}) \cdot \cos \beta}{\cos \gamma_{\text{R}}}} \right) = 90 - \tan^{-1} \left(\frac{(w - w_{\text{al}}) \cdot \sin \beta \cdot \cos \gamma_{\text{R}}}{PP - (w - w_{\text{al}}) \cdot \cos \beta} \right) \quad (4.11)$$

Where:

- θ_{next} is the zenith angle obstructed by the next row.
- γ_{view} is the azimuth view angle for which the next row zenith obstruction angle is being evaluated.
- w is the table width.
- w_{al} is the distance along the table width.
- β is the plane tilt.
- PP is the post to post distance.
- γ_{R} is the difference between the angle of a vector normal to the plane of array, and the azimuth being evaluated: $\gamma_{\text{R}} = \gamma_{\text{sur}} - \gamma_{\text{view}}$.

The value of θ_{next} should be 90 degrees if γ_{R} is greater than 90 degrees (the azimuth view angle is behind the plane of array), so that the only obstruction in this case is the ground.

The self row and next row obstructions are shown in Figure 4.6 as the black and red lines respectively. It should be noted that the self row obstruction will reach a maximum value of β when the azimuth view angle equals the back of the row, and that both obstructions tend to zero when the view azimuth is parallel to the row axis.

The Figure 4.6 was generated using 72m rows, themselves shown in Figure 4.7. The length value chose is not uncommon in photovoltaic power plants, and it can be seen that the error in the next

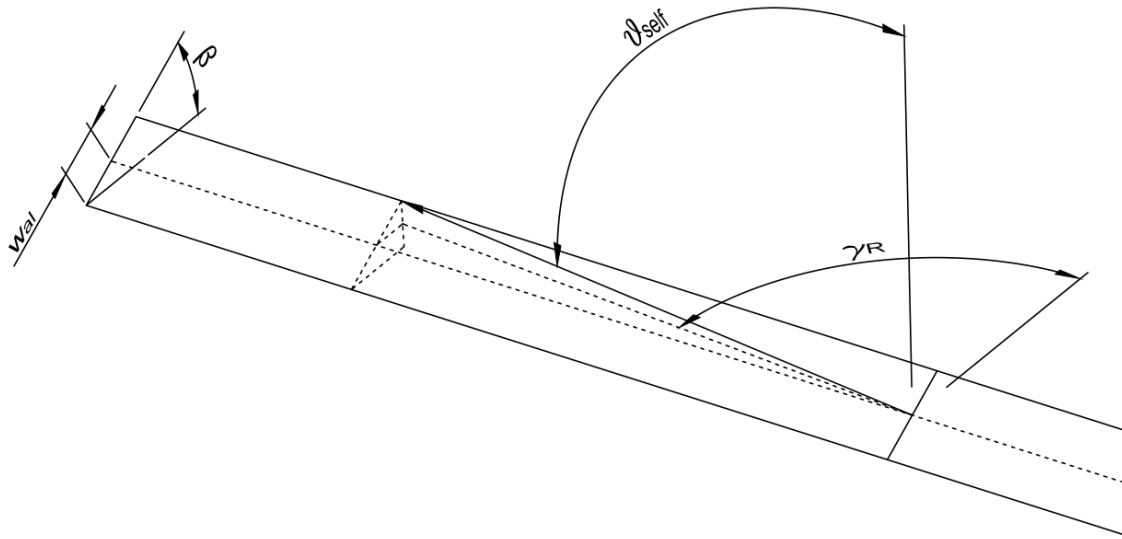


Figure 4.8: Obstructions caused by a row upon itself

row obstruction function only occurs when the azimuth view angle approaches the row axis, and is very low.

The next row elevation angle projected on the sphere surface shown in Figure 4.6 was not calculated using (4.11). Instead, a full 3D model was used to draw the figure.

The horizon is taken as a program input, and it is already presented as an array of azimuth values with their corresponding elevation values. These values can be used directly as obstruction angles to be taken into account when computing the integration limits. The values between available horizon points are interpolated linearly.

4.2.2 Formulation using the integration limits

With the integration limits defined in Subsection 4.2.1 it is now possible to compute the energy flux through the tilted plane after applying the obstructions. The equation (2.3) defined in Section 2.2 must be used to compute θ_{inc} , the angle of incidence on the tilted plane.

The flux intensity I_v is taken out of the equations, as it is constant for all values of θ and γ (isotropic assumption) and the results will be used in a factor. The resulting values of G are areas of visible sky, with weighting due to the angle of incidence.

The available area is calculated using equation (4.12).

$$G_{vis} = \int_0^{2\pi} \int_0^{\theta_{self}(\gamma)} \cos(\theta_{inc}(\theta, \gamma)) \cdot \sin \theta \, d\theta \, d\gamma \quad (4.12)$$

Where:

- G_{vis} is the area visible with no obstruction (only the area obstructed by the row itself).

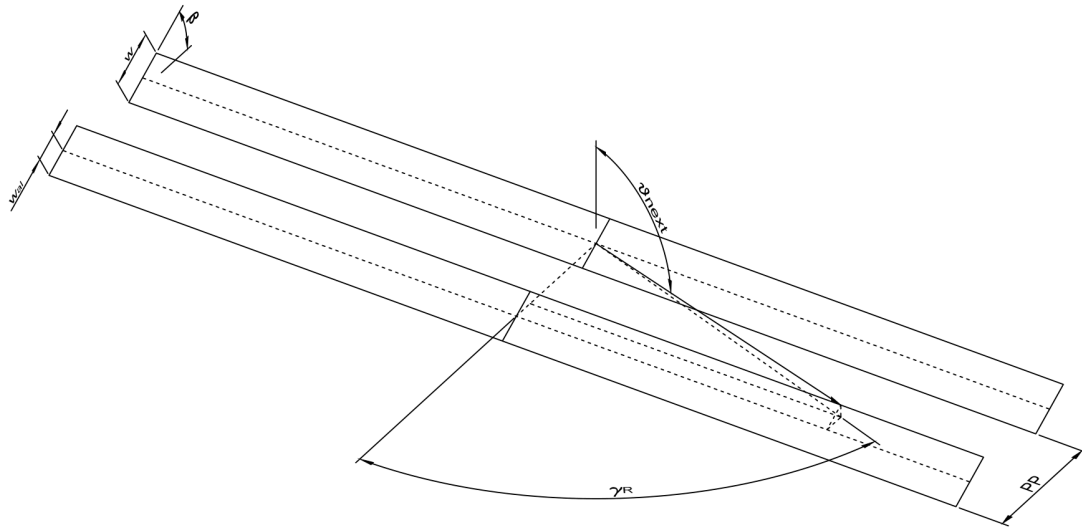


Figure 4.9: Obstructions caused by a row upon the next row

- θ_{self} is the zenith angle obstructed by the self-row. Whenever the γ value is in front of the row, it's value is 90 degrees, so that the integration area is a semi sphere obstructed by the self-row, as shown in Figure 4.6.
- θ is the zenith angle.
- γ is the azimuth angle.
- θ_{inc} is the angle of incidence on the tilted surface, calculated using equation (2.3).

The visible area after applying all obstructions is calculated with equation (4.13). The obstruction angle will be the minimum of the three obstruction angles (self-row, next row and horizon). The visible area can be calculated as a function of the position along the table width w_{al} , in order to integrate it's value along the whole table height.

$$G_{near} = \int_0^{2\pi} \int_0^{\min(\theta_{self}(\gamma), \theta_{next}(\gamma), \theta_{hor}(\gamma))} \cos(\theta_{inc}(\theta, \gamma)) \cdot \sin \theta \, d\theta \, d\gamma \quad (4.13)$$

Where:

- G_{near} is the area left after applying the self row, near and horizon obstructions.
- θ_{self} is the zenith angle obstructed by the self-row. Whenever the γ value is in front of the row, it's value is 90 degrees, so that the integration area is a semi sphere obstructed by the self-row, as shown in Figure 4.6.
- θ_{next} is the zenith angle obstructed by the next row. Whenever the γ value is behind the row, it's value is 90 degrees, so that the integration area is a semi sphere.
- θ_{hor} is the zenith angle obstructed by the horizon. It's value is interpolated linearly from the array of available horizon points.
- θ is the zenith angle.
- γ is the azimuth angle.
- θ_{inc} is the angle of incidence on the tilted surface, calculated using equation (2.3).

The visible area when only applying the horizon and the self row obstructions is calculated in the same way as the G_{near} , only removing the θ_{next} obstruction from the integration limits.

$$G_{\text{hor}} = \int_0^{2\pi} \int_0^{\min(\theta_{\text{self}}(\gamma), \theta_{\text{hor}}(\gamma))} \cos(\theta_{\text{inc}}(\theta, \gamma)) \cdot \sin \theta \, d\theta \, d\gamma \quad (4.14)$$

Where:

- G_{hor} is the area left after applying the self row and the horizon obstructions.
- θ_{self} is the zenith angle obstructed by the self-row. Whenever the γ value is in front of the row, it's value is 90 degrees, so that the integration area is a semi sphere obstructed by the self-row, as shown in Figure 4.6.
- θ_{hor} is the zenith angle obstructed by the horizon. It's value is interpolated linearly from the array of available horizon points.
- θ is the zenith angle.
- γ is the azimuth angle.
- θ_{inc} is the angle of incidence on the tilted surface, calculated using equation (2.3).

4.3 Ground-reflected component shading

The ground-reflected irradiance perceived by the front face can be calculated using the methodology described in Chapter 5. The model was developed for bifacial simulation, but is very suitable for calculating the front face irradiance accurately with a small simulation time penalty.

The reference system described in Section 5.1 holds for the front face. The α value will range from 180 to 360 degrees.

The ground reflected irradiance can be calculated using equation (5.13), evaluated for α values ranging from $360 - \beta$ to 360 degrees. There will only be one near vision obstacle, which is the structure directly in front of the one in evaluation.

The pertinent implementations of the equations described in Chapter 5 must therefore be programmed in such a way that they are safe to use when the α value is greater than 180 degrees.

The benefits of using an accurate model for the ground reflected irradiance far outweigh the simulation time penalty. The near shading effects can be evaluated with better precision, which is important because in well-designed systems (eg. systems with a sufficient pitch and appropriate tilt) the near shading loss is dominated by the ground reflected component loss and the diffuse component loss.

4.4 Incidence angle modifier loss

The incidence angle modifier is the ratio of the transmittance-absorptance product at a given incidence angle to the transmittance-absorptance product at normal incidence angle [5].

In this methodology, the IAM loss will be calculated using one of the three models described in Subsection 4.4.1, Subsection 4.4.2 or Subsection 4.5.1.

The application of the IAM loss on the beam component is straightforward. Using the angle of incidence for the sun rays on the plane of array, the IAM value is computed using (4.18). The beam component is multiplied by this value to obtain the effective irradiance after the IAM loss.

To compute the IAM loss on the diffuse and albedo components, however, a more complex approach must be taken. Since the IAM is dependent on the angle of incidence, it's effect won't be the same on the diffuse component if the most unfavorable angles (those which yield the highest angle of incidence) are blocked because of the plane tilt or other obstacles.

For the diffuse component shading, this effect is directly considered as the shades are integrated in a 3D scene. However, the ground reflected component, when calculated for either face of the plane of array, is evaluated in a 2D scene in a plane perpendicular to the axis of the rows, so a different approach is taken.

A method is proposed by Marion [15] to take this effect into account without needing to evaluate the scene in three dimensions.

To calculate the incidence angle modifier loss for the back face irradiance, the approach consists in evaluating the IAM loss in a plane which contains the viewing vector defined by the α value (see Figure 5.2), for a range of azimuth values. The IAM loss, corrected for the azimuth effect, will be for each α value the coefficient of the integral with the IAM function and the integral without it, as in equation (4.15).

The integral is described in equation (4.16). The process consists in, for each α value, evaluate azimuth values between 0 and 90 degrees (as the results will be simetrical to either side of the vertical plane). Each integration step uses as input an α value and an azimuth value. The pair defines a viewing direction, from which an incidence angle θ can be calculated using equation (4.17).

A profile corrected with this methodology is shown in Figure 4.10. The corrected profile can never reach a value of one (no loss), as the azimuth values always introduce a loss even if the α value yields an incidence angle of zero.

Therefore an IAM factor for the ground reflected component can be computed using the equations described in Section 4.2. This factor can be calculated using equation (4.15).

$$F_{IAM, \text{diff}} = \frac{G_{\text{vis, with IAM}}}{G_{\text{vis}}} \quad (4.15)$$

Where:

- $F_{IAM, \text{diff}}$ is the isotropic irradiance IAM factor used for the ground reflected components.
- $G_{\text{vis, with IAM}}$ is the flux visible with no obstruction (only the area obstructed by the row itself), including the IAM effect and calculated using equation (4.16).
- G_{vis} is the flux visible with no obstruction (only the area obstructed by the row itself), calculated using equation (4.12).

The integral part of the calculation is shown in equation (4.16).

$$G_{\text{vis, with IAM}} = \int_0^{2\pi} \int_0^{\theta_{\text{self}}(\gamma)} IAM(\theta_{\text{inc}}(\theta, \gamma)) \cdot \cos(\theta_{\text{inc}}(\theta, \gamma)) \cdot \sin \theta \, d\theta \, d\gamma \quad (4.16)$$

Where:

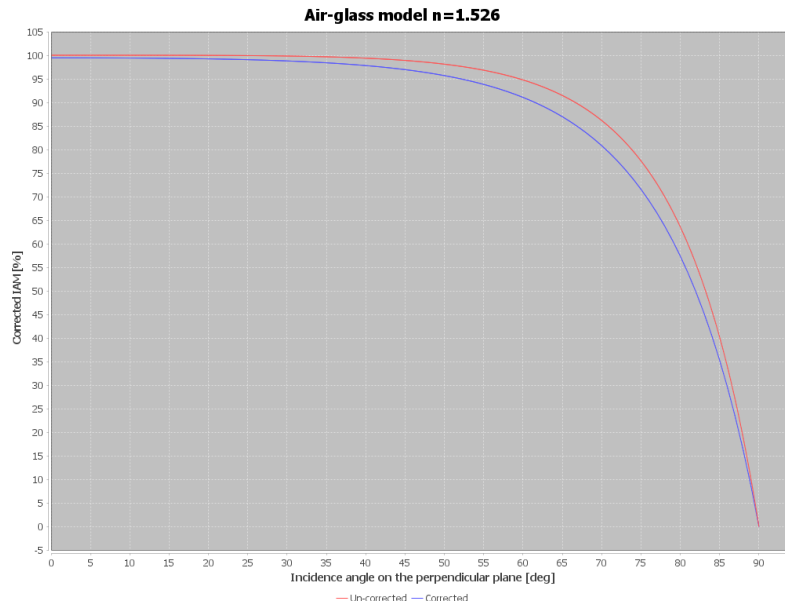


Figure 4.10: Air-glass model IAM profile, with profile corrected for the azimuth effect.

- $G_{vis, with IAM}$ is the flux visible with no obstruction (only the area obstructed by the row itself), including the IAM effect.
- θ_{self} is the zenith angle obstructed by the self-row. Whenever the γ value is in front of the row, it's value is 90 degrees, so that the integration area is a semi sphere obstructed by the self-row, as shown in Figure 4.6.
- $IAM(\theta_{inc})$ is the incidence angle modifier loss, calculated using one of the models described in this section.
- θ is the zenith angle.
- γ is the azimuth angle.
- θ_{inc} is the angle of incidence on the tilted surface, calculated using equation (2.3).

$$(\tan \theta)(\alpha, \gamma) = \frac{\sqrt{\sin^2(|90 - \alpha|) + \cos^2 \gamma}}{\cos(|90 - \alpha|)} \quad (4.17)$$

Where:

- θ is the incidence angle for which the incidence angle modifier loss will be evaluated.
- α is the angle on the vertical plane perpendicular to the table length, measured from the bottom of the table.
- γ is the azimuth value in evaluation.

4.4.1 ASHRAE incidence angle modifier model

The IAM definition used in this methodology was developed by Souka and Safwat [16], and is the model adopted by the ASHRAE. It is shown in equation (4.18). A plot of the values of the IAM given by this model is shown in Figure 4.11. In Figure 4.11 the IAM is floored at 0 to avoid unreasonable results if the incidence angle is too high.

$$IAM = 1 - b_0 \cdot \left(\frac{1}{\cos \theta_{inc}} - 1 \right) \quad (4.18)$$

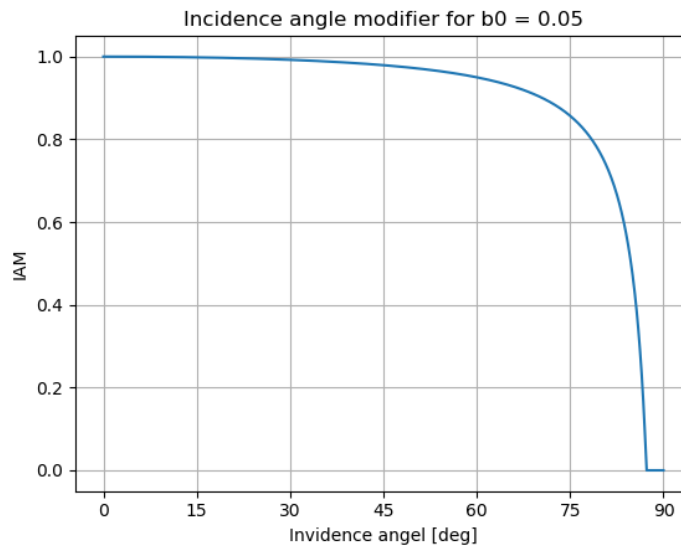


Figure 4.11: IAM calculated using the ASHRAE model

Where:

- IAM is the ASHRAE incidence angle modifier.
- b_0 is the incidence angle modifier coefficient. A. Mermoud [17] recommends a value of 0.05 as default value if no module-specific data is available.
- θ_{inc} is the angle of incidence on the tilted surface, calculated using equation (2.3).

4.4.2 Air-glass incidence angle modifier model

The air-glass model was recommended by Sjerps-Koomen, Alsema, and Turkenburg [18], after finding that the air-glass interface dominates the transmittance of light through the glass. The equations in this methodology for calculating the IAM loss using the air-glass model are found in the work by Marion [15].

The first step is to calculate the reflectance at normal incidence using equation (4.19).

$$r_0 = \left(\frac{n - 1}{n + 1} \right)^2 \tag{4.19}$$

Where:

- r_0 is the reflectance at normal incidence angles.
- n is the index of refraction for the cover material of the module. Common values are normal glass, with a value of $n = 1.526$, and $n = 1.3$ if an anti reflective coating is present. [15].

With the reflectance at normal incidence known, the angle of refraction at angles other than the normal can be calculated using equation (4.20). With the angle of refraction, the reflectance can be calculated using equation (4.21) for any angle of incidence.

$$\sin \theta_r = \frac{\sin \theta_{inc}}{2} \tag{4.20}$$

Where:

- θ_r is the angle of refraction.
- θ_{inc} is the angle of incidence on the module surface.
- n is the index of refraction for the cover material of the module.

$$r_\theta = \frac{1}{2} \cdot \left(\frac{\sin^2(\theta_r - \theta_{inc})}{\sin^2(\theta_r + \theta_{inc})} + \frac{\tan^2(\theta_r - \theta_{inc})}{\tan^2(\theta_r + \theta_{inc})} \right) \quad (4.21)$$

Where:

- r_θ is the reflectance at the angle of incidence θ_{inc} .
- θ_r is the angle of refraction.
- θ_{inc} is the angle of incidence on the module surface.

Finally, the incidence angle modifier loss is calculated using equation (4.22).

$$IAM_{agm} = \frac{1 - r_\theta}{1 - r_0} \quad (4.22)$$

Where:

- IAM_{agm} is the air-glass model incidence angle modifier loss.
- r_θ is the reflectance at the angle of incidence θ_{inc} , calculated using equation (4.21).
- r_0 is the reflectance at normal incidence angles, calculated using equation (4.19).

4.5 Soiling loss

The soiling loss encapsulates the irradiance deficit which appears whenever the photovoltaic module surface is not completely clean. This is very dependent on the site conditions and meteorology, and can be caused by dust, snow, or other depositions which may appear on the glass protecting the module.

A common way to model this losses is to reduce the global effective irradiance defined in Section 4.6 by a constant percentage (soiling factor) throughout the whole year. This soiling factor can only be determined accurately with knowledge about the site meteorology and presence of dust or other particles in the air. The global effective irradiance after applying the soiling loss is calculated using equation (4.23).

$$G_{eff, soil} = G_{eff} \cdot (1 - F_{soiling}) \quad (4.23)$$

Where:

- $G_{eff, soil}$ is the global effective irradiance after applying the soiling loss.
- G_{eff} is the global effective irradiance calculated using equation (4.26).
- $F_{soiling}$ is the soiling factor in parts per one.

4.5.1 Measured incidence angle modifier model

Photovoltaic module manufacturers usually include a measured IAM profile in the PAN files used by the PVSyst software [3].

The profile takes the form of a series of points, with each point being a two-value pair of incidence angle and the associated incidence angle modifier loss. For values other than the provided ones, cubic interpolation is used.

4.6 Effective irradiance on the plane of array

The effective irradiance at the plane of array is the irradiance that reaches the surface of the photovoltaic modules, after all shades are applied. It is separated in the three components which were calculated in Chapter 3.

The beam effective irradiance is calculated using equation (4.24).

$$B_{\text{eff}} = B_{\text{POA}} \cdot F_{\text{B, hor}} \cdot (1 - F_{\text{sh area}}) \cdot IAM_{\text{beam}} \quad (4.24)$$

Where:

- B_{eff} is the beam effective irradiance.
- B_{POA} is the beam irradiance transposed to the plane of array, calculated using equation (3.1).
- $F_{\text{B, hor}}$ is the horizon shading factor on the beam component, calculated using equation (4.1).
- $F_{\text{sh area}}$ is the shaded area factor, calculated using equation (4.6).
- IAM_{beam} is the incidence angle modifier, computed using equation (4.18) for the angle of incidence of the interval being calculated.

The diffuse effective irradiance is calculated using equation (4.25).

$$D_{\text{eff}} = D_{\text{POA}} \cdot F_{\text{sh diff}} \cdot F_{\text{IAM, diff}} \quad (4.25)$$

Where:

- D_{eff} is the diffuse effective irradiance.
- D_{POA} is the diffuse irradiance transposed to the plane of array, calculated using equation (3.3).
- $F_{\text{sh diff}}$ is the diffuse shading factor, calculated using equation (4.9).
- $F_{\text{IAM, diff}}$ is the diffuse irradiance IAM factor, calculated using equation (4.15).

The ground reflected effective irradiance is calculated using equation (5.13), as described in Section 4.3.

Finally, the global effective irradiance is calculated as the sum of the three separated components, as shown in equation (4.26).

$$G_{\text{eff}} = (B_{\text{eff}} + D_{\text{eff}} + GR_{\text{eff}}) \cdot (1 - F_{\text{soiling}}) \quad (4.26)$$

Where:

- G_{eff} is the global effective irradiance.
- B_{eff} is the beam effective irradiance, calculated using equation (4.24).
- D_{eff} is the diffuse effective irradiance, calculated using equation (4.25).

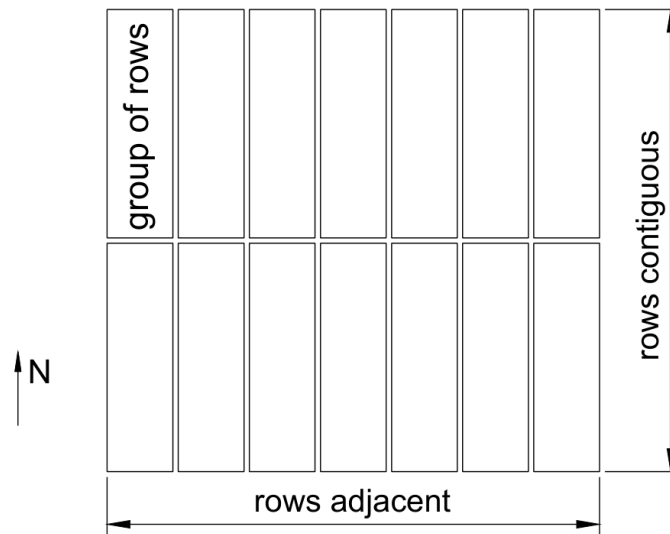


Figure 4.12: A diagram of the equivalent virtual field, using trackers

- GR_{eff} is the effective ground reflected irradiance, calculated using equation (5.13).
- F_{soiling} is the soiling factor in parts per one, defined in Section 4.5.

4.7 Virtual field dimensions

The equivalent field size is a plant disposition which reproduces the required number of modules in the plant, but as a square layout. A diagram is shown in Figure 4.12. The inter-group distances in Figure 4.12 are not taken into account.

This simplification is made because although in pvDesign the real position of all the structures is known, using them in the simulation would be prohibitively expensive in terms of computation time. However, it is desirable to consider the differences in row length which result from the size of the PV plant. For example, in a very big PV plant the rows will be very long and the edge effects will be nullified. In smaller plants, however, the rows may be so short the edge effects become significant, as shown in Figure 4.1.

The virtual field is sized calculating the number of rows in either direction required to match the number of modules in the plant. The number of adjacent rows shown in Figure 4.12 is calculated using equation (4.27).

$$n_{\text{rows adj}} = \text{truncate} \left(\sqrt{\frac{n_{\text{strings}} \cdot PP}{n_{\text{str/row}} \cdot L_{\text{row}}}} \right) \quad (4.27)$$

Where:

- $n_{\text{rows adj}}$ is number of adjacent rows, floored to 1.
- n_{strings} is the total number of strings in the power plant.
- PP is the post to post distance.
- $n_{\text{str/row}}$ is the number of strings per row.

- L_{row} is the row length.

The number of contiguous rows shown in Figure 4.12 is calculated using equation (4.28).

$$n_{\text{rows cont}} = \text{truncate} \left(\frac{n_{\text{strings}}}{n_{\text{str/row}} \cdot n_{\text{rows adj}}} \right) \quad (4.28)$$

Where:

- $n_{\text{rows cont}}$ is number of contiguous rows, increased by 1 if not an integer.
- n_{strings} is the total number of strings in the power plant.
- $n_{\text{str/row}}$ is the number of strings per row.
- $n_{\text{rows adj}}$ is number of adjacent rows, calculated using equation (4.27).

The $n_{\text{rows cont}}$ is increased by 1 to guarantee field will always be either exactly the required size or slightly over-sized, while retaining the square shape. The shape is essential to ensure the validity of the shading calculations.

The number of contiguous rows can be used to calculate an equivalent row length, which will be used in Section 4.1. The number of adjacent rows is used to de-rate the losses when the first row is unaffected.

Chapter 5

Back-face effective irradiance

The back-face irradiance is defined as the irradiance value perceived by the back side of the photovoltaic modules. There has been much interest in finding suitable models to predict the yield of bifacial modules, and comparisons have been published of the different options available. There are three types of models for calculating the back-face irradiance [19]:

- Ray-tracing models perform a realistic simulation in a 3D model space. Complex and localized near shading objects can be defined, and surface reflectance characteristics can be modeled, including specular reflection. One example of such model was developed by Lo, Lim, and Rahman [20] using the open source Radiance software [21]. Another analysis using Radiance was made by Deline et al. [22]. An example of the kind of complex scenes which can be modeled with Radiance is shown in Figure 5.1.
- View factor models use a 2D representation of the scene and configuration factors to compute the contribution of each irradiance source. The PVSyst software [3], NREL's SAM software [23] and Sunpower's pvFactors [24] are some examples.
- Empirical models can be deduced from real-world measurements to accurately predict the production of existing installations. However, they are less suitable for use cases which require greater system configuration flexibility.

Because the calculation model which is described in this methodology will be used in the pvDesign software, some requirements must be met. The most restrictive requirement is a simulation time requirement. The simulation of one year must be completed in a matter of seconds to avoid slowing down the software.

For this reason, ray-tracing models are deemed unsuitable for the pvDesign software. The analysis made by Ayala et al. [19] found that for sufficiently large DC fields (with long rows and a high enough number of rows), the edge effects can be neglected and view factor models are accurate enough for bifacial simulations. This is specially suitable for the pvDesign software, as it is designed to simulate utility scale photovoltaic power plants in the range of 1MW and above.

The back-face irradiance model presented in this methodology is a view-factor model based on the work by Marion et al. [23]. It is therefore a 2D model, which assumes infinite length rows and a flat terrain.

The following irradiance components will be considered in this model:

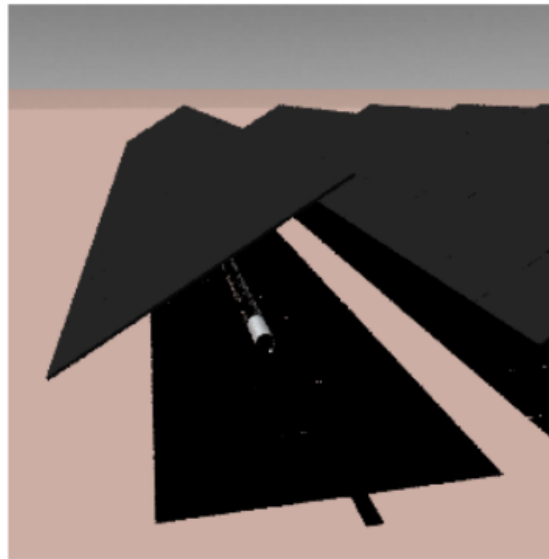


Figure 5.1: Single axis tracker with torque tube model in Radiance [25]

- The ground reflected irradiance, separated in two components. The first component is the beam irradiance, adding up the direct beam and the circumsolar component of the diffuse irradiance as described in [23]. The second component is the sky vault diffuse irradiance.
- The contribution of diffuse irradiance when directly impinging on the back-face.
- The contribution of beam irradiance when the sun is visible from the back-face.

Two more sources could be added in the future. One would be the irradiance reflected from the structure directly behind the one in evaluation. The other source would be reflections from the torque tube, if present. These sources of irradiance are not taken into account in this version of the methodology.

5.1 Geometrical reference system definition

The evaluation of the contribution of each component requires the definition of a geometrical reference system, needed to locate points in the table and viewing directions, and to locate points in the ground. The system described in this methodology is designed to facilitate integration of the irradiance components in the angular dimension and along the width of the table. As will be described later in this chapter, the integration in the angular dimension means splitting the view range in many smaller ranges defined by a looking direction.

The first definition, which is used to locate a point in the table and a viewing direction, is shown in Figure 5.2 (a), using a tracker as an example (the definition does not change for fixed structures). This reference system defines the two integration dimensions.

Any point in the table can be located by the d_{tb} coordinate, which is the distance to the bottom of the table. The d_{tb} coordinate can range from zero to the table width.

When evaluating the irradiance perceived by a point in the table as defined by its d_{tb} coordinate, the next dimension should define looking direction. This direction is defined by the α value,

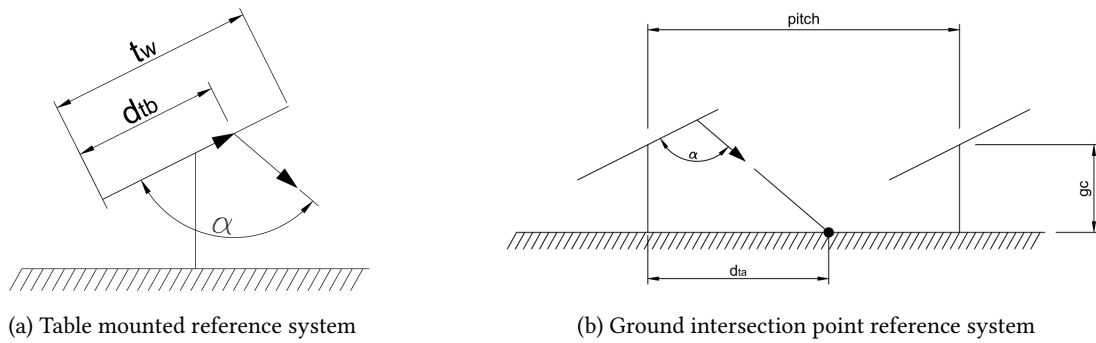


Figure 5.2: Reference systems used for the back-face irradiance calculation

which is the angle formed by the view vector and the table itself. The α value ranges from zero to 180 degrees.

In Figure 5.2 (b) the reference system used to locate points in the ground is shown. When looking towards the ground from the table, the intersection of the viewing vector and the ground is calculated, which yields the d_{ta} distance to axis coordinate. One additional parameter is required, the ground clearance g_c .

The ground clearance is defined as the distance from the ground to the axis of rotation of the tracker. For fixed structures, it will be the distance to the middle point of the table. Although this definition may not be the best for fixed structures, the benefits of having the same reference system for fixed structures and trackers outweigh the disadvantages.

One caveat with this definition is that it leads to an error when simulating trackers. The error consists in not considering the offset from the tracker rotation axis to the table, which can be clearly seen in Figure 5.6. This offset means that the actual ground clearance, as defined in Figure 5.2 (b), will change for trackers from one interval to the next.

To correct for that error, an effective ground clearance value is calculated for each interval in tracker structures, using equation (5.1). For fixed structures, the offset is zero, and therefore the effective ground clearance is the distance from the ground to the center of the table.

$$g_{c, \text{eff}} = g_c + d_{\text{off}} \cdot \cos \beta \tag{5.1}$$

Where:

- $g_{c, \text{eff}}$ is the effective ground clearance for trackers or fixed structures (for fixed structures, the offset is zero).
- g_c is the ground clearance to the rotation axis, as defined in Figure 5.2 (b).
- d_{off} is the offset from the rotation axis to the center of the table.
- β is the structure tilt angle in absolute value.

5.1.1 Ground intersection point calculation

To calculate the position of the point shown in Figure 5.2 (b), the distance to axis value d_{ta} must be calculated. The first step is to calculate the position of the reference point defined by the distance to table bottom. The height of the reference point is calculated using equation (5.2),

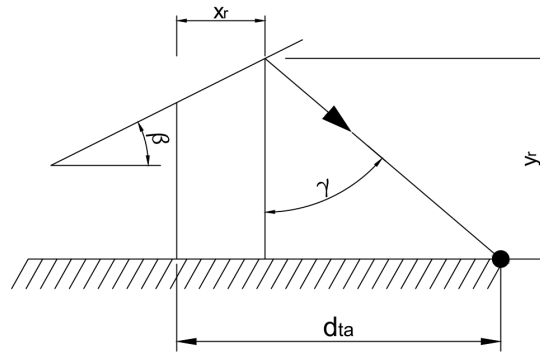


Figure 5.3: Diagram showing the variables used to calculate the distance to axis coordinate

and the distance of the reference point to the axis projected on the ground is calculated using equation (5.3).

$$y_r = g_c + \sin \beta \cdot \left(d_{tb} - \frac{t_w}{2} \right) \quad (5.2)$$

Where:

- y_r is the height of the reference point defined by d_{tb} , shown in Figure 5.3.
- g_c is the effective ground clearance value, calculated using (5.1).
- β is the structure tilt angle, in absolute value.
- d_{tb} is the distance from the bottom of the table to the reference point.
- t_w is the total table width, as shown in Figure 5.2 (a).

$$x_r = \cos \beta \cdot \left(d_{tb} - \frac{t_w}{2} \right) \quad (5.3)$$

Where:

- x_r is the distance from the structure axis to the reference point defined by d_{tb} , projected on the ground, shown in Figure 5.3.
- β is the structure tilt angle, in absolute value.
- d_{tb} is the distance from the bottom of the table to the reference point.
- t_w is the total table width.

Finally, to calculate the value of the distance to axis d_{ta} , it is convenient to define the angle γ , which is the angle between the viewing vector and the vertical.

$$d_{ta} = x_r + \frac{y_r}{\tan \gamma} \quad (5.4)$$

Where:

- d_{ta} is the distance to the structure axis of the point in the ground, as shown in Figure 5.3.
- x_r is the distance from the structure axis to the reference point defined by d_{tb} , projected on the ground, shown in Figure 5.3.
- y_r is the height of the reference point defined by d_{tb} , shown in Figure 5.3.
- γ is the angle shown in Figure 5.3.

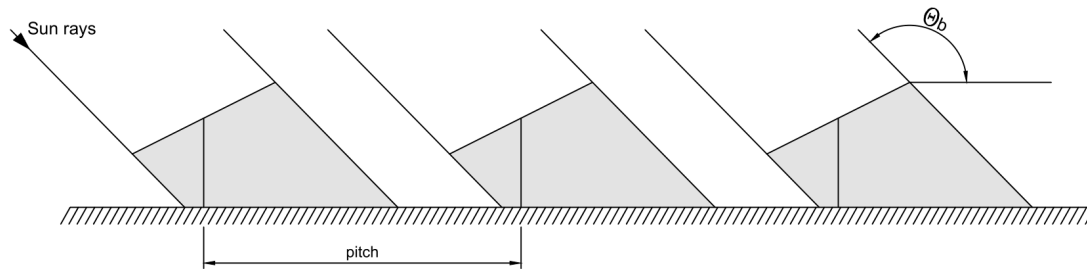


Figure 5.4: Diagram showing the shades cast by the tables on the ground

5.2 Beam irradiance perceived by the ground

When evaluating the contribution of the ground reflected irradiance from a given point in the ground (as defined by α and d_{tb}), the first step is to locate the point in relation to the structure axis using equation (5.4).

Defining the ground emitter point in relation to the structure axis is helpful because the shades cast from the tables to the ground are periodical in pitch increments, as shown in Figure 5.4.

In order to calculate the dimensions of the shaded segments, the beam theta angle θ_b must be calculated, shown in Figure 5.4. This angle is derived from the projection of the sun elevation on the vertical plane perpendicular to the structure axis. Using the true tracking algorithm described in Subsection 2.3.1, the true tracking tilt angle can be calculated with equation (2.4). The absolute value of the true tracking tilt is the sun elevation projected on the yz plane.

The θ_b angle is calculated using equation (5.5). Note that the true tracking tilt is in absolute value. An alternative formulation would be to use the sign of the true tracking tilt directly to ascertain whether the surface looks towards or away from the sun, but this formulation seems clearer.

$$\theta_b = \begin{cases} 90 + \beta_{tt} & \text{if } |\gamma_{sur} - \gamma_{sun}| < 90 \\ 90 - \beta_{tt} & \text{otherwise} \end{cases} \quad (5.5)$$

Where:

- θ_b is the beam theta angle, as shown in Figure 5.4.
- β_{tt} is the true tracking tilt, in absolute magnitude, calculated using equation (2.4).
- γ_{sur} is the surface azimuth, defined in Subsection 2.2.1.
- γ_{sun} is the sun azimuth angle, defined in Chapter 2.

The θ_b angle is defined such that it is always greater than 90 degrees if the sun is in front of the structures. This works well to avoid over-complicating the formulation for handling tracking structures, because it removes the dependency on the surface azimuth (eg it does not matter if the tracker looks east or west).

Once the beam theta angle is defined, the next step is to calculate whether a point in the ground is shaded or not. To do so, first the position of the shade in relation to the axis has to be calculated

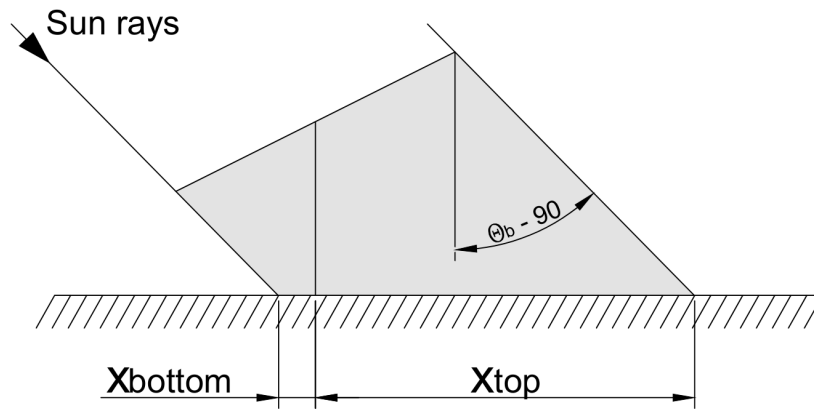


Figure 5.5: Diagram showing the position of the direct shade on the ground

using equation (5.6), as shown in Figure 5.5.

$$\begin{aligned} x_{\text{top}} &= \cos \beta \cdot \frac{t_w}{2} + \tan (\theta_b - 90) \cdot \left(g_c + \sin \beta \cdot \frac{t_w}{2} \right) \\ x_{\text{bottom}} &= -\cos \beta \cdot \frac{t_w}{2} + \tan (\theta_b - 90) \cdot \left(g_c - \sin \beta \cdot \frac{t_w}{2} \right) \end{aligned} \quad (5.6)$$

Where:

- x_{top} is the position of the shade end, caused by the top end of the table, in reference to the structure axis.
- β is the structure tilt angle, in absolute value.
- t_w is the total table width.
- θ_b is the beam theta angle, as shown in Figure 5.4.
- g_c is the effective ground clearance value, calculated using (5.1).
- x_{bottom} is the position of the shade start, caused by the bottom end of the table, in reference to the structure axis.

When the θ_b beam theta angle is lower than 90 degrees, the tangent result is negative and the shades move to the left of the vertical below each point. If θ_b is lower than β , then x_{top} is lower than x_{bottom} , and the shade is inverted.

The condition used to check if a point defined by its position in reference to the axis d_{ta} lies in a shaded segment is simple. If d_{ta} is greater than x_{bottom} and lower than x_{top} , then the point is shadowed. Care should be taken to check that x_{top} is greater than x_{bottom} , in which case the condition is inverted.

To compute the beam irradiance reflected from the ground, equation (5.7) is used. This equation assumes the ground reflects light as a lambertian surface.

One final detail is that the irradiance reflected by shaded segments is not necessarily zero, as the mounting structure table and the photovoltaic modules are not completely opaque. This partial transparency can be observed in Figure 5.6.

Because this transparency could only be realistically modeled using a ray tracing simulation, a simplification can be made to include the effect in view factor models. The simplification is to



Figure 5.6: Picture of a 2V tracker using bifacial modules [27]

assign a transparency alpha value, α_t , to the table, so that light is not completely blocked when impinging on the table surface. This transparency is applied to beam and diffuse sources alike. One example using this assumption is the PVSyst software [3]. Some recommendations on what value this parameter should take can be found in [26].

$$I_{br} = \begin{cases} 0 & \text{if the horizon blocks the sun} \\ (BHI + I_{cir}) \cdot \rho \cdot \alpha_t & \text{if } x_{bottom} < d_{ta} < x_{top} \text{ (shaded ground)} \\ (BHI + I_{cir}) \cdot \rho & \text{otherwise (illuminated ground)} \end{cases} \quad (5.7)$$

Where:

- I_{br} is the irradiance reflected from the ground attributed to the beam component.
- BHI is the beam horizontal irradiance component.
- I_{cir} is the circumsolar component of the diffuse irradiance, obtained from the Perez transposition model for a horizontal plane (the ground).
- ρ is the albedo value.
- α_t is the table transparency, ranging from zero for fully opaque to one for fully transparent table.
- x_{bottom} is the position of the shade start, caused by the bottom end of the table, in reference to the structure axis.
- d_{ta} is the distance to the structure axis of the point in the ground, as shown in Figure 5.3.
- x_{top} is the position of the shade end, caused by the top end of the table, in reference to the structure axis.

5.3 Diffuse irradiance perceived by the ground

The ground reflects the diffuse irradiance originating from the sky vault. For any given point in the ground determined by its position in relation to the structure axis d_{ta} , the amount of visible sky vault must be quantified.

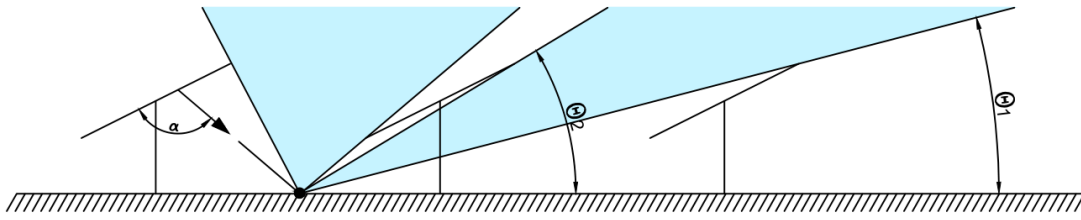


Figure 5.7: Arcs of sky vault visible through the gaps between structures.

To do so, a configuration factor calculation is used. The inputs for the configuration factors are the angles of obstructed vision caused by the presence of structures, as shown in Figure 5.7. The angles θ_1 and θ_2 are measured from ground and increase in the counter clockwise direction.

Creating an algorithm to compute the visible arcs is presents some difficulties, because at tilt zero (which may happen for trackers or fixed structures in the equator), the number of visible arcs is infinite. A simple solution was adopted in this methodology, which is to impose a limit on the number of structures which are looked at in either direction.

The algorithm is formulated in terms of how many structures away the evaluation point is. The limitation is that the furthest structure evaluated is 15 times the pitch distance away. Therefore, if evaluating the diffuse irradiance perceived by a point in the ground, it will looking for gaps between structures which are at most 15 times the pitch distance.

To calculate the θ angles for any given structure in view of the ground point defined by d_{ta} , the first step is to calculate the distance from the point to the structure axis

$$d_x = PP \cdot n_p - d_{ta} \tag{5.8}$$

Where:

- d_x is the distance from the evaluation point located at d_{ta} to the axis of the structure located at n_p pitch distances away.
- PP is the pitch distance (post to post distance).
- n_p is the number of pitch distances. At zero, the structure being evaluated may be directly above or to the right of the evaluation point. For n_p values greater than zero, the structures are to the right of the evaluation point, which are the structures contributing most of the sky visibility.
- d_{ta} is the distance to the structure axis of the point in the ground, as shown in Figure 5.3.

The vision angles of the lower and higher points of the structure, θ_{low} and θ_{high} respectively, are calculated using equation (5.9).

$$\begin{aligned} \tan \theta_{low} &= \frac{g_c - \sin \beta \cdot t_w/2}{d_x - \cos \beta \cdot t_w/2} \\ \tan \theta_{high} &= \frac{g_c + \sin \beta \cdot t_w/2}{d_x + \cos \beta \cdot t_w/2} \end{aligned} \tag{5.9}$$

Where:

- θ_{low} is the vision angle to the lower point of the structure.

- g_c is the ground effective clearance, calculated using (5.1).
- β is the structure tilt angle, in absolute value.
- t_w is the total table width.
- d_x is the distance from the evaluation point to the axis of the structure located at n_p pitch distances, calculated using equation (5.8).
- θ_{high} is the vision angle to the higher point of the structure.

A visible sky arc is defined as the visible sky arc between a structure at n_p to a structure at $n_p + 1$. The arc lower and higher angles, θ_1 and θ_2 in Figure 5.7 respectively, can be calculated using equation (5.10). If the θ_2 angle is greater than the θ_1 angle, then the sky is not visible between two structures.

$$\begin{aligned}\theta_1 &= \max(\theta_{low}(n_p + 1), \theta_{high}(n_p + 1)) \\ \theta_2 &= \min(\theta_{low}(n_p), \theta_{high}(n_p))\end{aligned}\tag{5.10}$$

Where:

- θ_1 is the vision angle at the start of the arc.
- θ_{low} is the vision angle to the lower point of the structure.
- n_p is the number of pitch distances.
- θ_{high} is the vision angle to the higher point of the structure.
- θ_2 is the vision angle at the start of the arc.

The irradiance perceived by the ground when in presence of a sky arc emitting isotropically, defined by θ_1 and θ_2 , is calculated using the configuration factor defined in equation (5.11). This equation is the configuration factor between a point (1) and a any infinitely long surface parallel to the plane to which the point belongs [28], as shown in Figure 5.8.

The configuration factor for each possibly transparent structure is calculated using equation (5.11), evaluated between the θ_{low} and θ_{high} angles calculated using equation (5.9).

$$F_{12} = \frac{1}{2} \cdot (\cos \theta_1 - \cos \theta_2)\tag{5.11}$$

Where:

- F_{12} is the configuration factor.
- θ_1 is the vision angle at the start of the arc.
- θ_2 is the vision angle at the start of the arc.

The diffuse irradiance reflected from the ground is calculated using equation (5.12). This equation adds up the contribution of the visible sky arcs and the contribution of the semi-transparent structures.

$$I_{dr} = \rho \cdot I_{dv} \cdot \left(\sum (F_{sky\ arc}) + \alpha_t \cdot \sum (F_{str\ arc}) \right)\tag{5.12}$$

Where:

- I_{dr} is the diffuse irradiance reflected from the ground.
- ρ is the albedo value.

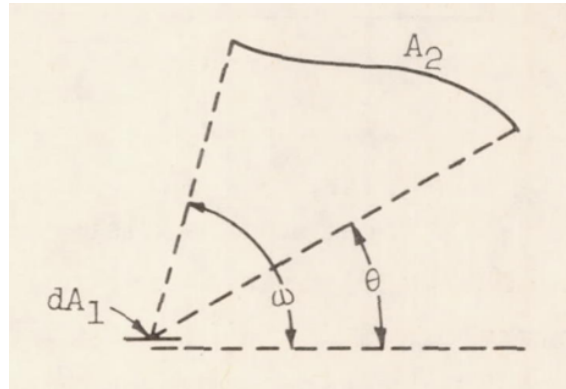


Figure 5.8: Configuration factor between a point in the ground and an arc of the sky vault [28]

- I_{dv} is the sky vault diffuse irradiance component, as perceived by a horizontal plane, calculated using the Perez model.
- $F_{sky\ arc}$ is the configuration factor of each visible arc.
- α_t is the table transparency, ranging from zero for fully opaque to one for fully transparent table.
- $F_{str\ arc}$ is the configuration factor of structure arc in between the visible arcs.

5.4 Contribution of ground reflected irradiance to the back face

Once the irradiance emitted by an arbitrary point in the ground is known, the next step is to quantify the irradiance perceived by the back face. It is important to keep in mind that the irradiance perceived by the back face changes along its width, not only in terms of the ground reflected but also in terms of the direct diffuse and beam sources.

The calculation consists of evaluating the irradiance emitted by the ground points which the back face can see. Then the irradiance is multiplied by the configuration factor calculated using (5.11), for the relevant α range. This evaluation yields the equivalent of a transposition to the plane of array, except the ground is not a homogeneous emitter like in Section 3.4.

The ground reflected irradiance perceived by the back face is calculated using equation (5.13). A simple diagram showing a single evaluation of an α range is shown in Figure 5.9.

$$I_{gr}(d_{tb}) = F_{soi} \left(\sum_{\alpha=0}^{\alpha=180-\beta} (I_{br}(d_{tb}, \alpha) + I_{dr}(d_{tb}, \alpha)) \cdot F_{cf}(\alpha) \cdot F_{near}(d_{tb}, \alpha) \cdot F_{iam}(|90 - \alpha|) \right) \quad (5.13)$$

Where:

- I_{gr} is the effective ground reflected irradiance perceived by the back face plane, evaluated at a point in the table as defined by d_{tb} .
- d_{tb} is the distance from the bottom of the table to the reference point.
- F_{soi} is the soiling factor for the back face irradiance.

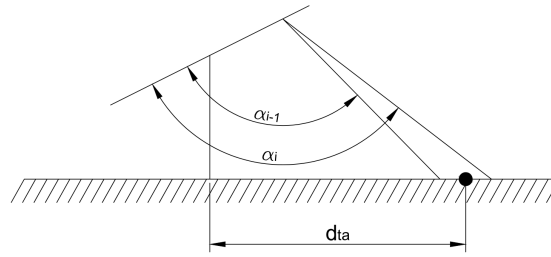


Figure 5.9: Evaluation of a ground segment from the back face

- α is the angle between the evaluation direction and the lower part of the table, ranging from zero to 180 degrees. For evaluating the ground reflected component the range can be shortened by removing the sky, yielding an upper range of $180 - \beta$.
- I_{br} is the irradiance reflected from the ground attributed to the beam component, calculated for the mid point of the range.
- I_{dr} is the diffuse irradiance reflected from the ground, calculated for the mid point of the range.
- F_{cf} is the configuration factor for the range, calculated using equation (5.11) for the angles α_{i-1} and α_i . The α_{i-1} is the lower value angle, otherwise the configuration factor will be negative.
- F_{near} is the near shading factor evaluated at the α range middle point, either 1 if the ground is visible or 0 if it isn't (because of the torque beam or the contiguous structure), calculated as described in Subsection 5.4.1.
- F_{iam} is the incidence angle modifier loss, evaluated at the incidence angle on the back face.

5.4.1 Near vision obstacles obstructing the ground reflected irradiance

The 2D model assumption means that only objects which are infinitely long in the direction perpendicular to the plane can be taken into account for the near shading model. Only two such objects are modeled in this methodology:

- The contiguous structure behind the one in evaluation, present in trackers and fixed structures.
- The torque beam in single axis trackers.

A simple graphical representation of this obstacles is shown in Figure 5.10. The evaluation of the near shading factor F_{near} is a geometrical problem which is formulated differently for the two previously described obstacles.

For the contiguous structure, the first step is to calculate the θ values which point to the lower and upper vertex of the obstructing structure, using equation (5.14). These values are referred to the horizontal plane, and increase in the counter clockwise direction.

$$\begin{aligned} \tan \theta_{low} &= \frac{-d_{tb} \cdot \sin \beta}{PP - d_{tb} \cdot \cos \beta} \\ \tan \theta_{high} &= \frac{(t_w - d_{tb}) \cdot \sin \beta}{PP - (t_w - d_{tb}) \cdot \cos \beta} \end{aligned} \tag{5.14}$$

Where:

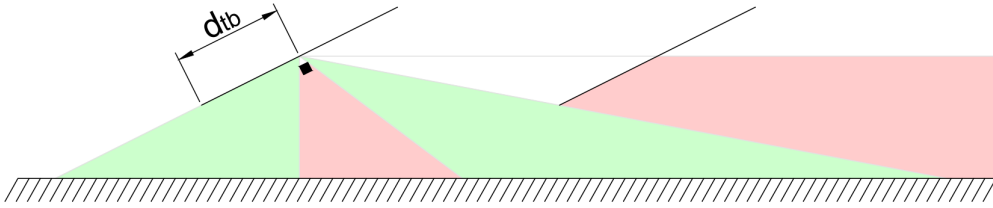


Figure 5.10: Ground reflected irradiance loss due to the near obstacles (torque beam and contiguous structure), evaluated at the middle point of the table for a worse case scenario representation.

- θ_{low} is the lower obstruction angle caused by the contiguous structure, with 0 being the horizontal and increasing counter clockwise.
- θ_{high} is the higher obstruction angle caused by the contiguous structure, with 0 being the horizontal and increasing counter clockwise.
- d_{tb} is the distance from the bottom of the table to the reference point.
- β is the structure tilt angle, in absolute value.
- PP is the pitch distance (post to post distance).
- t_w is the total table width.

If the α looking direction value, when referred to the horizontal plane, is between the θ_{low} and θ_{high} values calculated using equation (5.14), then the vision of the ground is blocked for that alpha value.

To compute if the torque beam is obstructing vision of the ground at a given α value, the geometry of the torque beam cross section is required. There are two types of torque beams in the market, namely the cylindrical torque beam and the squared torque beam.

To compute the limit angles when using either of the two types of torque beam, it is convenient to define a Cartesian coordinate system with the vertical Y axis matching the table, and the X axis being perpendicular to the table. The origin of the coordinate system is located at the bottom of the table.

For the cylindrical torque beam, the limit angles can be calculated if the center position of the beam is referenced in the previously defined coordinate system and the radius is known. First the α_c view angle to the center is calculated using equation (5.15). Then the γ value is calculated using equation (5.16), which is the angular sweep obstructed from the center to the circumference of the beam.

Finally, the limit angles are calculated by subtracting and adding the γ value to the α_c value of the center. If the α viewing direction angles lies within the resulting range, the ground is not visible.

$$\tan \alpha_c = \frac{d_{off}}{d_{tb} - t_w/2} \tag{5.15}$$

Where:

- α_c is the view angle to the center of the cylindrical torque beam.
- d_{off} is the offset from the rotation axis to the center of the table.

- d_{tb} is the distance from the bottom of the table to the reference point.
- t_w is the total table width.

$$\sin \gamma = \frac{r_{\text{beam}}}{\sqrt{(d_{tb} - t_w/2)^2 + (d_{\text{off}})^2}} \quad (5.16)$$

Where:

- γ is the angular sweep obstructed from the center of the beam to the circumference.
- r_{beam} is the radius of the torque beam.
- d_{tb} is the distance from the bottom of the table to the reference point.
- t_w is the total table width.
- d_{off} is the offset from the rotation axis to the center of the table.

For the square torque beam, it is convenient to define the beam as a polygon. For each vertex of the polygon, it's limit angle will be calculated using equation (5.17). The α_{vertex} angle is defined consistently with the previous definitions. After the limit angle of all vertexes is known, the minimum and maximum angles will be calculated. If the α viewing direction angles lies within the range defined by the minimum and maximum limit angles of all vertexes, the ground is not visible.

$$\tan \alpha_{\text{vertex}} = \frac{y_c - d_{tb}}{x_b} \quad (5.17)$$

Where:

- α_{vertex} is the limit angle for the vertex, starting at zero at the table and increasing counter clockwise.
- y_c is the Y coordinate of the polygon in the Cartesian coordinate system with its vertical axis parallel to the table.
- d_{tb} is the distance from the bottom of the table to the reference point.
- x_b is the X coordinate of the polygon in the Cartesian coordinate system with its vertical axis parallel to the table.

5.5 Contribution of diffuse irradiance to the back face

The back face is likely to be directly irradiated by the sky vault for tilt angles other than zero. To calculate the contribution of the diffuse irradiance, an equation analogous to equation (5.13) is used, using configuration factors to transpose the vault irradiance to the back face.

The effective diffuse irradiance on the back face is calculated using equation (5.18).

$$I_{db}(d_{tb}) = F_{\text{soi}} \cdot I_{dv} \cdot \left(\sum_{\alpha=180-\beta}^{\alpha=180} F_{cf}(\alpha) \cdot F_{\text{near}}(d_{tb}, \alpha) \cdot F_{\text{iam}}(|90 - \alpha|) \right) \quad (5.18)$$

Where:

- I_{db} is the effective diffuse irradiance on the back face, evaluated at a point in the table as defined by d_{tb} .
- d_{tb} is the distance from the bottom of the table to the reference point.

- F_{soi} is the soiling factor for the back face irradiance.
- I_{dv} is the sky vault diffuse irradiance component, as perceived by a horizontal plane, calculated using the Perez model.
- α is the angle between the evaluation direction and the lower part of the table, ranging from zero to 180 degrees. For evaluating the ground reflected component the range can be shortened by removing the sky, yielding an upper range of $180 - \beta$.
- F_{cf} is the configuration factor for the range, calculated using equation (5.11) for the angles α_{i-1} and α_i . The α_{i-1} is the lower value angle, otherwise the configuration factor will be negative.
- F_{near} is the near shading factor evaluated at the α range middle point, with value 1 if the sky vault is visible or 0 if it isn't, calculated as described in Subsection 5.4.1.
- F_{iam} is the incidence angle modifier loss, evaluated at the incidence angle on the back face.

5.6 Contribution of beam irradiance to the back face

In sunrise and sunset intervals, it is conceivable that depending on the location the sun could be directly visible from the back face. If the sun is visible from the back face, the contribution of beam irradiance is calculated using equation (5.19).

$$I_{bb}(d_{tb}) = (B_{bf} + I_{cir, bf}) \cdot F_{hor}(\gamma_{sun}, 90 - \theta_{sun}) \cdot F_{near}(d_{tb}, \alpha_{sun}) \cdot F_{iam}(\theta_{inc, b}) \cdot F_{soi} \quad (5.19)$$

Where:

- I_{bb} is the effective irradiance beam irradiance perceived by the back plane, evaluated at a point in the table as defined by d_{tb} .
- d_{tb} is the distance from the bottom of the table to the reference point.
- B_{bf} is the beam irradiance transposed to the back face, calculated as described in Section 3.4.
- $I_{cir, bf}$ is the circumsolar component of the diffuse irradiance, transposed to the back face, as described in Section 3.4.
- F_{hor} is the horizon shading factor, with value 0 if the horizon blocks the sun, or 1 otherwise. It is evaluated at the sun azimuth and elevation values of the interval.
- γ_{sun} is the sun azimuth angle.
- θ_{sun} is the sun zenith angle.
- F_{near} is the near shading factor evaluated at the α_{sun} value, with value 1 if the sun is visible or 0 if it isn't, calculated as described in Subsection 5.4.1.
- α_{sun} is the alpha value from which the sun is irradiating the back face, calculated as using equation (5.20).
- F_{iam} is the incidence angle modifier loss, evaluated at the sun incidence angle on the back face.
- $\theta_{inc, b}$ is the sun incidence angle on the back face, calculated with equation (2.3).
- F_{soi} is the soiling factor for the back face irradiance.

$$\alpha_{sun} = 180 + \theta_b - \beta \quad (5.20)$$

Where:

- α_{sun} is the alpha value from which the sun is irradiating the back face
- θ_b is the beam theta angle, as shown in Figure 5.4.
- β is the structure tilt angle, in absolute value.

5.7 Effective back face irradiance

The final step is to integrate the average effective back face irradiance along the table length, using equation (5.21). In this equation, the integration variable x is the distance to bottom d_{tb} variable.

$$I_b = \frac{1}{t_w} \cdot \int_0^{t_w} I_{\text{gr}}(x) + I_{\text{db}}(x) + I_{\text{bb}}(x) dx \quad (5.21)$$

Where:

- I_b is the average effective irradiance perceived by the back face.
- t_w is the total table width.
- x is the distance to bottom variable d_{tb} .
- I_{gr} is the effective ground reflected irradiance perceived by the back face plane, calculated using equation (5.13).
- I_{db} is the effective diffuse irradiance on the back face, calculated using equation (5.18).
- I_{bb} is the effective irradiance beam irradiance perceived by the back plane, calculated using equation (5.19).

The integration range in equation (5.21) should be changed if the mounting structure is a tracker. When using bifacial modules it is recommended to avoid placing modules directly on top of the torque beam. The shade cast by the torque beam on the back face of the modules results in mismatch losses due to the heterogeneous illumination of the back face.

If the point directly on top of the torque beam is evaluated but there is no photovoltaic module (eg, in a 2V structure or 2H), then the effective irradiance is artificially lowered. To avoid this issue, the integration range can be changed to less half a table width (accounting for the gap), and separated in two integrals.

If separating the evaluation in two integrals, the result of each integral is weighted by the evaluated length of each.

Chapter 6

Photovoltaic module model

The photovoltaic module model should predict the current and voltage generated by any given module when it is being irradiated.

The model described in this chapter is valid for mono and poly crystalline modules. It would require modifications if it was to be used for thin film modules, and additional losses should be added for amorphous silicon modules.

6.1 The one-diode model

The one-diode model used in this methodology can be found in [5], and the implementation is based on the paper by Mermoud and Lejeune [2].

The formulation of the one-diode model results from solving the electrical circuit shown in Figure 6.1.

The one-diode model has three components:

- The current generated by the photovoltaic cell, I_L .
- The current lost through the diode, I_D , shown in Figure 6.1.
- The current lost through the shunt resistance, I_{sh} , shown in Figure 6.1.

The one-diode model equation is shown in (6.1), as it appears in [2], [5]. It is not an explicit function, which means that in order to compute the current value when the voltage is known, an iterative process must be used, as will be described in Subsection 6.1.4. An example of the IV and power curves obtained with this model is shown in Figure 6.2.

$$I(V) = I_L - I_D - I_{sh} = I_L - I_0 \cdot \left(\exp \left(q \cdot \frac{V + I(V) \cdot R_s}{N_{cs} \cdot \gamma'_d \cdot k \cdot T_{cell}} \right) - 1 \right) - \frac{V + I(V) \cdot R_s}{R'_{sh}} \quad (6.1)$$

Where:

- $I(V)$ is the current generated by the module when it operates at voltage V , in [A].

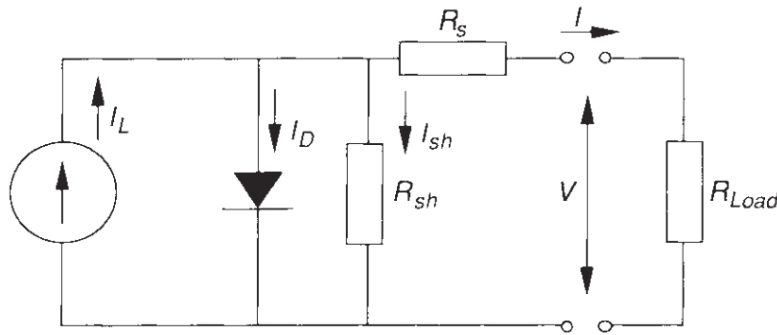


Figure 6.1: Equivalent circuit of a photovoltaic module [5]

- I_L is the light current (also known as photocurrent), the current generated by the module before any losses, calculated using equation (6.2).
- I_0 is the diode reverse saturation current, calculated using equation (6.3).
- q is the charge of an electron in coulombs, $q = 1.602 \cdot 10^{-19} \text{ C}$.
- R_s is the series resistance of the module, in $[\Omega]$.
- N_{cs} is the number of cells in series in the module.
- γ'_d is the temperature corrected diode ideality factor, a dimensionless parameter calculated using equation (6.12).
- k is Boltzmann's constant, $k = 1.381 \cdot 10^{-23} \frac{\text{m}^2\text{kg}}{\text{s}^2\text{K}}$.
- T_{cell} is the cell temperature, in $[\text{K}]$.
- R'_{sh} is the irradiance corrected shunt resistance of the module, in $[\Omega]$, calculated using (6.6).

In order to compute a value of $I(V)$, some values have to be computed in an initialization phase. These parameters which are computed initially are the reference parameters $I_{L, \text{ref}}$ and $I_{0, \text{ref}}$, needed to calculate I_L and I_0 , and diode ideality factor correction $\mu_{\gamma d}$. The equations to calculate them are found in sections 6.1.2 and 6.1.3 respectively.

When actually computing the value of $I(V)$, the corrected values of the diode ideality factor and the shunt resistance must be calculated, using equations (6.12) and (6.6) respectively. At this point the value of $I(V)$ can be calculated, using the equations (6.2) and (6.3).

The light current is dependent on the irradiance reaching the photovoltaic cell and its temperature. It is calculated using equation (6.2).

$$I_L = \frac{G}{G_{\text{ref}}} \cdot (I_{L, \text{ref}} + \mu_{\text{isc}}(T_{\text{cell}} - T_{\text{cell, ref}})) \tag{6.2}$$

Where:

- I_L is the light current (also known as photocurrent), the current generated by the module before any losses.
- G is the irradiance reaching the surface of the photovoltaic cell.
- G_{ref} is the reference irradiance, usually $G_{\text{ref}} = 1000 \text{ W/m}^2$.

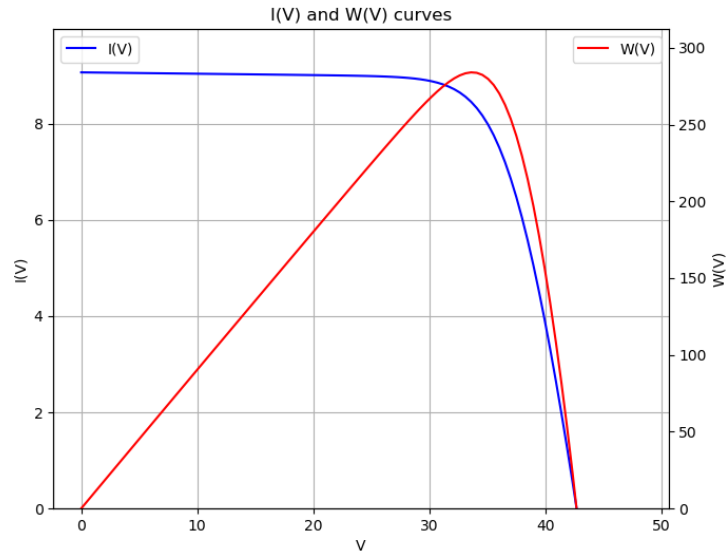


Figure 6.2: Example of the obtained IV curve for a photovoltaic module

- $I_{L, \text{ref}}$ is the reference light current, calculated using the procedure described in Subsection 6.1.2.
- μ_{IsC} is the short-circuit current temperature coefficient, in $[A/K]$.
- T_{cell} is the cell temperature in $[K]$.
- $T_{\text{cell, ref}}$ is the reference cell temperature in $[K]$, usually $T_{\text{cell, ref}} = 298 K$.

The diode saturation current is dependent on the cell temperature, and is calculated using equation (6.3).

$$I_0 = I_{0, \text{ref}} \cdot \left(\frac{T_{\text{cell}}}{T_{\text{cell, ref}}} \right)^3 \cdot \exp \left(\frac{q \cdot \varepsilon_G}{\gamma'_d \cdot k} \cdot \left(\frac{1}{T_{\text{cell}}} - \frac{1}{T_{\text{cell, ref}}} \right) \right) \quad (6.3)$$

Where:

- I_0 is the diode reverse saturation current.
- $I_{0, \text{ref}}$ is the reference diode reverse saturation current, calculated using the procedure described in Subsection 6.1.2.
- T_{cell} is the cell temperature in $[K]$.
- $T_{\text{cell, ref}}$ is the reference cell temperature in $[K]$, usually $T_{\text{cell, ref}} = 298 K$.
- q is the charge of an electron in coulombs, $q = 1.602 \cdot 10^{-19} C$.
- ε_G is the diode bandgap energy, of value $\varepsilon_G = 1.12 eV$ for silicon.
- γ'_d is the temperature corrected diode ideality factor, a dimensionless parameter calculated using equation (6.12).
- k is Boltzmann's constant, $k = 1.381 \cdot 10^{-23} \frac{m^2kg}{s^2K}$.

Once the value of $I(V)$ has been computed for a given voltage, the power can be calculated using equation (6.4).

$$W(V) = I(V) \cdot V \quad (6.4)$$

Where:

- $W(V)$ is the power generated by the module when it operates at voltage V , in $[W]$.
- $I(V)$ is the current generated by the module when it operates at voltage V , in $[A]$, calculated using equation (6.1).
- V is the operating voltage of the photovoltaic module, in $[V]$.

The module efficiency can be calculated using equation (6.5).

$$\eta_{\text{mod}} = \frac{W}{G \cdot A_{\text{mod}}} \quad (6.5)$$

Where:

- η_{mod} is the module efficiency.
- $W(V)$ is the power generated, in $[W]$.
- G is the irradiance reaching the surface of the photovoltaic cell, in $[W/m^2]$.
- A_{mod} is the module area being irradiated, in $[m^2]$

The reference parameters $I_{L, \text{ref}}$ and $I_{0, \text{ref}}$ can be calculated using the equations found in Subsection 6.1.2.

6.1.1 Correction of the shunt resistance

The shunt resistance is strongly dependent on the irradiance reaching the cell [2], [5]. The correction described here can be found in [2], and the equations are described in detail by Hansen [29]. The corrected shunt resistance is calculated using (6.6).

$$R'_{\text{sh}} = R_{\text{sh, base}} + (R_{\text{sh, dark}} - R_{\text{sh, base}}) \cdot \exp\left(-\alpha_{\text{exp}} \cdot \frac{G}{G_{\text{ref}}}\right) \quad (6.6)$$

Where:

- R'_{sh} is the irradiance corrected shunt resistance of the module.
- $R_{\text{sh, base}}$ is calculated using equation (6.7).
- $R_{\text{sh, dark}}$ is the module shunt resistance at zero irradiance, usually found in the module datasheet, in $[\Omega]$.
- α_{exp} is the exponential factor for the shunt resistance correction, which has a default value of $\alpha_{\text{exp}} = 5.5$ in [3].
- G is the irradiance reaching the surface of the photovoltaic cell.
- G_{ref} is the reference irradiance, usually $G_{\text{ref}} = 1000 \text{ W}/m^2$.

The base shunt resistance is calculated using equation (6.7).

$$R_{sh, base} = \max \left(0, \frac{R_{sh, ref} - R_{sh, dark} \cdot \exp(-\alpha_{exp})}{1 - \exp(-\alpha_{exp})} \right) \quad (6.7)$$

Where:

- $R_{sh, base}$ is the base shunt resistance, used to calculate the corrected shunt resistance.
- $R_{sh, ref}$ is the reference shunt resistance, taken directly from the module datasheet, in $[\Omega]$.
- $R_{sh, dark}$ is the module shunt resistance at zero irradiance, usually found in the module datasheet, in $[\Omega]$.
- α_{exp} is the exponential factor for the shunt resistance correction, which has a default value of $\alpha_{exp} = 5.5$ in [3].

6.1.2 Reference parameters

The calculation of the reference parameters for the one diode model is a topic on which there is ample literature. Generally speaking, there are two branches of research: calculating the reference parameters given experimental results, and calculating them when given module datasheet values from the manufacturer. In this methodology, we are interested in the second option. Jordehi [30] published a review of different methods for estimating the reference parameters.

The parameters to be determined are [5]:

- The reference light current.
- The reference diode saturation current.
- The reference diode ideality factor.
- The series resistance.
- The shunt resistance.

In this methodology, the shunt resistance reference value is taken directly from the module datasheet (PAN file). That leaves four parameters to be determined.

The following procedure is based on the one described by [3]. The maximum series resistance value is determined iteratively, as described in this section. If the series resistance is known, the three remaining reference parameters can be calculated using equations (6.8), (6.9) and (6.10), which result from substituting into equation (6.1) the conditions at short circuit current, open circuit voltage, and maximum power point [5] respectively.

The four reference values (short circuit current I_{sc} , open circuit voltage V_{oc} , maximum power point current I_{mpp} , maximum power point voltage V_{mpp}) are taken from the module datasheet, at reference STC conditions.

$$I_{sc} = I_{L, ref} - I_{0, ref} \cdot \left(\exp \left(\frac{I_{sc} \cdot R_s}{a_{ref}} \right) - 1 \right) - \frac{I_{sc} \cdot R_s}{R_{sh}} \quad (6.8)$$

$$0 = I_{L, ref} - I_{0, ref} \cdot \left(\exp \left(\frac{V_{oc}}{a_{ref}} \right) - 1 \right) - \frac{V_{oc}}{R_{sh}} \quad (6.9)$$

$$I_{mpp} = I_{L, ref} - I_{0, ref} \cdot \left(\exp \left(\frac{V_{mpp} + I_{mpp} \cdot R_s}{a_{ref}} \right) - 1 \right) - \frac{V_{mpp} + I_{mpp} \cdot R_s}{R_{sh}} \quad (6.10)$$

Where:

- I_{sc} is the short circuit current in STC conditions, as found in the module datasheet, in [A].
- $I_{L, ref}$ is the reference light current, one of the three unknown parameters, in [A]. If the module is a thin film module, this parameter is adjusted according to Subsection 6.6.2.
- $I_{0, ref}$ is the reference diode saturation current, one of the three unknown parameters, in [A].
- a_{ref} is a made up parameter used to simplify the formulation, calculated using equation , and which contains the last unknown parameter (diode ideality factor).
- R_s is the series resistance of the module, in [Ω]. The value of this parameter changes depending on the stage of the calculation, as explained in this section. To solve this system of equation, it is assumed to be known.
- R_{sh} is the shunt resistance of the module, in [Ω], at reference conditions and taken directly from the module datasheet.
- V_{oc} is the open circuit voltage of the module, in [V], at reference conditions, taken directly from the module datasheet.
- I_{mpp} is the maximum power point current in [A], at reference conditions, taken directly from the module datasheet.
- V_{mpp} is the maximum power point voltage in [V], at reference conditions. taken directly from the module datasheet.

The light current is adjusted if the module is a thin film module, using the recombination loss correction of Subsection 6.6.2. When calculating the light current, the obtained value is divided by the recombination loss correction. When the light current value is used to calculate the diode saturation current, or used in equation (6.10), it is multiplied by the recombination loss correction. In each case, the recombination loss correction is calculated at the relevant operation point (short circuit current, open circuit voltage, or maximum power point).

$$a_{ref} = \frac{N_{cs} \cdot \gamma_{ref} \cdot k \cdot T_{cell, ref}}{q} \quad (6.11)$$

Where:

- a_{ref} is a calculated reference parameter which simplifies the formulation of the one diode equation.
- N_{cs} is the number of cells in series in the module.
- γ_{ref} is the reference diode ideality factor, one of the three unknown parameters.
- k is Boltzmann's constant, $k = 1.381 \cdot 10^{-23} \frac{m^2kg}{s^2K}$.
- $T_{cell, ref}$ is the cell temperature at reference conditions, in [K], usually 298.15 K.
- q is the charge of an electron in coulombs, $q = 1.602 \cdot 10^{-19} C$.

Solving this system of equations is not perfectly straightforward, because the a_{ref} parameter, which contains the diode ideality factor, is part of an exponential. To solve it the following iterative procedure is used:

1. Assume a diode ideality factor.
2. Substitute the diode saturation current in equation (6.8) by the expression obtained from equation (6.9).
3. Calculate the photo current using the modified equation (6.8).
4. Calculate the diode saturation current using equation (6.9), with the obtained photo current result.
5. Substitute the photo current and diode saturation current in equation (6.10), and calculate the result.
6. Assume a new diode ideality factor, with the objective being to minimize the residual of equation (6.10).
7. When the result of equation (6.10) is zero, the correct values have been found for the three reference parameters (photo current, diode saturation current, and diode ideality factor).

This is done using an iterative process, similar to the Newton-Raphson method, in which the result of equation (6.10) must be zero (in other words, finding the root of equation (6.10) is the objective, with the diode ideality factor being the variable).

The remaining unknown parameter is the series resistance of the model. In this methodology the procedure of PVsyst is followed [3]. The first step is to calculate the maximum admissible value of the series resistance. The procedure used by PVsyst to calculate this value is not documented, and it is necessary to calculate it if reading PAN files. For this reason, the follow iterative procedure was developed to approximate the value of the maximum series resistance.

1. Read the diode ideality factor value from the PAN file.
2. Assume an initial maximum series resistance value.
3. Calculate the reference light current, reference diode saturation current, and diode ideality factor value.
4. Minimize the difference between the calculated diode ideality factor, and the diode ideality factor value from the PAN file.

In each iteration, only the series resistance changes. The maximum series resistance is found once the diode ideality factor difference is zero.

To calculate the series resistance value used in the model, the value found in the PAN file is compared with the maximum series resistance. If it is lower than the maximum, it is directly used in the model. Otherwise, the maximum series resistance is used as the corrected model resistance.

Finally, once the corrected series resistance value is known, the final reference parameters are calculated, including the final diode ideality factor.

6.1.3 Correction of the diode ideality factor

The diode ideality factor is dependent on the cell temperature according to Mermoud [3], and should be corrected. The correction to be applied can be found in [3], defined as linear model. The corrected diode ideality factor γ'_d is calculated using equation (6.12).

$$\gamma'_d = \gamma_d + \mu_{\gamma d} \cdot (T_{\text{cell}} - T_{\text{cell, ref}}) \quad (6.12)$$

Where:

- γ'_d is the temperature corrected diode ideality factor, a dimensionless parameter.
- γ_d is the uncorrected diode ideality factor, a dimensionless parameter.
- $\mu_{\gamma d}$ is the slope of the linear correction, in $[1/K]$.
- T_{cell} is the cell temperature in $[K]$.
- $T_{\text{cell, ref}}$ is the reference cell temperature in $[K]$, usually $T_{\text{cell, ref}} = 298 K$.

The calculation of the $\mu_{\gamma d}$ slope is an iterative process which takes place after the reference parameters have been calculated according to Subsection 6.1.2. The $\mu_{\gamma d}$ parameter is adjusted to find a value such that the maximum power at 65 °C cell temperature and 1000 W/m² is equal to the value specified in the datasheet (calculated using the $\mu_{W, \text{req}}$ parameter).

The power required at a cell temperature of 65 °C is calculated using equation (6.13), with the parameters obtained from the photovoltaic module manufacturer.

$$W_{65, \text{req}} = W_{\text{STC, req}} - (T_{\text{cell, STC}} - T_{\text{cell, 65}}) \cdot (W_{\text{STC, req}} \cdot \mu_{W, \text{req}}) \quad (6.13)$$

Where:

- $W_{65, \text{req}}$ is the maximum power at a cell temperature $T_{\text{cell}} = 338 K$ and irradiance $G = 1000 W/m^2$.
- $W_{\text{STC, req}}$ is the required maximum power at STC conditions, a parameter usually found in the photovoltaic module datasheet.
- $T_{\text{cell, STC}}$ is the cell temperature in STC conditions, $T_{\text{cell}} = 298 K$.
- $T_{\text{cell, 65}}$ is the cell temperature of value $T_{\text{cell}} = 338 K$.
- $\mu_{W, \text{req}}$ is the required temperature coefficient for power, in $[1/K]$, usually found in the module datasheet.

6.1.4 Numerical resolution using an iterative method

The non-explicit nature of equation (6.1) means an iterative process must be used to compute the value of $I(V)$. The process will consist in finding a value of I which yields an equal $I(V)$ calculated using equation (6.1).

The simplest way to obtain this result was found to be to use a root search function. A root search function is a program which when given a function $f(x)$ finds the x values which satisfy the condition $f(x) = 0$ (roots of the equation) [31].

The function for which the roots must be found is defined in equation (6.14). When the value of this function reaches zero (within the desired tolerance), a valid value of I has been found, and the search ends.

$$f_{\text{to zero}}(I) = I(I, V) - I \quad (6.14)$$

Where:

- $f_{\text{to zero}}$ is the function for which the roots are to be found. In this case, the independent variable is the photovoltaic module current.
- $I(I, V)$ is the current value calculated using equation (6.1) for a given operating voltage.

Another important value which must be computed is the maximum power which could be generated by the module at some given irradiance and temperature conditions. This operating point is known as the maximum power point. To find this operating point, a maximizing function can be used, which finds the point where the maximum value of some $f(x)$ is reached within a given interval of x .

The function to be maximized in this case would be $W(V)$, calculated using equation (6.4).

6.1.5 Input parameters

The input parameters used by the one diode model, and which must be provided by the photovoltaic module manufacturer, are:

- The module series resistance, R_s .
- The number of cells connected in series, N_{cs} .
- The short-circuit current temperature coefficient, μ_{Isc} .
- The shunt resistance of the module at reference irradiance, R_{sh} .
- The module shunt resistance at zero irradiance, $R_{sh, \text{dark}}$.
- The exponential factor for the shunt resistance correction, α_{exp} .
- The short circuit current, I_{sc} .
- The open circuit voltage, V_{oc} .
- The maximum power point current at reference conditions, I_{mpp} .
- The maximum power point voltage at reference conditions, V_{mpp} .
- The diode ideality factor, γ_d .
- The power temperature coefficient, $\mu_{W, req}$.
- The reference irradiance, G_{ref} .
- The reference cell temperature, $T_{cell, ref}$.

The following additional parameters are needed for later steps in the process:

- The module surface area, computed using the module length and width.
- The module power tolerance, separated in two values (high and low).

6.2 Cell temperature

The cell temperature is dependent on the ambient conditions (temperature and wind), heat transfer coefficient from module to ambient, and module generated power (as it is power being dissipated from the module). The model used in this methodology is based on the model by Faiman [32], used in [3].

The model is based on a simplified energy balance. It is defined in equation (6.15).

$$T_{\text{cell}} = T_{\text{amb}} + \frac{1}{U} \cdot (\alpha_{\text{ac}} \cdot G \cdot (1 - \eta_{\text{mod}})) \quad (6.15)$$

Where:

- T_{cell} is the cell temperature, in $[K]$.
- T_{amb} is the ambient temperature, in $[K]$.
- U is the global heat transfer coefficient, calculated using equation (6.16), in $\left[\frac{W}{m^2K}\right]$.
- α_{ac} is the absorption coefficient of solar radiation, of recommended value $\alpha_{\text{ac}} = 0.9$ according to [3].
- G is the irradiance reaching the photovoltaic module, in $[W/m^2]$.
- η_{mod} is the module efficiency, calculated using (6.5).

The heat transfer coefficient can be calculated using equation (6.16).

$$U = U_c + U_v \cdot w_{\text{sp}} \quad (6.16)$$

Where:

- U is the global heat transfer coefficient, in $\left[\frac{W}{m^2K}\right]$.
- U_c is the heat transfer coefficient constant component, in $\left[\frac{W}{m^2K}\right]$.
- U_v is the heat transfer coefficient wind component, in $\left[\frac{W \cdot s}{m^3K}\right]$.
- w_{sp} is the wind speed, in $[m/s]$.

When calculating solar photovoltaic utility-scale plants, the recommended value for the constant heat transfer coefficient is $U_c = 29 W/m^2K$ according to [3], if no wind data is available. Should wind data be available in hourly resolution, the recommended values are $U_c = 25 W/m^2K$ and $U_v = 1.2 W \cdot s/m^3K$ [3].

Because of the dependence of T_{cell} upon η_{mod} in equation (6.15), the IV model itself must be used to be able to compute the cell temperature. Unfortunately this results in another loop in the calculation, which will now need to iterate in search of both the current value (assuming the voltage is the fixed variable), and the cell temperature, which will depend on the power output of the module at each operating point.

There are at least two different approaches to this problem. The first approach is to choose a starting value for the T_{cell} , compute the electrical power output of the module using the IV model, and then calculate a new T_{cell} value. This results in a function which can be solved using a root search, as is shown in equation (6.17).

The starting value may be approximated using the module efficiency in STC conditions, or directly using the ambient temperature as the cell temperature.

$$f_{\text{to zero}}(T_{\text{cell}}) = T_{\text{cell, new}}(T_{\text{cell}}) - T_{\text{cell}} \quad (6.17)$$

Where:

- $f_{\text{to zero}}$ is the function for which the roots are to be found. In this case, the independent variable is the cell temperature.
- $T_{\text{cell, new}}$ is the new cell temperature calculated using the T_{cell} passed to the function.

However, it becomes apparent that this approach is not the best in terms of computational efficiency. Although it may reach a very good accuracy level, it results in a total number of iterations which is the sum of the iterations performed by each time the IV model is solved (eg if for computing the cell temperature ten calls to the IV model are performed, and each call required 20 IV model iterations, then the total is 200 calls).

The second approach consists of computing a new cell temperature value at the end of each IV model iteration. In each iteration, when the current value is obtained, a new cell temperature value can be calculated. This new value can then be used in the next iteration. When the result of equation (6.14) is within the required tolerance values, it can be safely assumed that the cell temperature values converged as well.

This approach results in a higher number of iterations than if the cell temperature value is fixed, but a much lower overall number of iterations when the cell temperature is unknown and must be calculated with the ambient temperature.

6.3 Bifacial photovoltaic modules

The electrical characterization of bifacial photovoltaic modules is very similar to monofacial modules. A method to characterize the electrical response of bifacial modules is described in [33].

In this methodology, a simplified approach is taken which uses the bifaciality factor to account for the increased energy input in the previously described one diode model. This is an approximation which is also used in software such as PVSyst [3] and NREL's SAM [34].

A bifaciality factor is the ratio between the front and back response for any given module parameter, when operating in the same conditions (eg same irradiance for front and back) [35]. The bifaciality is also usually defined as the ratio between rear and front side efficiency, referred to module power output in STC conditions [36].

The bifaciality factor for module power can be calculated using equation (6.18) [35].

$$\varphi_{P_{\max}} = \frac{P_{\max, r}}{P_{\max, f}} \quad (6.18)$$

Where:

- $\varphi_{P_{\max}}$ is the bifaciality factor for power output.
- $P_{\max, r}$ is the maximum power output in STC conditions when only the rear side is illuminated.
- $P_{\max, f}$ is the maximum power output in STC conditions when only the front side is illuminated.

When simulating bifacial modules, the irradiance value used in equation (6.2) is replaced by the value calculated using equation (6.19). The model is otherwise identical to the monofacial model.

$$G_{\text{bif}} = G_f + \varphi_{P_{\max}} \cdot G_r \quad (6.19)$$

Where:

- G_{bif} is the effective irradiance used to calculate the photo current in the one diode model for bifacial modules.
- G_f is the effective irradiance on the front face of the cell.
- $\varphi_{P_{\max}}$ is the bifaciality factor for power output.
- G_r is the effective irradiance on the back face of the cell.

Finally, the method for calculating the cell temperature described in Section 6.2 remains unchanged. The irradiance heating the module is considered to be the front face irradiance only.

6.4 Module degradation

Module degradation causes a power loss over the years [37], [38]. Some of the processes which give rise to this power loss are [39]:

- Optical degradation due to ultraviolet (UV) exposure (yellowing, browning and discoloration).
- Corrosion of the cell-interconnect bus bars (which may occur in humid environments) and other components of the module result in an increase in the module series resistance (R_s). This in turns reduces the voltage produced by the cell, lowering the overall module maximum power point voltage, as shown in Figure 6.3 (a).
- Appearance of shunts (parallel high-conductivity paths through the solar cell or on the cell edges), which lowers the shunt resistance (R_{sh}) of the module. This effect will mostly mean a reduced maximum power point current, due to the increased shunt current I_{sh} in equation (6.1), as shown in Figure 6.3 (b).
- Inter-cell mismatch, which appears due to front surface soiling, encapsulant degradation, cell cracking, manufacturing defects, etc.

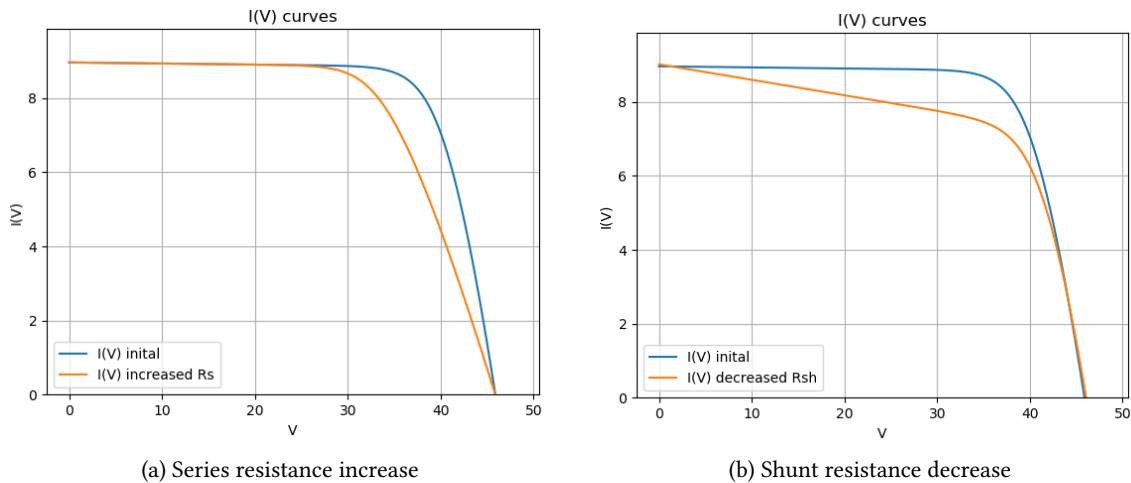


Figure 6.3: Effect of modifying the module resistances on the IV curve

The degradation of the module resistances is shown in Figure 6.3. Increasing the series resistance R_s will cause the slope of the I(V) curve to decrease at the open circuit point, and decreasing the shunt resistance R_{sh} will cause the slope of the curve to increase at the short circuit point. The change observed in Figure 6.3 is only due to a very exaggerated degradation of the resistances, for demonstrative purposes. Normal degradation will cause much subtler changes. However, the combined effect of degradation on both resistances and the aggregated effect over the years will yield a significantly reduced fill factor.

However, most of this degradation modes are very dependent on the manufacturing process and materials used, and thus will show a strong dependency on the module manufacturer and model. Furthermore, some types of degradation which were very common in the early mass-manufactured modules have been mitigated or completely eliminated in modern modules, while new types have appeared, such as the PID (potential induced degradation) which has been observed some in 1500V modules.

Because of this reasons, the module degradation model to be used must be applicable to modules of any manufacturer. The approach taken in this methodology is to use a model which mimics the results found by Jordan, Wohlgemuth, and Kurtz [37] in 2012, shown in Figure 6.4. The authors of [37] found the I_{sc} degradation to be the largest contributor to the loss in P_{max} .

The degradation model used by pvDesign consists of a linear degradation model, with a power loss calculated using equation (6.20).

The power loss is applied as a reduction of the I_{sc} parameter of the one diode model. Reducing the short circuit current I_{sc} yields the results shown in Figure 6.5. To find the reduction of I_{sc} required to match the power loss calculated using equation (6.20), an iterative process is used.

$$W_{degraded} = W_{STC, n=0} \cdot (1 - x_{degr, n=0} - x_{degr} \cdot n) \quad (6.20)$$

Where:

- $W_{degraded}$ is the power generated by a photovoltaic module after n years have passed.

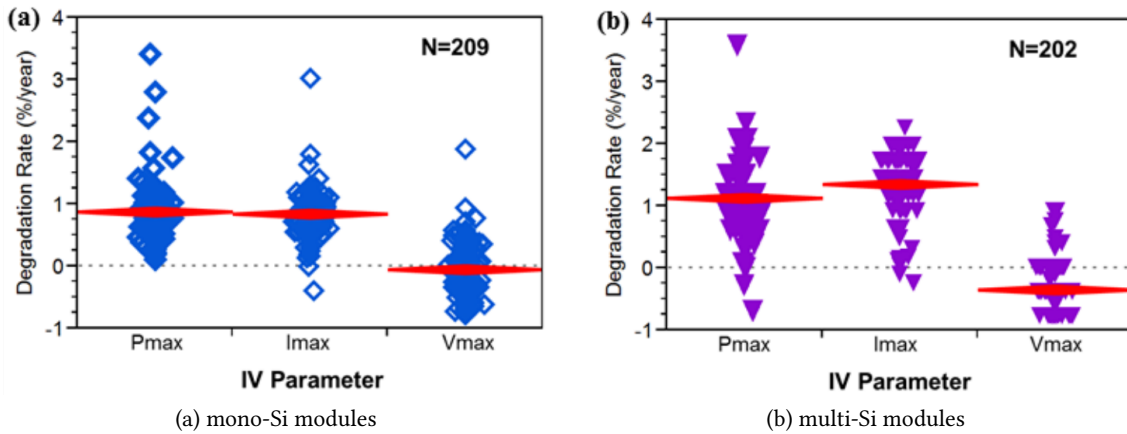


Figure 6.4: Degradation of maximum power point values [37]

- $W_{STC, n=0}$ is the power generated by the module at STC conditions in the year zero.
- $x_{degr, n=0}$ is the power loss factor for the first year.
- x_{degr} is the linear power loss factor for the subsequent years.
- n is the number of years.

6.5 Module losses: quality, LID and mismatch

There are three additional losses to be applied to the generated power. These losses reflect issues of great physical complexity, but are calculated using simple models (percentage loss) due to their usually very low values. The losses are applied sequentially.

The quality loss reflects the fact that the power generated by a photovoltaic module varies between different modules of the same model. Usually a module manufacturer will guarantee a power within a range of the STC power, giving a low and high tolerance value. For example, for a module of $W_{STC} = 300\text{ W}$ with a tolerance of $\pm 3\%$, the manufacturer guarantees that the power generated by the individual modules will be within the range 291-309 W.

The module power after applying the quality loss can be calculated using equation (6.21).

$$W_{\text{after qua}} = W_{\text{mod}} \cdot (1 - F_{\text{qua}}) \quad (6.21)$$

Where:

- $W_{\text{after qua}}$ is the power generated by a photovoltaic module after applying the quality loss.
- W_{mod} is the power generated by the module.
- F_{qua} is the quality loss factor, in parts per one.

Light-induced degradation losses arise due to boron-oxygen defects in the silicon wafer used to manufacture a photovoltaic module [40]. This defect appears on prolonged exposure of Czochralski (CZ) wafers to light. Sopori et al. [40] found the degradation to occur mostly during the first minutes of exposure to light, followed by a much lower degradation rate, and stabilization

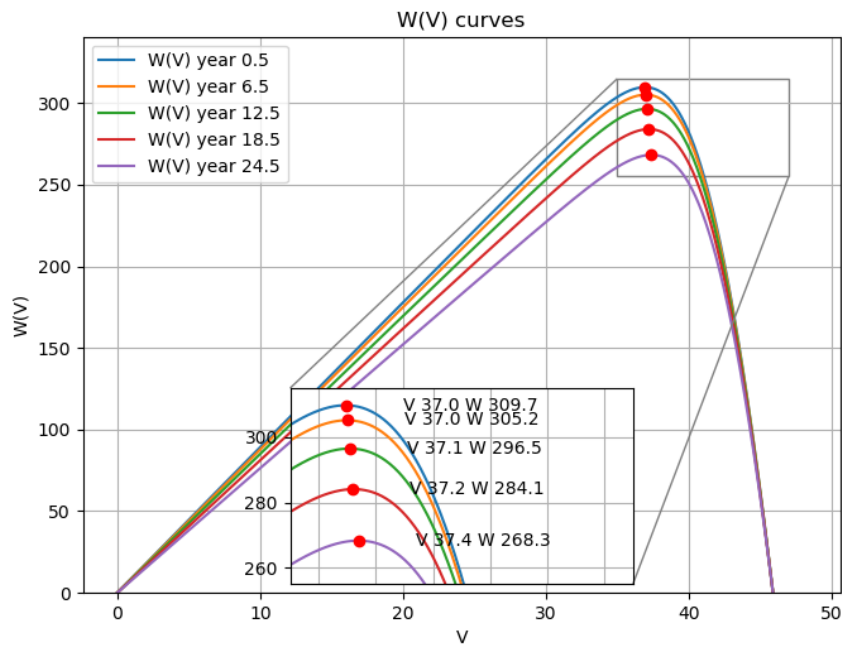


Figure 6.5: Degradation of the module maximum power after 25 years

at around 72h. The overall loss of module efficiency due to LID was found to be no grater than 0.5%.

The consequences of LID on the production of a photovoltaic module are very complex and module dependent. However, the low loss and the long time periods being simulated means a simple percentage-loss model can be used. The loss is expressed in (6.22).

$$W_{\text{after LID}} = W_{\text{after qua}} \cdot (1 - F_{\text{LID}}) \tag{6.22}$$

Where:

- $W_{\text{after LID}}$ is the power generated by a photovoltaic module after applying the LID loss.
- $W_{\text{after qua}}$ is the power generated by a photovoltaic module after applying the quality loss.
- F_{LID} is the LID loss factor, in parts per one.

The mismatch loss appears in a string of photovoltaic modules due to the differences from one module to another. The small variations in the IV curves from one module to another means any given module is unlikely to be operating at it’s maximum power point, because in a string all modules are subject to the same current.

The mismatch loss is applied according to equation (6.23).

$$W_{\text{after mis}} = W_{\text{after LID}} \cdot (1 - F_{\text{mis}}) \tag{6.23}$$

Where:

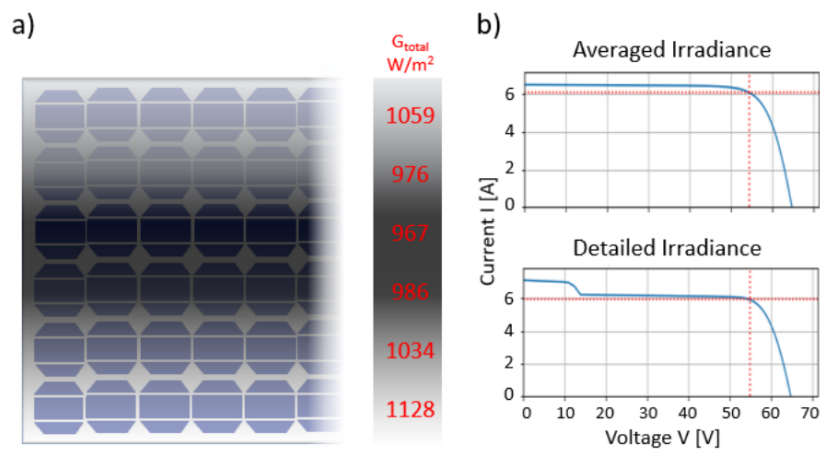


Figure 6.6: Loss caused by mismatch when using bifacial modules [41]

- $W_{\text{after mis}}$ is the power generated by a photovoltaic module after applying the mismatch loss.
- $W_{\text{after LID}}$ is the power generated by a photovoltaic module after applying the LID loss.
- F_{mis} is the mismatch loss factor, in parts per one.

6.5.1 Bifacial mismatch

Bifacial simulations must consider one additional loss, caused by the heterogeneous illumination of the back face. This loss is specially significant when the back face is shaded by the torque tube [41], as shown in Figure 6.6.

Although it would be desirable to simulate the effects of the mismatch using a cell by cell one diode model, such a simulation would be too expensive computationally. A simplified approach is taken, using a percentage loss model.

The value of the bifacial mismatch should be applied proportionally to the proportion of back face irradiance of each interval. The loss is calculated using equation (6.24).

$$W_{\text{after bif mis}} = W_{\text{after LID}} \cdot \left(1 - F_{\text{bif mis}} \cdot \frac{G_r}{G_r + G_f} \right) \tag{6.24}$$

Where:

- $W_{\text{after bif mis}}$ is the power generated by a photovoltaic module after applying the bifacial mismatch loss.
- $W_{\text{after LID}}$ is the power generated by a photovoltaic module after applying the LID loss.
- $F_{\text{bif mis}}$ is the bifacial mismatch loss, with 0 representing no loss.
- G_f is the effective irradiance on the front face of the cell.
- G_r is the effective irradiance on the back face of the cell.

Technology	b_0	b_1	b_2	b_3	b_4	b_5
CdTe	0.7946	-0.05423	-0.01319	0.1724	0.08372	-0.004376
FirstSolar	0.86273	-0.0389480	-0.012506	0.098871	0.084658	-0.0042948

Table 6.1: Parametrization coefficients for spectral correction [42]

6.6 CdTe photovoltaic modules

The structure and distribution of cells in CdTe modules make them behave differently under certain circumstances. To model them, some additional considerations must be taken into account:

- Spectral correction: STC conditions consider a normalised solar spectrum, according to ASTM G173 standard. The mismatch between the distribution of the prevailing spectrum and the distribution according to ASTM G173 standard can be negligible in terms of module operation in the case of Silicon modules [3], but not for CdTe modules. In Subsection 6.6.1, the model of the spectral correction is presented.
- Recombination losses: in the case of CdTe modules, the recombination losses that occur in the intrinsic layer of the junction must be considered. Those will affect the one-diode model as explained in Subsection 6.6.2.
- Electrical shading: CdTe modules have cells distributed longitudinally along the module so, when one module is shaded, all the cells will be shaded regularly and there won't be any electrical mismatch between the cells. For this reason, truetracking will be used instead of backtracking to increase the energy production.

6.6.1 Spectral correction

The power produced by CdTe modules is affected by the spectrum that characterizes the prevailing sun light.

To calculate the correction that has to be applied, a simple model which facilitates the spectral correction according to the air mass and the precipitable water content is presented in [42]. This model is represented by Equation 6.25. The value obtained for the spectral shift is multiplied to the current calculated using the one-diode model (see Equation 6.1), being a gain if it is greater than 1 and a loss if it is less than 1.

$$M = b_0 + b_1 \cdot AM_a + b_2 \cdot p_{\text{wat}} + b_3 \cdot \sqrt{AM_a} + b_4 \cdot \sqrt{p_{\text{wat}}} + b_5 \cdot \frac{AM_a}{\sqrt{p_{\text{wat}}}} \quad (6.25)$$

Where:

- M is the spectral shift.
- AM_a is the absolute optical air mass, obtained using the SOLPOS library described in Chapter 2.
- p_{wat} is the precipitable water, in [cm]. This value is obtained from the meteorological data or, if not present, calculated using Equation 6.26.
- $b_0, b_1, b_2, b_3, b_4, b_5$ are the parametrization coefficients, which depend on the technology that is being evaluated (see Table 6.1).

The precipitable water can be calculated using the approach presented in [43], by using Equation 6.26.

$$p_w = 0.1 \cdot H_v \cdot \rho_v \quad (6.26)$$

Where:

- p_w is the precipitable water, in $[cm]$.
- H_v is the apparent water vapour scale height, in $[km]$, which can be calculated using Equation 6.27.
- ρ_v is the surface water vapour density, in $[g/m^3]$, which can be calculated using Equation 6.28.

The apparent water vapour scale height can be calculated using the approach presented in [43], by using Equation 6.27.

$$H_v = 0.4979 + 1.5265 \cdot \theta + \exp(13.6897 \cdot \theta - 14.9188 \cdot \theta^3) \quad (6.27)$$

Where:

- H_v is the apparent water vapour scale height, in $[km]$.
- θ is T/T_0 , being T the temperature in $[K]$ and T_0 273.15 K .

The surface water vapour density can be calculated using the approach presented in [44], by using Equation 6.28.

$$\rho_v = \frac{216.7 \cdot R_H \cdot \varrho_s}{T} \quad (6.28)$$

Where:

- ρ_v is the surface water vapour density, in $[g/m^3]$.
- R_H is the relative humidity, in parts per one. This value can be obtained from the meteorological data.
- ϱ_s is the saturation water pressure, in $[mb]$, which can be calculated using Equation 6.29.
- T is the ambient temperature, in $[K]$.

The saturation water pressure can be calculated using the approach presented in [45], by using Equation 6.29.

$$\begin{aligned} \varrho_s = & 6.1104546 + 0.4442351 \cdot t + 1.4302099 \cdot 10^{-2} \cdot t^2 + 2.6454708 \cdot 10^{-4} \cdot t^3 \\ & + 3.0357098 \cdot 10^{-6} \cdot t^4 + 2.0972268 \cdot 10^{-8} \cdot t^5 + 6.0487594 \cdot 10^{-11} \cdot t^6 - 1.469687 \cdot 10^{-13} \cdot t^7 \end{aligned} \quad (6.29)$$

Where:

- ϱ_s is the saturation water pressure, in [mb].
- t is the ambient temperature, in [C].

6.6.2 Recombination losses

To characterize the recombination losses that occur in the intrinsic layer of CdTe modules, a correction has to be applied to the one-diode model, as presented in [46]. This correction adjusts the light current generated, and is represented by Equation 6.30.

$$I'_L = I_L \cdot \left(1 - \frac{d^2 \mu \tau}{V_{bi} \cdot N_{cs} - V + I(V) \cdot R_s} \right) \quad (6.30)$$

Where:

- I'_L is the corrected light current.
- I_L is the light current (also known as photocurrent), the current generated by the module before any losses, calculated using equation (6.2).
- $d^2 \mu \tau$ is the recombination coefficient, provided by the manufacturer.
- V_{bi} is the intrinsic voltage of the junction. This value is 0.9 V for CdTe modules.
- N_{cs} is the number of cells in series in the module.
- $I(V)$ is the current generated by the module when it operates at voltage V , in [A].
- R_s is the series resistance of the module, in [Ω].

Chapter 7

Production of an array of photovoltaic modules

An array is a group of photovoltaic modules connected to an inverter. The way the panels are connected to each other induces losses due to mismatch, and the electrical cables themselves lose energy in the form of heat due to the Joule effect.

The inverters themselves are usually packed together in power stations. Power stations may also house electrical transformers which raise the voltage of the inverter AC output to more effectively transmit the electrical power to the plant substation.

7.1 Electrical connections in an array

In utility-scale photovoltaic plants, the modules are connected in series in "strings", and the strings are connected in parallel to form an array. Every array is connected to an electrical inverter, which converts the DC power to AC power. A simplified diagram of the connections used in photovoltaic power plants is shown in Figure 7.1.

Physically, the strings are actually connected to a string-box, which serves as a junction point for the DC cables before reaching the inverter input. The string-boxes serve the purpose of reducing the number of cables used (and thus cost). The string boxes are represented in Figure 7.1.

The connection of the modules in strings in series serves the purpose of increasing the voltage in the system. A higher voltage leads to lower electrical losses due to the Joule effect, due to the lower current needed to conduct power (the Joule effect losses are directly proportional to the resistance and the square of the current, equation (7.1)). Hence the efficiency of the electrical transmission of DC power is improved.

$$P \propto R \cdot I^2 \tag{7.1}$$

Where:

- P is heat loss in a cable.
- R is the electrical resistance of the cable.
- I is the current flowing through the cable.

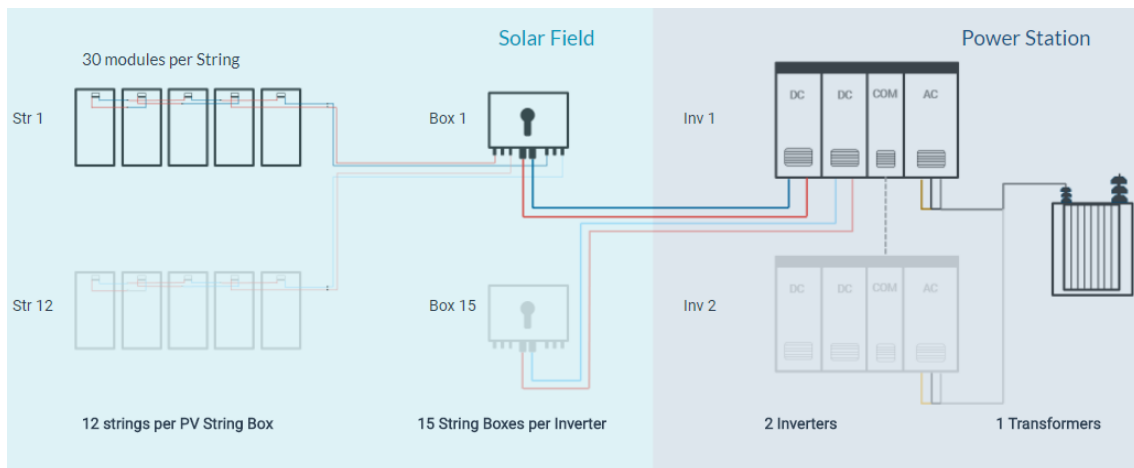


Figure 7.1: Electrical connections in a photovoltaic power plant [47]

The number of modules in series determines the voltage which the string may reach when irradiated. Given they are connected in series, a higher number of modules will mean a higher voltage can be reached. The voltage is usually limited by the module design, with modules having a maximum voltage rating which directly limits the maximum number of modules which can be connected in series.

The inverter will also have a maximum DC input voltage, which forces the plant designer to carefully match the photovoltaic modules, electrical configuration and inverter model. Poorly designed configurations will lead to situations where the inverter limits the production or can't produce at all.

The DC/AC_{ratio} calculated using equation (7.2) plays an important role in the design of the electrical configuration. It is a function of the number of strings in any given array (and the number of modules per string), or in other words, the size of the array. High DC/AC_{ratio} arrays will usually exceed the maximum power the inverter can generate, thus producing losses due to power cutoff.

$$DC/AC_{ratio} = \frac{W_{DC \text{ array}}}{W_{AC \text{ inverter}}} \quad (7.2)$$

Where:

- DC/AC_{ratio} is the ratio of DC power to AC power.
- $W_{DC \text{ array}}$ is the power generated at STC conditions by the DC array of photovoltaic modules.
- $W_{AC \text{ inverter}}$ is the rated AC output power of the inverter.

In Figure 7.2, an array of modules is shown connected to a power station (red box in the center of Figure 7.2). The blue boxes represent the structures where the panels are mounted. Each structure (either fixed or sun-tracking) may contain one or several module strings. The individual strings are connected to the inverter in parallel using low-voltage DC cables (yellow lines in Figure 7.2).

The distances which any given DC cable may have to gap in order to reach the inverter input can be sufficient to produce significant losses in the DC cables. The minimization of the cable length in photovoltaic power plants thus serves a double purpose: both minimizing cost and

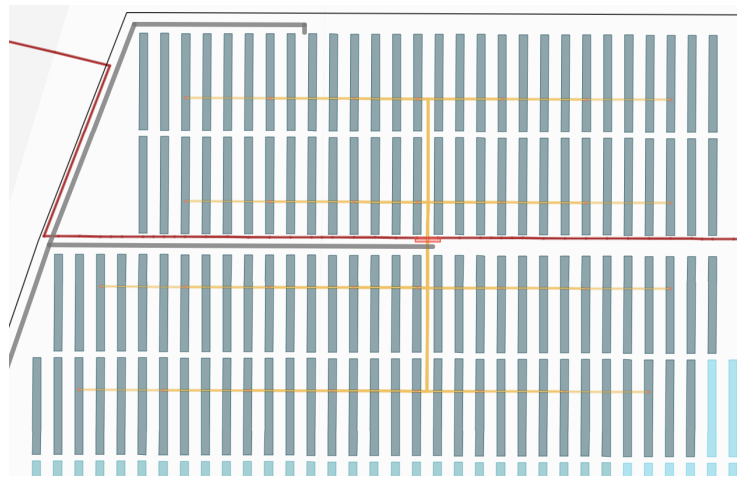


Figure 7.2: Array disposition in plant and connection to power station [47]

power losses. The DC cables can reach length in excess of 100m in arrays like the one shown in Figure 7.2.

In recent years efforts have been made by the photovoltaic industry to reduce the losses and costs due to the electrical connections. Some of the innovations resulting from this efforts are:

- Smaller inverters which are connected to a lower number of strings, known as string-inverters. The use of string inverters greatly reduces the ratio of DC cables to AC cables, at the cost of having more inverters vs. the central inverter configuration. However the higher number of inverters also leads to an improved reliability, as less power is lost if any single inverter should fail.
- DC bus configurations allow for the removal of string boxes, thus simplifying the electrical connections and reducing cost.

7.2 Power production of an array

In order to compute the output of an array (voltage, current and power), the output of the individual modules of the array must be known. However, it would not be reasonable to compute the production of each individual module, thus only the production and operation point of one module is calculated. The losses due to module mismatch are very small, and can be taken into account as described in Section 6.5.

Knowing the operation point of the module, the array voltage is calculated using equation (7.3), knowing that the modules are connected in series. The voltage is always forced by the inverter for the whole array. However, during the resolution process, the module maximum power point is calculated first, and it is assumed the inverter can operate at that optimum value, thus calculating the array voltage using equation (7.3).

If the inverter can't operate at the maximum power point voltage, then additional steps must be taken, as is explained in Chapter 8 and in particular in Section 8.5. If the inverter is forcing the operating voltage of the array, it can be assumed that each module in the string will increase the voltage equally, hence the voltage can be solved for using equation (7.3).

$$V_{array} = V_{mod} \cdot n_{mod/str} \tag{7.3}$$

Where:

- V_{array} is the voltage at the array output.
- V_{mod} is the voltage generated by a single module.
- $n_{\text{mod/str}}$ is the number of modules per string.

The array current can be calculated using equation (7.4), given the strings are connected in parallel.

$$I_{\text{array}} = I_{\text{mod}} \cdot n_{\text{str/array}} \quad (7.4)$$

Where:

- I_{array} is the current at the array output.
- I_{mod} is the current generated by a single module.
- $n_{\text{str/array}}$ is the number of strings per array.

The power generated by the array can be calculated using equation (7.5).

$$W_{\text{array}} = V_{\text{array}} \cdot I_{\text{array}} \quad (7.5)$$

Where:

- W_{array} is the power generated by the array.
- V_{array} is the voltage at the array output.
- I_{array} is the current at the array output.

7.2.1 Losses in DC power cables

The array DC power cable losses are defined using a single parameter, the DC loss ratio, to calculate an equivalent circuit resistance. This ratio multiplies the array electrical resistance at STC, as shown equation (7.6). The array resistance at STC is calculated applying Ohm's law to the array voltage and current at the maximum power point in STC conditions, calculated using the module voltage and current at STC.

$$R_{\text{DC loss}} = F_{\text{DC loss}} \cdot \frac{V_{\text{STC}} \cdot n_{\text{mod/str}}}{I_{\text{STC}} \cdot n_{\text{str/array}}} \quad (7.6)$$

Where:

- $R_{\text{DC loss}}$ is the circuit equivalent circuit resistance used to compute the DC power loss.
- $F_{\text{DC loss}}$ is the DC loss ratio, in parts per one.
- V_{STC} is the module voltage at the maximum power point in STC conditions.
- $n_{\text{mod/str}}$ is the number of modules per string.
- I_{STC} is the module current at the maximum power point in STC conditions.
- $n_{\text{str/array}}$ is the number of strings per array.

Once the equivalent resistance has been calculated, the power loss in the DC cables can be calculated using equation (7.7).

$$W_{\text{DC loss}} = R_{\text{DC loss}} \cdot I^2 \quad (7.7)$$

Where:

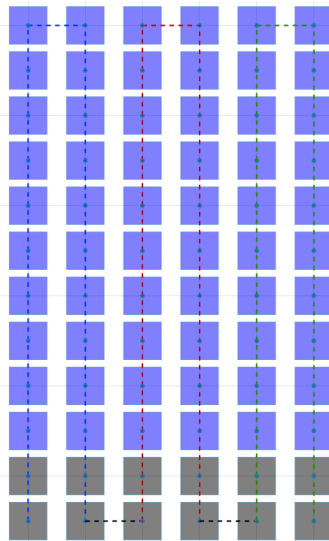


Figure 7.3: Partially shaded photovoltaic module

- $W_{DC\ loss}$ is the power loss in the array DC cables.
- $R_{DC\ loss}$ is the circuit equivalent circuit resistance used to compute the DC power loss, calculated using equation (7.6).
- I is the current at the array output.

7.2.2 Array production loss due to partial shadings

All the effects described in this section only apply to arrays of traditional crystalline Si photovoltaic modules. Other technologies behave differently.

The one diode model described in Section 6.1 is formulated under the assumption that the whole photovoltaic module is being irradiated with the same intensity.

However, this assumption does not hold when the module is partially shaded, as shown in Figure 7.3. It may seem that this situation can be modeled by reducing the irradiance used on the one-diode model proportionally to the shaded area. But this does not represent the irradiance actually reaching the individual cells in a module, some of which are still receiving the full beam irradiance.

The impact of partial shading on the production of utility-scale photovoltaic plants is minimal, given they only appear in the moments of the day when the production is lowest with or without shadows, and even then, most plants are designed in a way which guarantees shadows will only occur during short periods of time in the day. Or not at all if the plant uses backtracking.

When one cell is shaded, it affects the electrical behaviour of the whole module (as cells are connected in series working at the same current), that module affects the electrical behaviour of the whole string (as modules are connected in series working at the same current) and the string affects the behaviour of the whole array (as strings are connected in parallel working at the same voltage). This would incur an electrical mismatch whenever some of the strings in an array are shaded and others aren't.

However, it is not practical to model the cells individually representing the electrical connections and the way shades affect these electrical connections. A common way to estimate the losses that are incurred under partial shadings is according to the strings that are being shaded, as explained by Mermoud and Lejeune [48].

This method will assume that the beam radiation that one shaded string will receive is zero, and the energy produced by these shaded strings will come from the diffuse and ground reflected radiation.

By doing this consideration, the total losses due to near shading have to be divided into linear losses that reduce the radiation perceived by the module (Section 4.1) and electrical losses. Equation (7.8) is used to calculate the electrical shading loss factor.

The first term in equation (7.8) reflects the assumption that the module will still produce power proportionally to the available diffuse and ground reflected irradiance. The second term introduces the actual loss due to the shaded strings, and compensates for the power which has already been lost due to the linear shading loss factor $F_{\text{shd, beam}}$.

$$F_{\text{shd, elect}} = \frac{B_{\text{after, far}}}{G_{\text{after, far}}} \cdot \left(\frac{n_{\text{str, shaded}}}{n_{\text{str, un-shaded}}} - F_{\text{shd, beam}} \right) \quad (7.8)$$

Where:

- $F_{\text{shd, elect}}$ is the electrical shading loss factor, in parts per one.
- $B_{\text{after, far}}$ is the beam irradiance after applying the far shading losses, calculated by multiplying the beam irradiance at the POA, equation (3.1), by the far shading loss factor, equation (4.1).
- $G_{\text{after, far}}$ is the global irradiance after applying the far shading losses. It is calculated by multiplying the diffuse irradiance at the POA, equation (3.3), by the diffuse shading horizon factor, equation (4.8), and then adding the beam after far shading $B_{\text{after, far}}$, and the ground reflected irradiance including the horizon effect.
- $n_{\text{str, shaded}}$ is the number of shaded strings in the table.
- $n_{\text{str, un-shaded}}$ is the number of un-shaded strings in the table.
- $F_{\text{shd, beam}}$ is the near shading beam irradiance loss factor, in parts per one, calculated using equation (4.6).

Chapter 8

Electrical inverter production and performance

The electrical inverter converts the DC power generated by the photovoltaic array to AC power. Although the efficiency of this conversion is very high in modern inverters, its direct impact on the production makes its correct modeling critical.

Other inverter characteristics, such as the inverter operation window, can become major losses should the inverter be poorly chosen in relation to the photovoltaic array.

Therefore, the inverter calculation process will consist of two steps (not necessarily sequential): computing the inverter efficiency and checking whether or not the operating point is inside the operation window.

An essential component of any inverter is the maximum power point tracking (MPPT) algorithm. However, it is not practical to implement any particular MPPT system, as they vary greatly from one inverter model to another. Instead, it is assumed that the DC array is operating at its maximum power point, and afterwards the validity of the maximum power point against the operation window is checked.

8.1 Inverter conversion performance model

The inverter efficiency is the ratio of converted active AC power to input DC power, as shown in equation (8.1). The efficiency is a function of input power and voltage, as detailed in Subsection 8.1.1 and Subsection 8.1.2.

$$\eta_{inv}(V_{DC}, W_{DC}) = \frac{W_{inv}}{W_{DC}} \quad (8.1)$$

Where:

- η_{inv} is the inverter efficiency.
- V_{DC} is the input DC voltage, calculated using equation (7.3).
- W_{DC} is the input DC power, calculated using equation (7.5).
- W_{inv} is the active output AC power of the inverter.

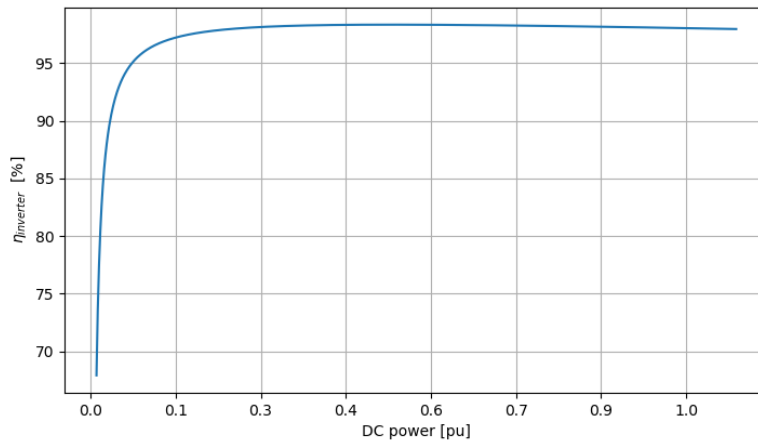


Figure 8.1: Example of efficiency curve obtained with synthetic model

The inverter efficiency η_{inv} is a function of input DC power and voltage. It is also a function of ambient temperature, given the dependency of auxiliary consumption on the cooling needs of the device, but this dependency is not usually modeled and its impact is very low at the usual operating power. The efficiency can be modeled using either a synthetic performance model, Subsection 8.1.1, which uses an equation for the efficiency, or by interpolating values from a series of curves provided by the inverter manufacturer, Subsection 8.1.2.

8.1.1 Synthetic performance model

The mathematical model used in this methodology to model the inverter efficiency when no manufacturer curves are available was described by Demoulias [49]. A procedure to compute the parameters needed to use this model is detailed in [50]. The model equation is (8.2), and an example of the curve obtained is shown in Figure 8.1. This model drops the dependency on input voltage.

$$\eta_{inv}(W_{DC}) = A + B \cdot W_{DC} + \frac{C}{W_{DC}} \tag{8.2}$$

Where:

- η_{inv} is the inverter efficiency.
- A , B and C are the equation coefficients.
- W_{DC} is the inverter input DC power.

In equation (8.2), the B coefficient commands losses at high input power, the C governs losses at very low input power, and the A coefficient is the constant component which dominates efficiency at the middle of the input power envelope.

The values of the parameters A , B and C are computed using the following data:

- An averaged efficiency value.
- The maximum efficiency value.
- The efficiency at the power threshold.

The power threshold is the minimum DC power by the inverter to generate any AC output. Therefore, at the power threshold, the efficiency value will be zero. Using this condition, along with the averaged and maximum efficiency values, a system of linear equations with three variables (the A , B and C parameters) can be established and solved.

The most accepted averaged efficiency definitions are the European efficiency, defined by Hotopp [51] and shown in equation (8.3), and the California Energy Commission (CEC) efficiency, found in [52] and shown in equation (8.4). The maximum efficiency value is defined as the efficiency at AC power equal to 60% of the nominal AC power.

The European averaged efficiency can be calculated using equation (8.3), as defined in [51].

$$\eta_{inv, euro} = 0.03 \cdot \eta_{5\%} + 0.06 \cdot \eta_{10\%} + 0.13 \cdot \eta_{20\%} + 0.10 \cdot \eta_{30\%} + 0.48 \cdot \eta_{50\%} + 0.20 \cdot \eta_{100\%} \quad (8.3)$$

Where:

- $\eta_{inv, euro}$ is the averaged inverter efficiency according to the European definition.
- $\eta_{x\%}$ is the inverter efficiency at $x\%$ of the nominal AC power.

The California Energy Commission (CEC) averaged efficiency can be calculated using equation (8.4), as defined in [52].

$$\eta_{inv, CEC} = 0.04 \cdot \eta_{10\%} + 0.05 \cdot \eta_{20\%} + 0.12 \cdot \eta_{30\%} + 0.21 \cdot \eta_{50\%} + 0.53 \cdot \eta_{75\%} + 0.05 \cdot \eta_{100\%} \quad (8.4)$$

Where:

- $\eta_{inv, CEC}$ is the averaged inverter efficiency according to the California Energy Commission (CEC) definition.
- $\eta_{x\%}$ is the inverter efficiency at $x\%$ of the nominal AC power.

8.1.2 Interpolated performance model

Whenever the efficiency curves provided by the manufacturer are available they should be used. The data may be available as:

- A set of three efficiency curves for three different DC input voltage values.
- A single efficiency curve for all DC input voltage values.

If three curves at different voltage values are available, the efficiency is calculated for the given DC power value for the three curves, and then the final efficiency value is interpolated given the input DC voltage. An example of efficiency curves provided by a manufacturer is shown in Figure 8.2. The interpolation is linear between the available values (that is, between the efficiency value at the minimum DC power value and the efficiency at the maximum DC power value). A linear interpolation was chosen because of its simplicity and predictability, and the error due to its use is very low in most cases because of the very small changes in efficiency at normal power values.

At low DC power values (between the efficiency value for the minimum DC power given and the power threshold), a linear interpolation is insufficient, because the inverter efficiency value rises quickly to high values once it starts production. In order to correctly model this section, the synthetic model described in Subsection 8.1.1 was used. The equation coefficients are solved using a system of three linear equations, built using the DC power threshold (with zero efficiency) plus the two first points of the available curves.

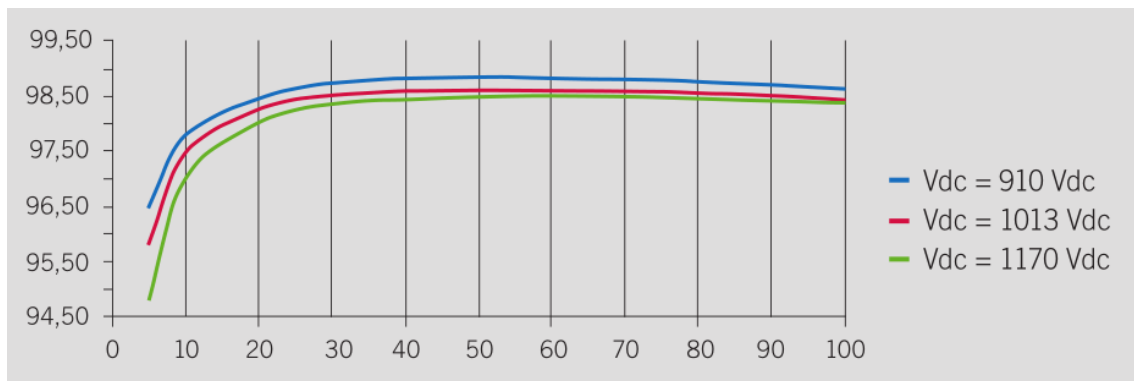


Figure 8.2: Example of inverter efficiency curves provided by a manufacturer [53]

8.2 Inverter operation window

The inverter can only generate AC power if certain conditions are met by the DC input. These conditions are:

- The input voltage is within a minimum and maximum value.
- The DC power exceeds the power threshold (related to the inverter self-consumption).
- The output AC power does not exceed the maximum inverter rated power.

These limitations mean not all operation points are possible, as shown in Figure 8.3. The curve shown in black is the $W(V)$ curve of the DC array (not an accurate representation). When the maximum power point of the DC array is outside the operation window, losses will be incurred due to the inverter being forced to change the operation point to a suitable voltage. In extreme cases no operation point may exist, causing the inverter not to produce any AC output.

Some instances where the inverter may be forced to change the operation point away from the maximum power point are shown in Figure 8.4. The curves shown in Figure 8.4 are just for representation purposes.

These are the possible scenarios in which the DC array operating point will change:

- If the MPP voltage does not exceed the minimum input voltage of the inverter, the operation point will slide to the minimum voltage, as shown in Figure 8.4 (a). If the power generated at V_{\min} does not reach the power threshold, the inverter will cut off production.
- If the MPP voltage exceeds the maximum voltage, the operation point will slide to the maximum voltage, as shown in Figure 8.4 (a). It may occur that at maximum voltage the power exceeds the maximum input power, in which case the voltage will be reduced until a possible operation point is found.
- If the power at the maximum power point does not exceed the power threshold, as shown in Figure 8.4 (b), no output AC power will be generated.
- If the power at the maximum power point exceeds the maximum power, as shown in Figure 8.4 (b), the operation point will slide towards the maximum voltage. This may happen not only because of excessive DC power, but also due to power factor requirements, as explained in Section 8.4.

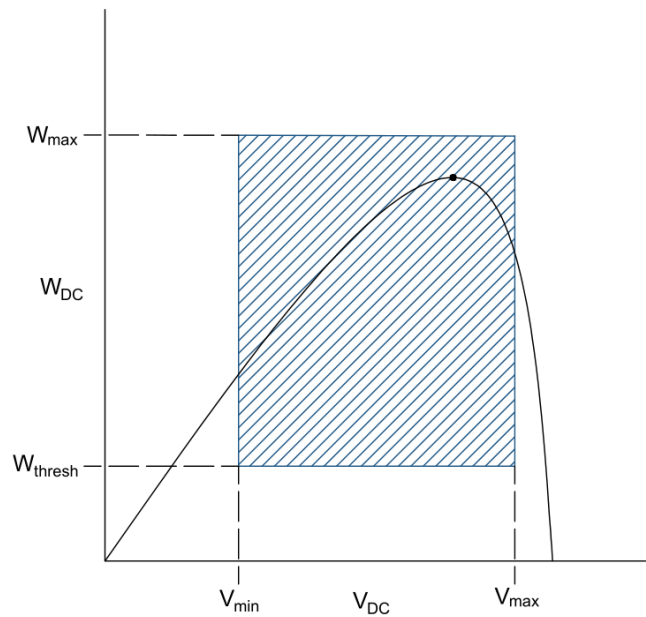


Figure 8.3: Graphical representation of the inverter operation window

The specific maximum power point tracking algorithm (MPPT) used by the inverter may change how the inverter responds to the situations described in Figure 8.4. Usually, MPPT systems will attempt to find a valid operation point by gradually decreasing the array voltage from the maximum input voltage, until reaching the minimum voltage. Operation points outside the operation window can therefore never be reached (the "slides" described in Figure 8.4 only serve representative purposes).

As explained in the introduction to this chapter, this methodology does not use a real, commercial MPPT algorithm. Instead, the algorithm tries to operate at the maximum power point of the DC array. If it is not possible to operate at that point (because of the power or voltage limits), then the DC array voltage is changed to the closest possible value in order to maximize production (shown in Figure 8.4). The process is described in Section 8.5.

8.3 Multiple MPPT inverter configuration

A single inverter may have several MPPT systems, each connected to a DC array. Multiple MPPT inverters present some challenges when programming a mathematical model to compute their operation. For instance, the efficiency model is referred to the whole inverter, as is the output power limit.

A conceptual representation of an MPPT array is shown in Figure 8.5.

In this methodology, the proposed solution is to let each MPPT compute the operation within the its voltage range, and the inverter model applies further changes to the operation point regarding overall power limits.

The process is described in detail in Section 8.5. When the inverter needs to lower the MPPT array output, because of the maximum output power limit, a specific DC power is calculated for each MPPT. The DC power value is calculated based on how much of the total DC power

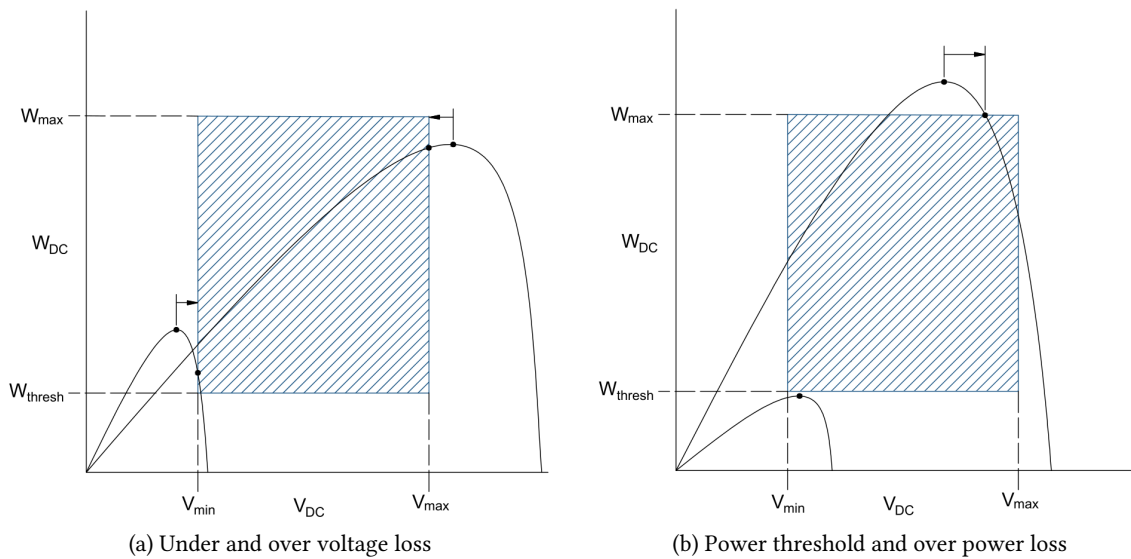


Figure 8.4: Losses due to MPP outside operation window

available each MPPT contributes. The total maximum admissible DC power value is calculated using the efficiency at maximum AC power output.

Then, each MPPT adjusts its operating point to match the required power output using the sliding operations described in Section 8.2. If the MPPT cannot match the required power output, an additional loss is perceived.

This approach has the additional advantage that it makes it easier to compute the different contributions of each loss type. First the contribution of the MPPT voltage limits is calculated when computing the "raw" MPPT output, and later on the output power limit is applied if exceeded.

8.4 Inverter apparent power output limit and power factor adjustment

In section Section 8.1 the inverter efficiency model is described. Equation (8.1) can be used to calculate the active power output of the inverter. To consider the effects of the inverter apparent power output limit and the power factor adjustment, further calculations have to be performed.

The inverter apparent power output limit is dependent on the ambient temperature. Inverter manufacturers usually specify the power limit of the inverter at different ambient temperature values, which yields a curve of power limit points (known as *kVA* curve).

The limits mandated by the *kVA* curve may be overridden by a modified inverter rating (e.g. if the inverter is de-rated because of elevation).

To compute the power limit at an unknown ambient temperature value, a linear interpolation methodology is recommended. In Figure 8.6 an example of the results obtained using linear interpolation is shown.

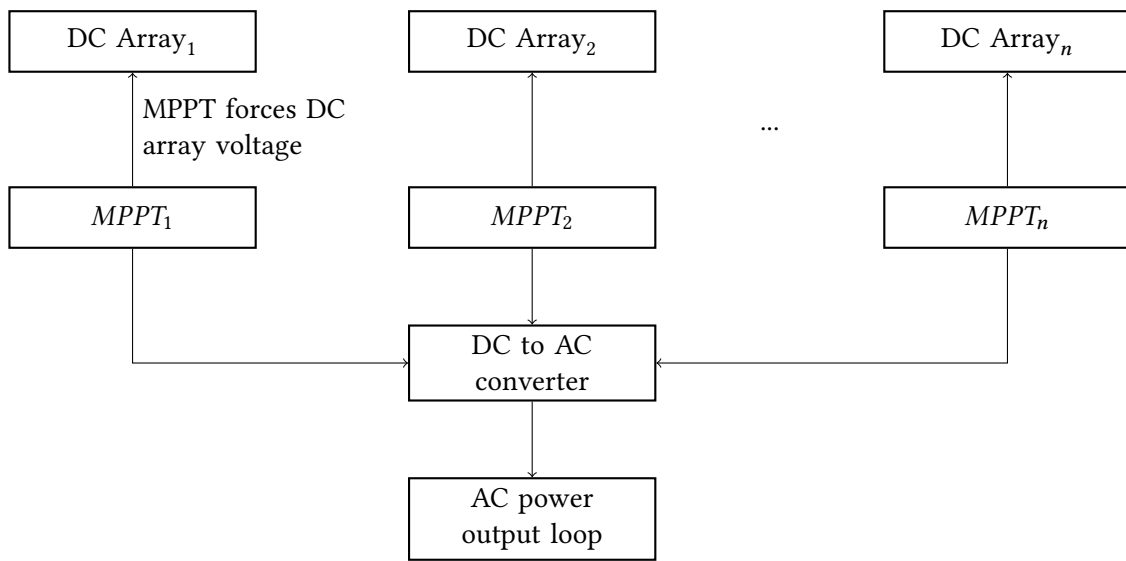


Figure 8.5: Array of MPPT systems in an inverter

The power factor adjustment is a requirement which mandates that at any given interval, the inverter should produce AC power at a given power factor value. To meet this requirement, the following calculation process is followed:

1. The active output power is calculated using equation (8.1).
2. The reactive power output is calculated using equation (8.5).
3. The apparent power output is calculated using equation (8.6).
4. The resulting apparent power output must be below the inverter apparent power output limit. If the power limit is exceeded, the inverter output is adjusted, and over power losses are incurred.

The inverter apparent power output and the power factor requirements are closely linked. With a power factor of 1, the power limit is directly translated to active power. However, as the power factor decreases, the apparent power output increases for the same active power output from the inverter efficiency model. This means that the power limit may be exceeded, resulting in over power losses.

The reactive power can be calculated using equation (8.5). The inverter apparent output power is calculated using equation (8.6).

$$Q_{inv} = W_{inv} \cdot \tan \phi \tag{8.5}$$

Where:

- Q_{inv} is the reactive power output of the inverter.
- W_{inv} is the active power output of the inverter.
- ϕ is the phase angle, which can be derived from the power factor as $\phi = \cos^{-1} \text{ pf}$, where pf is the desired inverter power factor.

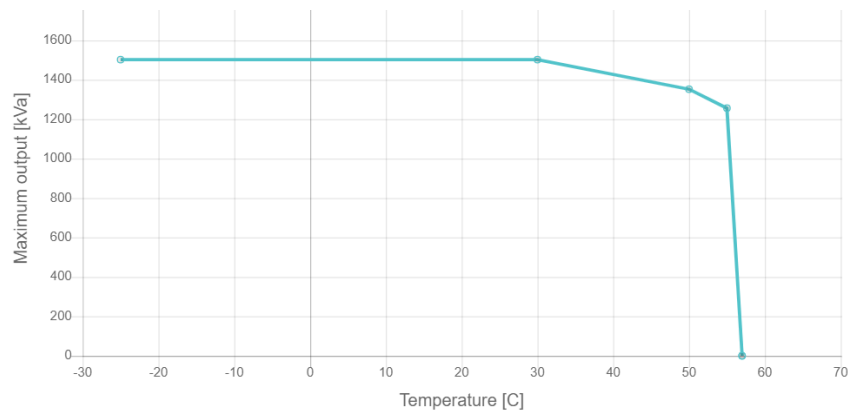


Figure 8.6: A sample kVA curve

$$S_{inv} = \sqrt{W_{inv}^2 + Q_{inv}^2} \tag{8.6}$$

Where:

- S_{inv} is the apparent power at the inverter output.
- W_{inv} is the active power output of the inverter.
- Q_{inv} is the reactive power output of the inverter.

8.5 Process diagram of the inverter power calculation

A process diagram showing the steps which are taken to calculate the power generated by an inverter is shown in Figure 8.7. The first step is for the MPPT array to compute the power in maximum power point conditions. The DC arrays will compute their power output at the maximum power point, and then the MPPT will apply its voltage limits. If the voltage threshold is not met (eg, the maximum power point voltage is below the threshold), the operation point will slide to the minimum MPPT voltage. If the maximum MPPT voltage is exceeded, the operation point slides to the maximum voltage. If in either case the production drops to zero, the array production will be zero and the loss will be attributed to the voltage limits.

After computing the power output of each MPPT, the inverter will check if the DC power exceeds the DC power threshold. If at this point the DC power threshold is not met, the inverter cannot start and the AC power production will be zero.

If the DC power threshold is exceeded, the conditions required for the inverter production are met. The next step is to compute the inverter efficiency, as described in Section 8.1. Because the efficiency model is referred to the entire inverter, the input for the model is the DC power output of the MPPT array, which is the sum of the individual MPPTs.

Finally, the inverter power output limit has to be respected. If the maximum apparent output power $S_{KVA\ lim}$ (the kVA limit described in Section 8.4) is exceeded by the apparent power calculated using equation (8.6), then the output of the MPPT array must be adjusted so that production does not exceed the limit. The power limit may be exceeded in two conditions:

- The MPPT array is producing too much DC power, which mostly happens if the DC/AC ratio is high.
- The power factor requirement is low.

In both conditions, a DC array voltage must be found which gives a production equal to $S_{KVA \text{ lim}}$. The MPPT array is responsible for finding the operating point at which the required power output is matched. A solution may not exist if the curve is completely "above" the operation window; however, this should be a rare occurrence, only possible in systems with high DC/AC ratio. The discarded DC power is the over power loss of the inverter.

Logically, the new operating point must also respect the MPPT voltage limits. If it was not possible to find an operating power point which meets the conditions, then production would be zero, and the loss would be assigned to over power losses. This may happen if, for example, the power at both the minimum voltage and the maximum voltage exceeds the required power output of the MPPT.

After applying the maximum power output limit, the production of the inverter has been found and the calculation process ends.

8.6 Auxiliary consumption inverter losses

A small part of the energy which feeds the inverter will be used by the inverter itself to power its own systems. The auxiliary power may be used to supply cooling systems (fans are the most significant auxiliary consumption), power electronics, and other control systems.

The auxiliary losses model presented in this methodology is equivalent to the PVSyst model [3]. The data required for the model is usually provided by the inverter manufacturers themselves.

To apply the auxiliary loss in the production intervals, a production threshold value must be exceeded, otherwise the loss will be null. The threshold is referred to DC input power in this methodology. In equation (8.7) the calculation model is shown.

$$W_{\text{aux}} = \begin{cases} 0 & \text{if } W_{\text{DC}} \leq W_{\text{thresh}} \\ W_{\text{aux load}} & \text{if } W_{\text{DC}} > W_{\text{thresh}} \end{cases} \quad (8.7)$$

Where:

- W_{aux} is the loss due to the inverter auxiliary consumption in production intervals.
- W_{DC} is the DC input power perceived by the inverter.
- W_{thresh} is minimum DC power threshold which must be exceeded in order for the loss at load to be applied.
- $W_{\text{aux load}}$ is the value of the auxiliary loss when the threshold is exceed.

The loss value calculated using equation (8.7) is then subtracted from the DC input power, before converting the power value to AC production.

In night intervals, a constant power value is consumed by the inverter in all intervals.

8.7 Inverter model input parameters

The inverter model must be supplied with the following parameters:

- The efficiency model for η_{inv} , in either of its two forms. The synthetic efficiency model requires:
 - The maximum efficiency of the inverter (assumed to be for a power value of $0.6 \cdot \eta_{nom}$).
 - The European averaged efficiency value. The CEC value is not yet implemented.

The interpolated performance model can take either one or three curves of efficiency. The following values are needed for each curve:

- The value of the power for each point (either input DC power or output AC power).
- The value of the efficiency for each point.
- If three curves are supplied, the input DC voltage for each.
- The nominal AC power.
- The DC power threshold, W_{thresh} .
- The minimum DC voltage for MPP search, V_{min} .
- The maximum DC voltage for MPP search, V_{max} .
- The AC output voltage, V_{AC} .
- The auxiliary consumption loss, $W_{aux\ load}$, and the loss activation threshold.
- The kVA curve, which requires, for each point:
 - The kVA apparent output power limit value.
 - The ambient temperature value.

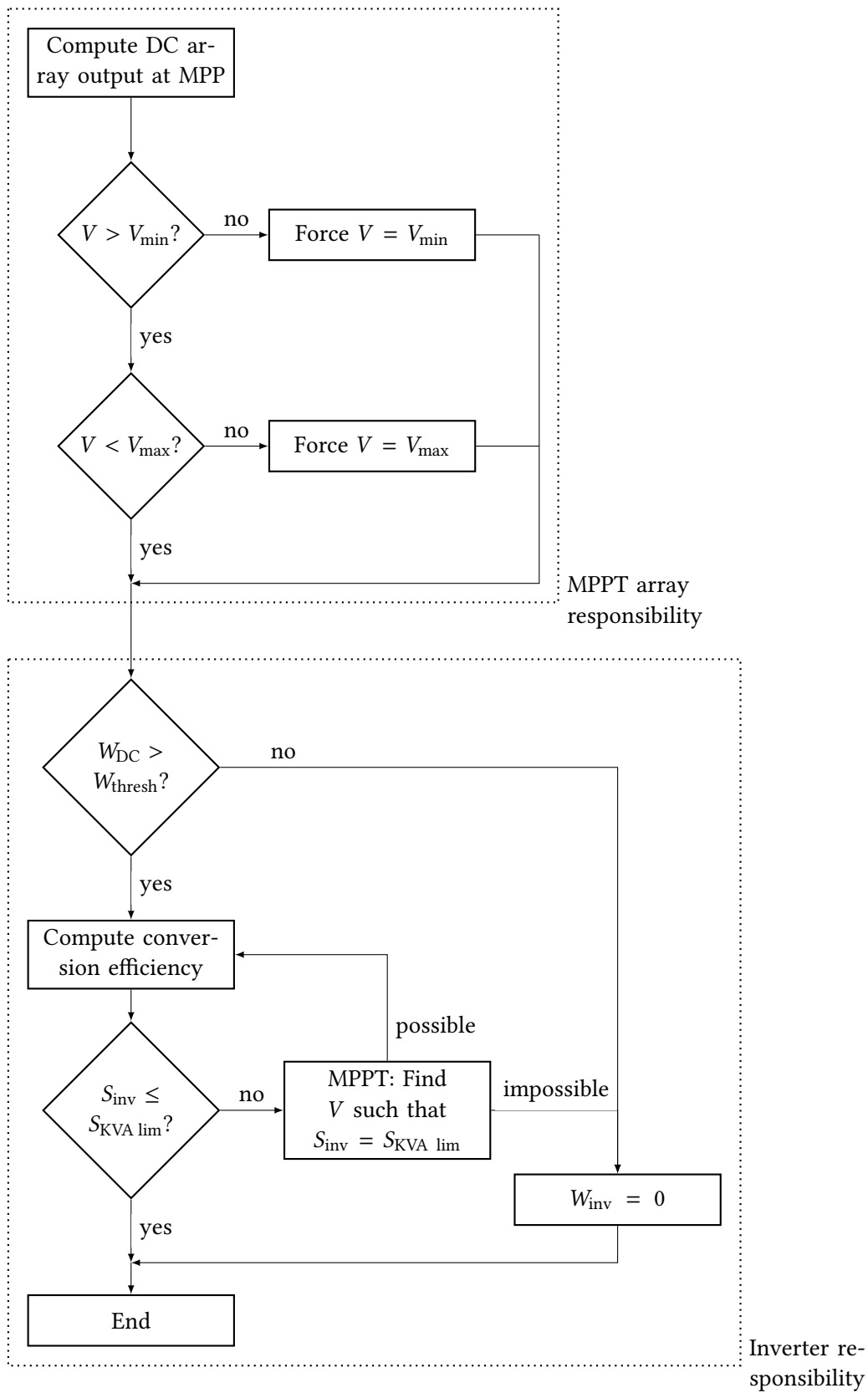


Figure 8.7: Simplified resolution process of a single interval

Chapter 9

Photovoltaic plant AC losses

The AC losses are defined as all the losses which take place after the conversion of DC power to AC power, excluding the losses incurred in the inverter itself. A basic diagram of these losses is shown in Figure 9.1. They are, in order:

1. Power lost in the cable from inverter to power station transformer. This loss is relevant in string inverter configurations.
2. Power station transformer loss (iron loss and copper loss).
3. Power lost in the cable from power station to substation.
4. Plant auxiliary consumption.
5. Substation loss, which is the loss in the substation transformer.
6. Power lost in the cable from substation to grid.
7. Availability loss.

In any AC electrical power transmission system, the power factor (cosine of ϕ) plays an important when sizing the system and calculating its operating conditions.

Photovoltaic plant inverters operate at a power factor other than the unit, in order to compensate reactive power consumption in the transmission system or to meet grid requirements. Depending on the specific value of the power factor at the inverter output, the reactive power consumption will have an important effect on the final energy production results.

In most cases, the power factor in the inverter output will be very close to the unit and can be disregarded. However, when stringent grid requirements must be met, the power factor may be lower, and thus it becomes necessary to take it into account when calculating the losses in the AC transmission system.

9.1 AC power cable losses

The three phase power cables in the power plant are modeled using the maximum admissible voltage drop used for sizing the cables in the pvDesign simulation.

The inverters are connected to the power station transformers in a Y (wye) layout. The power stations are connected to the substation in a Δ (delta) layout.

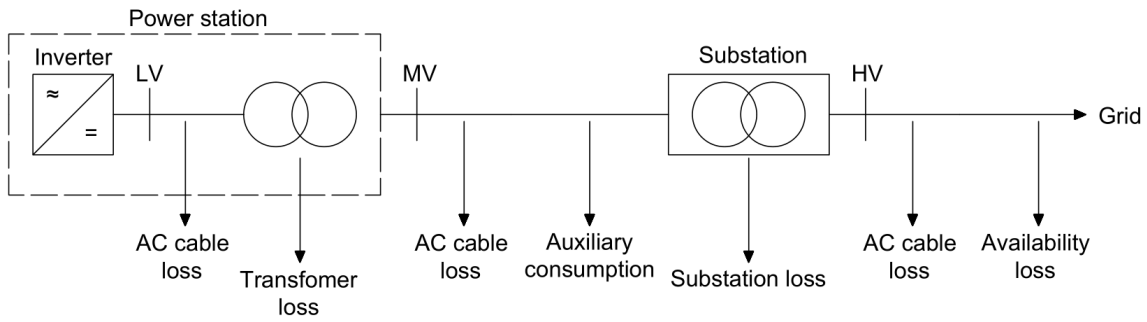


Figure 9.1: AC system losses

The first step is to calculate a phase resistance value using the maximum admissible voltage drop, using equation (9.1). The equation is formulated so that it can be used for Y and Δ configurations.

$$R_p = \frac{U_L \cdot \Delta V_{\max} \cdot \frac{1}{\text{pvm}}}{I_L \cdot \frac{1}{\text{pcm}}} \quad (9.1)$$

Where:

- R_p is the phase resistance.
- U_L is the cable line voltage.
- ΔV_{\max} is the maximum admissible voltage drop.
- pvm is the phase voltage multiplier, $\sqrt{3}$ for Y connection or 1 for Δ connection.
- I_L is the cable line current.
- pcm is the phase current multiplier, 1 for Y connection or $\sqrt{3}$ for Δ connection.

The three phase transmission line power loss can be calculated using equation (9.2).

$$W_{\text{loss}} = 3 \cdot R_p \cdot \left(I_L \cdot \frac{1}{\text{pcm}} \right)^2 \quad (9.2)$$

Where:

- W_{loss} is the transmission power loss.
- R_p is the cable phase resistance, calculated using equation (9.1).
- I_L is the transmission phase current.
- pcm is the phase current multiplier, 1 for Y connection or $\sqrt{3}$ for Δ connection.

9.2 Transformer losses

As shown in Figure 9.1, the photovoltaic power plant will have two transformers in different stages before the injection to grid. The first transformer is the power station transformer, and the second one is the substation transformer which raises the voltage to grid levels.

Any electrical transformer will lose energy in the process of raising voltage. The losses will be [54]:

- Core losses (iron loss), due to hysteresis and eddy-current in the core, a constant loss at all loads.
- Winding loss (copper loss), due to Joule heating in the conductor, dependent on the square of the current.

Because the transformers are inductive loads, the power factor at their output differs from the power factor at their input. This change can be modeled as reactive power consumption by the transformers, and combining the reactive power consumption with the active power losses yields the power factor the transformer output. Using the mathematical model described by Joksimovic [55], it is possible to compute the reactive power losses, given the active power losses and some basic transformer data.

Finally, if the active and reactive power losses are known, it is possible to compute the power factor at the transformer output.

9.2.1 Active power losses

The active power losses due to the core and winding components are calculated using equations (9.3) and (9.4).

$$W_{\text{iron}} = F_{\text{iron}} \cdot S_{\text{rated}} \quad (9.3)$$

Where:

- W_{iron} is the transformer iron loss.
- F_{iron} is the iron loss, in parts per one.
- S_{rated} is the transformer rated power, in [VA].

$$W_{\text{copper}} = F_{\text{copper}} \cdot S_{\text{rated}} \cdot x^2 \quad (9.4)$$

Where:

- W_{copper} is the transformer copper loss.
- F_{copper} is the copper loss, in parts per one.
- S_{rated} is the transformer rated power, in [VA].
- x is the load factor, calculated as the division of the apparent power at the transformer input by the rated power of the transformer.

9.2.2 Reactive power losses

The reactive power losses are calculated using the model described by Joksimovic [55]. The model uses an empirical approximation to calculate the no load current shown in equation (9.6), and the short circuit voltage to calculate the copper component reactive consumption.

The iron component of the reactive power consumption is calculated using equation (9.5).

$$Q_{\text{iron}} = \sqrt{\left(\frac{i_0}{100} \cdot S_{\text{rated}}\right)^2 - W_{\text{iron}}^2} \quad (9.5)$$

Where:

- Q_{iron} is the reactive consumption in the transformer due to the iron losses, in [VAR].

- i_0 is the no load current, in percentage value, calculated using (9.6).
- S_{rated} is the transformer rated power, in [VA].
- W_{iron} is the transformer iron loss, calculated using equation (9.3).

The no load current can be estimated using equation (9.6). In Joksimovic [55], this equation is referred to the transformer rated power in MVA.

$$i_0 = 0.0421 \cdot (\log(S_{\text{rated}} \cdot 10^{-6}))^2 - 0.4384 \cdot \log(S_{\text{rated}} \cdot 10^{-6}) + 1.6064 \quad (9.6)$$

Where:

- i_0 is the no load current, in percentage value.
- S_{rated} is the transformer rated power, in [VA].

The copper component of the reactive power consumption is calculated using equation (9.7).

$$Q_{\text{copper}} = x^2 \cdot \sqrt{\left(\frac{u_{\text{sc}}}{100} \cdot S_{\text{rated}}\right)^2 - W_{\text{copper}}^2} \quad (9.7)$$

Where:

- Q_{copper} is the reactive consumption in the transformer due to the copper losses, in [VAR].
- x is the load factor, calculated as the division of the apparent power at the transformer input by the rated power of the transformer.
- u_{sc} is the short circuit voltage percentage.
- S_{rated} is the transformer rated power, in [VA].
- W_{copper} is the transformer copper loss, calculated using equation (9.4).

The short circuit voltage percentage, u_{sc} , takes a value of 8 for power station transformers and 12.5 for the substation transformer [56].

9.3 Auxiliary consumption

The photovoltaic power plant will consume electrical energy to operate, in order power its own systems. These systems may be the electrical motors in sun-tracking systems, control electronics, lighting and security, etc.

The auxiliary consumption can be modeled as having two components, one constant and one variable. A third component may be introduced which would be the auxiliary consumption during nighttime, which would have a constant value. All losses are applied before the substation transformer losses are applied, as shown in Figure 9.1.

The constant auxiliary consumption at load and off-load is directly subtracted from the plant output AC power. The variable loss is computed as a percentage of the output AC power. The final AC output power at the substation input is computed using equation (9.8).

$$W_{\text{in, subs}} = W_{\text{out, pss}} - W_{\text{aux, const}} - W_{\text{out, pss}} \cdot F_{\text{aux, var}} \quad (9.8)$$

Where:

- $W_{\text{in, subs}}$ is the power at the substation input after applying auxiliary losses.

- $W_{\text{out, pss}}$ is the combined output power of all the power stations in the photovoltaic power plant, after applying the AC power cable loss.
- $W_{\text{aux, const}}$ is the constant auxiliary consumption.
- $F_{\text{aux, var}}$ is the variable auxiliary consumption factor.

9.4 Availability losses

The photovoltaic power plant may be unable to produce due to scheduled stops for maintenance or because of equipment failure. It is also possible for the grid to be unavailable in some countries.

These losses are modeled as a constant loss at every instant of the year, applied at the point of injection to grid. The final power injected to grid is calculated using equation (9.9). The loss factor may be split into two components, one for the plant availability and one for the grid availability.

$$W_{\text{grid}} = W_{\text{inj, grid}} \cdot F_{\text{availability}} \quad (9.9)$$

Where:

- W_{grid} is the power injected to the grid.
- $W_{\text{inj, grid}}$ is the power at the grid injection point, having applied the AC power loss in the cable from substation to grid.
- $F_{\text{availability}}$ is the availability loss factor, in parts per one, for either plant or grid.

Chapter 10

Annual aggregate results and losses

The annual aggregate results are the total yearly production and overall losses. The losses are particularly important, as they reflect specific aspects of the photovoltaic plant performance and may be used to compare different designs.

Another critical indicator is the Performance Ratio (PR), which is used to measure the plant efficiency.

10.1 Annual energy production

The annual production can be calculated by adding up the production of each individual hourly or sub-hourly interval. The production is considered positive if the plant is injecting energy to the grid and negative if it is consuming (which may happen in nighttime if certain auxiliary consumption are enabled).

Another key aspect of computing the yearly production is the treatment of sunrise and sunset intervals. Synthetic TMY hourly generators will multiply this intervals by the irradiated time to make them equivalent to fully-irradiated hours [57] (e.g. an hour in which only 20 minutes were irradiated with an intensity of 300 W/m^2 will yield a final irradiance value of $20/60 \cdot 300 = 100 \text{ W/m}^2$). However, this does not mean the sun position is calculated as if the interval was fully irradiated, as explained in Subsection 2.1.1.

Therefore, the partially irradiated sunrise and sunset intervals of each day are not treated any differently from the other fully irradiated intervals, and the yearly value is calculated adding up all intervals. Thus, for any given annual aggregate variable to be computed, the equation (10.1) is used.

$$x_{\text{annual}} = \sum_{i=1}^{i=n_{\text{interval}}} x_i \quad (10.1)$$

Where:

- x_{annual} is the annual aggregate of any particular variable x .

- $n_{interval}$ is the number of intervals in one year. For hourly TMYs, 8760; for 15-minute TMYs, 35040; for 5-minute TMYs, 105120; and for 1-minute TMYs, 525600.
- x_i is the value of the variable in each interval.

The variables for which the annual aggregate is computed are:

- GHI Global horizontal irradiance.
- G_{eff} Global effective irradiance.
- $E_{arr\ STC}$ The energy generated by the DC array feeding an inverter if it operated at STC conditions in all intervals.
- $E_{arr\ MPP}$ The energy generated by the DC array feeding an inverter if it operated at its maximum power point in all intervals.
- E_{inv} The energy generated by the inverter.
- E_{plant} The energy generated by the photovoltaic plant (at the substation output, the cable from plant to grid is not included and availability losses are not included).
- $E_{to\ grid}$ The energy injected to grid, including all losses.

10.2 Photovoltaic plant performance ratio

The performance ratio for photovoltaic power plants was defined by the IEC (International Electrotechnical Commission) in 1998 [58]. A detailed analysis of the parameter can be found in [59]. The performance ratio can be calculated using equation (10.2).

$$PR = \frac{\sum_i E_{to\ grid, i}}{n_{mods} \cdot W_{mod\ STC} \cdot \sum_i \frac{G_{POA, i}}{G_{STC, i}}} \quad (10.2)$$

Where:

- PR is the plant performance ratio.
- $E_{to\ grid, i}$ is the energy injected to grid, including all losses, for the interval i .
- n_{mods} is the total number of photovoltaic modules in the plant.
- $W_{mod\ STC}$ is the power generated by a module in STC conditions.
- $G_{POA, i}$ is the irradiance on the plane of array, for the interval i .
- $G_{STC, i}$ is the reference irradiance of the STC test (same for all intervals), for the interval i .

When performing bifacial simulations, the value of $G_{POA, i}$ will be the front face irradiance. This may result in performance ratios higher than 100% in some instances, specially if the ground albedo is high.

10.3 Specific production

The specific production is defined as the ratio of energy production to peak DC power of a photovoltaic plant. It can be calculated using equation (10.3). The specific production is usually given in kWh/kWp.

$$E_{spec} = \frac{E_{to\ grid, i}}{W_{peak}} \quad (10.3)$$

Where:

- E_{spec} is the specific production of the PV plant.
- $E_{\text{to grid}}$ is the energy injected to grid, including all losses, for one year of production.
- W_{peak} is the peak DC power of the PV plant.

10.4 Bifaciality gain

When simulating the production of PV plants using bifacial modules, it is interesting to quantify the gain obtained from using bifacial modules. This methodology uses the bifaciality gain definition found in [19], which removes the effect of the bifacial mismatch effect.

$$BG = \varphi_{\text{Pmax}} \cdot (1 - F_{\text{bif mis}}) \cdot \frac{I_r}{I_f} \quad (10.4)$$

Where:

- BG is the bifacial gain in parts per one.
- φ_{Pmax} is the bifaciality factor for power output, described in Section 6.3.
- $F_{\text{bif mis}}$ is the bifacial mismatch loss, with 0 representing no loss.
- I_r is the yearly back face irradiance.
- I_f is the yearly front face irradiance.

10.5 Computing the aggregate loss factors

The loss factors should be a quick indicator of the losses in each step of the calculation process. Furthermore, they should be defined to yield the final energy injected to grid if applied successively to the power generated by the array in STC efficiency (that is, if the module converted the solar energy at its maximum efficiency). This condition is expressed in general terms in equation (10.5). The positive sign is due to the definition of loss factor, which takes negative value if it's a loss.

$$x_1 = x_0 \cdot (1 + f_1) \cdot (1 + f_2) \cdot \dots \cdot (1 + f_n) \quad (10.5)$$

Where:

- x_1 is the final value of the variable x after all losses were applied.
- x_0 is the initial value of the variable x before any losses.
- f_n is a loss factor, in parts per one.

The losses will be separated in three categories, depending on the kind of energy being converted. The final irradiance after all losses, global effective irradiance G_{eff} , can be converted to electrical energy using the module efficiency at STC conditions, calculated using equation (6.5).

The process of calculating the loss factors will involve using the energy generated at each step sequentially to compute the loss factors.

The factors will be called "losses" regardless of whether or not they are actually a loss (e.g. the loss due to the plane tilt will actually always be a gain). Thus, losses may be of positive value if they are a gain, or negative if they are a loss.

Loss factor	Equation
Transposition to the plane of array	$f_{\text{plane}} = \frac{I_{\text{POA}}}{I_{\text{GHI}}} - 1$
Far shadings	$f_{\text{far shadings}} = \frac{I_{\text{after far}}}{I_{\text{POA}}} - 1$
Near shadings	$f_{\text{near shadings}} = \frac{I_{\text{after near}}}{I_{\text{after far}}} - 1$
Incidence angle modifier	$f_{\text{IAM}} = \frac{I_{\text{after IAM}}}{I_{\text{after near}}} - 1$
Soiling	$f_{\text{soiling}} = -F_{\text{soiling}}$

Table 10.1: Irradiance loss factors

Unless otherwise stated, the energies (E variables) and irradiances (I variables) are the annual aggregates.

10.5.1 Irradiance losses and shadows

The irradiance losses encompass any effect which reduces (or increases) the amount of irradiance which reaches the plane of array. The factors are calculated using the equations shown in Table 10.1.

In Table 10.1, the values used to compute the loss factors are:

- I_{POA} is the irradiance on the plane of array.
- I_{GHI} is the global horizontal irradiance.
- $I_{\text{after far}}$ is the irradiance after applying the horizon effect.
- $I_{\text{after near}}$ is the irradiance after applying the near shading effects.
- $I_{\text{after IAM}}$ is the irradiance after applying the incidence angle modifier.
- F_{soiling} is the soiling factor in parts per one.

10.5.2 Photovoltaic module and DC array losses

The photovoltaic conversion of irradiance to electrical energy which takes place in the photovoltaic modules is represented as a series of losses shown in Table 10.2. The starting energy value for the losses in this table is calculated using equation (10.6)

$$E_{\text{STC}} = \eta_{\text{STC}} \cdot I_{\text{GHI}} \cdot n_{\text{mods}} \cdot A_{\text{mod}} \cdot (1 + f_1) \cdot (1 + f_2) \cdot \dots \cdot (1 + f_n) \quad (10.6)$$

Where:

- E_{STC} is the energy generated by the photovoltaic module at STC efficiency.
- η_{STC} is the module efficiency in STC conditions, calculated using equation (6.5).
- I_{GHI} is the global horizontal irradiance.
- n_{mods} is the total number of photovoltaic modules in the plant.
- A_{mod} is the receptive surface area of a module.
- f_n are the loss factors, in parts per one, calculated using Table 10.1.

The loss factors for the photovoltaic module and DC array are calculated using Table 10.2.

Loss factor	Equation
Irradiance level	$f_{\text{irrad}} = \frac{E_{\text{mod at STC temp}}}{E_{\text{STC}}} - 1$
Cell temperature	$f_{\text{temp}} = \frac{E_{\text{mod at MPP}}}{E_{\text{mod at STC temp}}} - 1$
Module quality	$f_{\text{qua}} = \frac{E_{\text{after qua}}}{E_{\text{mod at MPP}}} - 1$
Light induced degradation	$f_{\text{LID}} = \frac{E_{\text{after LID}}}{E_{\text{after qua}}} - 1$
Mismatch factor	$f_{\text{mis}} = \frac{E_{\text{after mis}}}{E_{\text{after LID}}} - 1$
Partial shadings	$f_{\text{par shadings}} = \frac{E_{\text{after partial shadings}}}{E_{\text{after mis}}} - 1$
DC cables	$f_{\text{DC cables}} = \frac{E_{\text{after cable loss}}}{E_{\text{after partial shadings}}} - 1$

Table 10.2: Photovoltaic module and DC array loss factors

In Table 10.2, the values used to compute the loss factors are:

- $E_{\text{mod at STC temp}}$ is the energy that the photovoltaic module would produce if it was at a constant temperature equal to the STC temperature.
- E_{STC} is the energy generated by the photovoltaic module at STC efficiency, calculated using equation (10.6).
- $E_{\text{mod at MPP}}$ is the energy the photovoltaic modules produce at their maximum power point.
- $E_{\text{after qua}}$ is the energy the photovoltaic modules produce after applying the module quality loss.
- $E_{\text{after LID}}$ is the energy the photovoltaic modules produce after applying the light induced degradation loss.
- $E_{\text{after mis}}$ is the energy the photovoltaic modules produce after applying the mismatch loss.
- $E_{\text{after partial shadings}}$ is the energy produced by the DC array after applying the loss which arises due to partial shadings in the array (the mismatch loss generated by shadows).
- $E_{\text{after cable loss}}$ is the energy produced by the DC array after applying the transmission loss of the cables.

10.5.3 Inverter losses

The losses incurred in the inverter are calculated using the equations shown in Table 10.3.

In Table 10.3, the energy values used to compute the loss factors are:

- $E_{\text{inv after efficiency}}$ is the inverter output energy after applying the inverter efficiency.
- $E_{\text{inv after max pow}}$ is the inverter output energy after applying the maximum power limit.
- $E_{\text{inv after W thresh}}$ is the inverter output energy after applying the power threshold.
- $E_{\text{inv after max V}}$ is the inverter output energy after applying the maximum input voltage limit.
- $E_{\text{inv after V thresh}}$ is the inverter output energy after applying the voltage threshold.
- $E_{\text{inv after aux}}$ is the inverter energy output after subtracting the inverter auxiliary losses.

Loss factor	Equation
Inverter efficiency	$f_{inv\ eff} = \frac{E_{inv\ after\ efficiency}}{E_{after\ cable\ loss}} - 1$
Inverter over power	$f_{inv\ over\ W} = \frac{E_{inv\ after\ max\ pow}}{E_{inv\ after\ efficiency}} - 1$
Inverter power threshold	$f_{inv\ W\ thresh} = \frac{E_{inv\ after\ W\ thresh}}{E_{inv\ after\ max\ pow}} - 1$
Inverter over voltage	$f_{inv\ over\ V} = \frac{E_{inv\ after\ max\ V}}{E_{inv\ after\ W\ thresh}} - 1$
Inverter voltage threshold	$f_{inv\ V\ thresh} = \frac{E_{inv\ after\ V\ thresh}}{E_{inv\ after\ max\ V}} - 1$
Inverter auxiliary consumption	$f_{inv\ aux} = \frac{E_{inv\ after\ aux}}{E_{inv\ after\ V\ thresh}} - 1$

Table 10.3: Inverter loss factors

Loss factor	Equation
Inverter to transformer line	$f_{inv\ to\ trafo} = \frac{E_{PS\ trafo\ input}}{E_{inv\ after\ aux}} - 1$
Power station transformer	$f_{PS\ trafo} = \frac{E_{after\ PS\ trafo}}{E_{PS\ trafo\ input}} - 1$
Power station to substation line	$f_{PS\ to\ sub} = \frac{E_{sub\ input}}{E_{after\ PS\ trafo}} - 1$
Plant auxiliary consumption	$f_{plant\ aux} = \frac{E_{after\ plant\ aux}}{E_{sub\ input}} - 1$
Substation transformer	$f_{sub\ trafo} = \frac{E_{after\ sub\ trafo}}{E_{after\ plant\ aux}} - 1$
Substation to grid line	$f_{sub\ to\ grid} = \frac{E_{to\ grid}}{E_{after\ sub\ trafo}} - 1$
Availability	$f_{ava} = \frac{E_{after\ availability}}{E_{to\ grid}} - 1$

Table 10.4: AC transmission loss factors

10.5.4 AC transmission losses

The losses which occur between the inverter output and the final grid injection point (plus availability losses) are calculated using the equations shown in Table 10.4.

In Table 10.4, the energy values used to compute the loss factors are:

- $E_{PS\ trafo\ input}$ is the energy at the power station transformer input (after applying the transmission loss from inverter to transformer).
- $E_{after\ PS\ trafo}$ is the power station transformer output energy.
- $E_{sub\ input}$ is the energy at the substation input (after applying the transmission loss from power station to substation).
- $E_{after\ plant\ aux}$ is the energy at the substation input after subtracting the plant auxiliary consumption.
- $E_{after\ sub\ trafo}$ is the substation transformer output energy.
- $E_{to\ grid}$ is the energy at the grid injection point (after applying the transmission loss from substation to grid).

- $E_{\text{after availability}}$ is the energy injected to grid after applying the availability loss.

10.6 Energy production in sub-hourly timesteps

To aggregate the results of each interval into the yearly production, a conversion is necessary. The instant power generated at each interval is converted into energy produced, using equation (10.7).

$$E_{\text{interval}} = W_{\text{interval}} \cdot \frac{t_{\text{interval}}}{60} \quad (10.7)$$

Where:

- E_{interval} is the energy produced during the interval [Wh].
- W_{interval} is the power generated at the reference instant of the interval [W].
- t_{interval} is resolution of the interval in minutes (15 minutes, 5 minutes or 1 minute).

Bibliography

- [1] SolarGIS, *Solar resource maps of world*. [Online]. Available: <https://solargis.com/maps-and-gis-data/download/world>.
- [2] A. Mermoud and T. Lejeune, "Performance assessment of a simulation model for pv modules of any available technology," in (Proceedings of the 25th European Photovoltaic Solar Energy Conference), Proceedings of the 25th European Photovoltaic Solar Energy Conference. München: WIP, 2010, ISBN: 3936338264. [Online]. Available: <https://archive-ouverte.unige.ch/unige:38547>.
- [3] A. Mermoud, "Pvsyst: Software for the study and simulation of photovoltaic systems," *ISE, University of Geneva*, www.pvsyst.com, 2012.
- [4] NREL MIDC. "National Renewable Energy Laboratory Measurement and Instrumentation Data Center (NREL MIDC) Solar Position and Intensity (SOLPOS) Calculator." (2010), [Online]. Available: <http://www.nrel.gov/midc/solpos/solpos.html>.
- [5] J. A. Duffie and W. A. Beckman, *Solar engineering of thermal processes*. John Wiley & Sons, 2013.
- [6] P. Gilman, *SAM photovoltaic model technical reference*, 2015.
- [7] W. F. Marion and A. P. Dobos, *Rotation angle for the optimum tracking of one-axis trackers*, 2013.
- [8] R. Perez, P. Ineichen, R. Seals, J. Michalsky, and R. Stewart, "Modeling daylight availability and irradiance components from direct and global irradiance," *Solar Energy*, vol. 44, no. 5, pp. 271–289, 1990.
- [9] R. Perez, R. Stewart, R. Seals, and T. Guertin, *The development and verification of the Perez diffuse radiation model*, 1988.
- [10] T. Markvart, A. McEvoy, and L. Castaner, *Practical Handbook of Photovoltaics: Fundamentals and Applications*. Elsevier Science, 2003, ISBN: 9781856173902.
- [11] "Modis bidirectional reflectance distribution function (brdf) / albedo parameter." (2020), [Online]. Available: <https://modis.gsfc.nasa.gov/data/dataproduct/mod43.php>.
- [12] "Solargis: Methodology - albedo data." (2020), [Online]. Available: <https://solargis.com/docs/methodology/albedo>.
- [13] M. Gul, Y. Kotak, T. Muneer, and S. Ivanova, "Enhancement of albedo for solar energy gain with particular emphasis on overcast skies," *Energies 2018*, vol. 11, 2018. DOI: <https://doi.org/10.3390/en1112881>.

- [14] M. Iqbal, *An Introduction To Solar Radiation*. Elsevier Science, 1983, ISBN: 9780323151818. DOI: <https://doi.org/10.1016/B978-0-12-373750-2.X5001-0>.
- [15] B. Marion, “Numerical method for angle-of-incidence correction factors for diffuse radiation incident photovoltaic modules,” *Solar Energy*, vol. 147, pp. 344–348, May 2017. DOI: [10.1016/j.solener.2017.03.027](https://doi.org/10.1016/j.solener.2017.03.027).
- [16] A. Souka and H. Safwat, “Determination of the optimum orientations for the double-exposure, flat-plate collector and its reflectors,” *Solar Energy*, vol. 10, no. 4, pp. 170–174, 1966.
- [17] A. Mermoud, “Conception et dimensionnement de systèmes photovoltaïques : Introduction des modules pv en couches minces dans le logiciel pvsyst,” CUEPE, Tech. Rep., 2005. [Online]. Available: <https://archive-ouverte.unige.ch/unige:38786>.
- [18] E. Sjerps-Koomen, E. Alsema, and W. Turkenburg, “A simple model for PV module reflection losses under field conditions,” *Solar Energy*, vol. 57, no. 6, pp. 421–432, Dec. 1996. DOI: [10.1016/S0038-092X\(96\)00137-5](https://doi.org/10.1016/S0038-092X(96)00137-5).
- [19] S. Ayala, C. Deline, S. M. MacAlpine, B. Marion, J. S. Stein, and R. K. Kostuk, “Comparison of bifacial solar irradiance model predictions with field validation,” *IEEE Journal of Photovoltaics*, vol. 9, no. 1, pp. 82–88, Jan. 2019. DOI: [10.1109/jphotov.2018.2877000](https://doi.org/10.1109/jphotov.2018.2877000).
- [20] C. K. Lo, Y. S. Lim, and F. A. Rahman, “New integrated simulation tool for the optimum design of bifacial solar panel with reflectors on a specific site,” *Renewable Energy*, vol. 81, pp. 293–307, Sep. 2015. DOI: [10.1016/j.renene.2015.03.047](https://doi.org/10.1016/j.renene.2015.03.047).
- [21] G. Larson and R. Shakespeare, *Rendering with Radiance: The Art and Science of Lighting Visualization* (Computer Graphics and Geometric Modeling Series). Morgan Kaufmann, 1998, ISBN: 9781558604995.
- [22] C. Deline, S. MacAlpine, B. Marion, F. Toor, A. Asgharzadeh, and J. S. Stein, “Assessment of bifacial photovoltaic module power rating methodologies—inside and out,” *IEEE Journal of Photovoltaics*, vol. 7, no. 2, pp. 575–580, Mar. 2017. DOI: [10.1109/jphotov.2017.2650565](https://doi.org/10.1109/jphotov.2017.2650565).
- [23] B. Marion, S. MacAlpine, C. Deline, et al., “A practical irradiance model for bifacial PV modules,” in *2017 IEEE 44th Photovoltaic Specialist Conference (PVSC)*, IEEE, Jun. 2017. DOI: [10.1109/pvsc.2017.8366263](https://doi.org/10.1109/pvsc.2017.8366263).
- [24] M. A. Anoma, D. Jacob, B. C. Bourne, J. A. Scholl, D. M. Riley, and C. W. Hansen, “View factor model and validation for bifacial PV and diffuse shade on single-axis trackers,” in *2017 IEEE 44th Photovoltaic Specialist Conference (PVSC)*, IEEE, Jun. 2017. DOI: [10.1109/pvsc.2017.8366704](https://doi.org/10.1109/pvsc.2017.8366704).
- [25] S. Ayala, C. Deline, P. Greenberg, J. S. Stein, and R. K. Kostuk, “Model and validation of single-axis tracking with bifacial PV,” *IEEE Journal of Photovoltaics*, vol. 9, no. 3, pp. 715–721, May 2019. DOI: [10.1109/jphotov.2019.2892872](https://doi.org/10.1109/jphotov.2019.2892872).
- [26] J. Guerrero-Perez and J. Navarro, “Bitec: How to simulate bifacial projects?,” 2019. [Online]. Available: https://www.solarnews.es/wp-content/uploads/2019/07/BiTEC-whitepaper-2_en_compressed.pdf.
- [27] “Soltec - manufacturer of solar trackers.” (2020), [Online]. Available: <https://soltec.com/>.
- [28] D. Hamilton and W. Morgan, “Radiant-interchange configuration factors,” 1952. [Online]. Available: <https://ntrs.nasa.gov/search.jsp?R=19930083529>.

- [29] C. Hansen, “Estimating parameters for the pvsyst version 6 photovoltaic module performance model,” Sandia National Lab.(SNL-NM), Albuquerque, NM (United States), Tech. Rep., 2015.
- [30] A. R. Jordehi, “Parameter estimation of solar photovoltaic (pv) cells: A review,” *Renewable and Sustainable Energy Reviews*, vol. 61, pp. 354–371, 2016.
- [31] J. Kiusalaas, *Numerical methods in engineering with Python 3*. Cambridge university press, 2013.
- [32] D. Faiman, “Assessing the outdoor operating temperature of photovoltaic modules,” *Progress in Photovoltaics: Research and Applications*, vol. 16, no. 4, pp. 307–315, 2008.
- [33] J. P. Singh, A. G. Aberle, and T. M. Walsh, “Electrical characterization method for bifacial photovoltaic modules,” *Solar Energy Materials and Solar Cells*, vol. 127, pp. 136–142, Aug. 2014. DOI: [10.1016/j.solmat.2014.04.017](https://doi.org/10.1016/j.solmat.2014.04.017).
- [34] N. DiOrio and C. Deline. “Bifacial simulation in sam.” (Sep. 2018), [Online]. Available: <https://www.nrel.gov/docs/fy18osti/72360.pdf>.
- [35] J. Libal and R. Kopecek, Eds., *Bifacial Photovoltaics: Technology, applications and economics*. Institution of Engineering and Technology, Oct. 2018. DOI: [10.1049/pbpo107e](https://doi.org/10.1049/pbpo107e).
- [36] R. Kopecek, Y. Veschetti, E. Gerritsen, et al., “Bifaciality: One small step for technology, one giant leap for kwh cost reduction,” 2014.
- [37] D. C. Jordan, J. H. Wohlgemuth, and S. R. Kurtz, *Technology and climate trends in pv module degradation: Preprint*, 2012.
- [38] R. M. Smith, D. C. Jordan, and S. R. Kurtz, *Outdoor PV Module Degradation of Current-voltage Parameters: Preprint*, 2012.
- [39] E. L. Meyer and E. E. V. Dyk, “Assessing the reliability and degradation of photovoltaic module performance parameters,” *IEEE Transactions on Reliability*, vol. 53, no. 1, pp. 83–92, 2004.
- [40] B. Sopori, P. Basnyat, S. Devayajanam, et al., “Understanding light-induced degradation of c-si solar cells,” in *Photovoltaic Specialists Conference (PVSC), 2012 38th IEEE*, IEEE, 2012, pp. 001 115–001 120.
- [41] C. Deline, S. Ayala, S. MacAlpine, and C. Olalla, “Bifacial pv system mismatch loss estimation and parameterization,” Oct. 2019. [Online]. Available: <https://www.nrel.gov/docs/fy20osti/73541.pdf>.
- [42] M. Lee and A. Panchula, “Spectral correction for photovoltaic module performance based on air mass and precipitable water,” in *2016 IEEE 43rd Photovoltaic Specialists Conference (PVSC)*, IEEE, 2016, pp. 1351–1356.
- [43] C. Gueymard, “Analysis of monthly average atmospheric precipitable water and turbidity in canada and northern united states,” *Solar Energy*, vol. 53, no. 1, pp. 57–71, 1994.
- [44] J. D. Garrison and G. P. Adler, “Estimation of precipitable water over the united states for application to the division of solar radiation into its direct and diffuse components,” *Solar Energy*, vol. 44, no. 4, pp. 225–241, 1990.

- [45] C. Gueymard, "Assessment of the accuracy and computing speed of simplified saturation vapor equations using a new reference dataset," *Journal of Applied Meteorology and Climatology*, vol. 32, no. 7, pp. 1294–1300, 1993.
- [46] J. Merten, J. Asensi, C. Voz, A. Shah, R. Platz, and J. Andreu, "Improved equivalent circuit and analytical model for amorphous silicon solar cells and modules," *IEEE Transactions on electron devices*, vol. 45, no. 2, pp. 423–429, 1998.
- [47] RatedPower. "pvDesign: software to make the design and engineering of Solar Photovoltaic plants." (2017), [Online]. Available: <https://www.ratedpower.com/>.
- [48] A. Mermoud and T. Lejeune, "Partial shadings on pv arrays: By-pass diode benefits analysis," 2010.
- [49] C. Demoulias, "A new simple analytical method for calculating the optimum inverter size in grid-connected pv plants," *Electric Power Systems Research*, vol. 80, no. 10, pp. 1197–1204, 2010.
- [50] R. S. Faranda, H. Hafezi, S. Leva, M. Mussetta, and E. Ogliari, "The optimum pv plant for a given solar dc/ac converter," *Energies*, vol. 8, no. 6, pp. 4853–4870, 2015.
- [51] R. Hotopp, "Private photovoltaik-stromerzeugungsanlagen im netzparallelbetrieb," *RWE Energie AG, Essen*, 1990.
- [52] B. Brooks, C. Whitaker, and C. S. Ramon, "Guideline for the use of the performance test protocol for evaluating inverters used in grid-connected photovoltaic systems," *California Energy Commission*, 2005.
- [53] Ingeteam. "Ingeteam Solar Photovoltaic Inverters." (2018), [Online]. Available: <https://www.ingeteam.com>.
- [54] A. E. Fitzgerald, C. Kingsley, S. D. Umans, and B. James, *Electric machinery*. McGraw-Hill New York, 2003, vol. 5.
- [55] G. Joksimovic, "Transformer reactive power compensation - fixed capacitor bank calculation," *IEEE Transactions on Power Delivery*, vol. 30, Oct. 2014. DOI: [10.1109/TPWRD.2014.2373039](https://doi.org/10.1109/TPWRD.2014.2373039).
- [56] International Electrotechnical Commission, *IEC 60076-5:2006 Power transformers - Part 5: Ability to withstand short circuit*. 2006.
- [57] J. Remund, S. Müller, S. Kunz, B. Huguenin-Landl, C. Studer, and C. Schilte, "Meteonorm global meteorological database—handbook part ii: Theory, version 7.1," 2014.
- [58] I. E. Commission, "Photovoltaic system performance monitoring - guidelines for measurement, data exchange and analysis," *IEC 61724*, 1998.
- [59] T. Dierauf, A. Growitz, S. Kurtz, J. L. B. Cruz, E. Riley, and C. Hansen, *Weather-corrected performance ratio*, 2013.
- [60] M. C. Alonso-García, J. Ruiz, and W. Herrmann, "Computer simulation of shading effects in photovoltaic arrays," *Renewable Energy*, vol. 31, no. 12, pp. 1986–1993, 2006.
- [61] R. G. Chamberlain and W. H. Duquette, *Some algorithms for polygons on a sphere*, 2007.
- [62] A. Driesse, P. Jain, and S. Harrison, "Beyond the curves: Modeling the electrical efficiency of photovoltaic inverters," in *Photovoltaic Specialists Conference, 2008. PVSC'08. 33rd IEEE*, IEEE, 2008, pp. 1–6.

- [63] S. Hess and V. I. Hanby, "Collector simulation model with dynamic incidence angle modifier for anisotropic diffuse irradiance," *Energy Procedia*, vol. 48, pp. 87–96, 2014.
- [64] P. Ineichen, O. Guisan, and R. Perez, "Ground-reflected radiation and albedo," *Solar Energy*, vol. 44, no. 4, pp. 207–214, 1990.
- [65] P. Ineichen, A. Zelenka, O. Guisan, and A. Razafindraibe, "Solar radiation transposition models applied to a plane tracking the sun," *Solar Energy*, vol. 41, no. 4, pp. 371–377, 1988.
- [66] O. P. Lamigueiro, "Energía solar fotovoltaica," *Versión 1.22.Marzo 2011*, 2013.
- [67] E. Lorenzo, L. Narvarte, and J. Muñoz, "Tracking and back-tracking," *Progress in Photovoltaics: Research and Applications*, vol. 19, no. 6, pp. 747–753, 2011.
- [68] A. Mermoud, "Optimization of row-arrangement in pv systems, shading loss evaluations according to module positioning and connexions," in *27th Eur. Photovolt. Sol. Energy Conf*, 2012.
- [69] M. A. Torrero and M. Chinchilla, "Desarrollo de herramienta para el diseño, cálculo y análisis de viabilidad de una planta fotovoltaica con seguidor a un eje norte-sur," Universidad Carlos III de Madrid, 2016.
- [70] T. A. Olukan and M. Emziane, "A comparative analysis of pv module temperature models," *Energy Procedia*, vol. 62, pp. 694–703, 2014.
- [71] Ó. P. Lamigueiro, "Grandes centrales fotovoltaicas: Producción, seguimiento y ciclo de vida," 2008.
- [72] V. Quaschnig and R. Hanitsch, "Shade calculations in photovoltaic systems," in *ISES Solar World Conference, Harare*, 1995.
- [73] D. Schneider, "Control algorithms for large-scale single-axis photovoltaic trackers," *Acta Polytechnica*, vol. 52, no. 5, 2012.
- [74] J. Stein, *PV Performance Modeling Methods and Practices: Results from the 4th PV Performance Modeling Collaborative Workshop.*, 2017.
- [75] D. Yang, "Solar radiation on inclined surfaces: Corrections and benchmarks," *Solar Energy*, vol. 136, pp. 288–302, 2016.
- [76] E. Strobach, D. Faiman, S. J. Bader, and S. J. Hile, "Effective incidence angles of sky-diffuse and ground-reflected irradiance for various incidence angle modifier types," *Solar Energy*, vol. 89, pp. 81–88, 2013.
- [77] A. A. Abood, "A comprehensive solar angles simulation and calculation using matlab," *International Journal of Energy and Environment*, vol. 6, no. 4, p. 367, 2015.
- [78] Plant Predict. "Plant predict models & algorithms." (2018), [Online]. Available: <https://plantpredict.com/algorithm/introduction/>.
- [79] H. te Heesen, M. Baron, C. Kurz, and R. Pfatischer, "Definition of the euro efficiency of solar modules," in *Proc. of the 25th European Photovoltaic Solar Energy Conf. and Exhibition*, 2010.
- [80] E. L. Meyer and E. E. V. Dyk, "Assessing the reliability and degradation of photovoltaic module performance parameters," *IEEE Transactions on Reliability*, vol. 53, no. 1, pp. 83–92, 2004.